Arturo E. Corte *
Bahia Blanca

RELATIONSHIP BETWEEN FOUR GROUND PATTERNS, STRUCTURE OF THE ACTIVE LAYER, AND TYPE AND DISTRIBUTION OF ICE IN THE PERMAFROST

Abstract

Four ground patterns were investigated by means of trenches cut in the outwash near Thule, Greenland: circular and linear depressions in unsorted material, polygonal troughs in unsorted material, sorted circles, and irregular mounds and depressions of low relief formed in unsorted finer grained material. Correlation is made between surface pattern, grain size and structure of the active layer, and type and distribution of ground ice for the patterns investigated. Classification of the active layer as disturbed, slightly disturbed, and undisturbed is based on the condition of primary depositional bedding and the presence or absence of vertical sorting. Other features of the active layer, depending upon its type, are an accumulation of fines at the bottom of the active layer and on top of stones, and a siliceous calcareous evaporite on the under surface and clean washed coarser particles beneath the larger stones.

Fabric analysis of four kinds of ground ice is presented: ice wedge, relict ice, ice mass, and ice lens, as well as analysis of the contact of ice wedges with relict and mass ice.

Practical applications, based on the conclusions, are given for the selection of foundation sites and the location of non-frost-susceptible building materials.

A glossary of selected terms and appendices concerning the use of geophysical and plant ecological studies as indicators of various features of the active layer and permafrost, recommendations for further field and laboratory studies, and recommendations on field and laboratory techniques are presented.

PREFACE

This report presents data and analysis from a field study conducted near Thule, Greenland during the summer of 1957. The investigation is a part of a comprehensive project conducted by the Frozen Ground Basic Research Branch, USA SIPRE, entitled Field and Laboratory study of patterned ground.

The work was performed under the direct supervision of Dr. Arturo E. Corte, Contract Scientist, with technical and administrative supervision from Dr. Henri Bader, Chief Scientists, and Mr. W. K. Boyd, Acting Chief, Frozen Ground Basic Research Branch. The report also includes data from investigations carried on by Mr. Jack Arthur, project leader during the 1956 field season. The results of studies on the plant ecology of patterned ground sites by Dr. John W. Marr, and on geophy-

* U.S. Army Cold Regions Research and Engineering Laboratory, Hanover, New Hampshire. Present address: Universidad del Sud, Bahia Blanca, Argentina.

sical prospecting for ground ice by Anthony D. Nicolaou are presented in an appendix. Grateful acknowledgement is made to Mr. John T. Tangermann who prepared the maps and diagrams, carefully edited the entire munuscript, made many valuable suggestions and contributed substantially to the improvement of its form and contents.

It is the author's pleasure to acknowledge the helpful assistance provided by the US Army Engineer Arctic Task Force and the following scientific project personnel: Eugene F. Farrell, Bevan M. French, Donald R. Peacor, and Alfred W. Stuart.

INTRODUCTION

The surface of the outwash near Thule, northwest Greenland (fig. 1) is marked by four distinctive patterns, three of which are of widespread occurrence. These patterns are shown in plate 1, labeled as follows:

Pattern type 1 is characterized by depressions in the form of kettles or valleys of about one meter relief in coarse unsorted gravel and sand, spaced from 6 to 10 meters on centers. This pattern type is not listed in the international nomenclature (Commission de Morphologie Périglaciaire 1952) for patterned ground and occurs in only a few places in the Thule area.

Pattern type 2 is the very well known ice-wedge polygon investigated by Leffingwell (1919) and Black (1951, 1952, 1954) in Alaska. In the Thule area these polygons commonly have a mesh diameter of 20 to 30 meters.

Pattern type 3 consists of sorted circles or centers of fines surrounded by coarse washed particles. There is a wide size variation in those observed about Thule, ranging from a few centimeters to several meters in diameter. This pattern and its many variations have been fully described in the literature, and many conflicting theories have been advanced on its origin. Summaries and criticisms of these theories have been published recently by Cailleux and Taylor (1954) and Washburn (1956), to which the reader is referred for background material.

Pattern type 4 is characterized by elevations and depressions of low relief, without surface sorting. The humps in this pattern are flatter and less well developed than those of type 1 and are formed in finer material. Vegetation growing in the depressions, outlines the mounds more distinctly. This pattern has been described often, but little is understood as to its origin (Washburn 1956, p. 829). It is widespread in the Thule area.

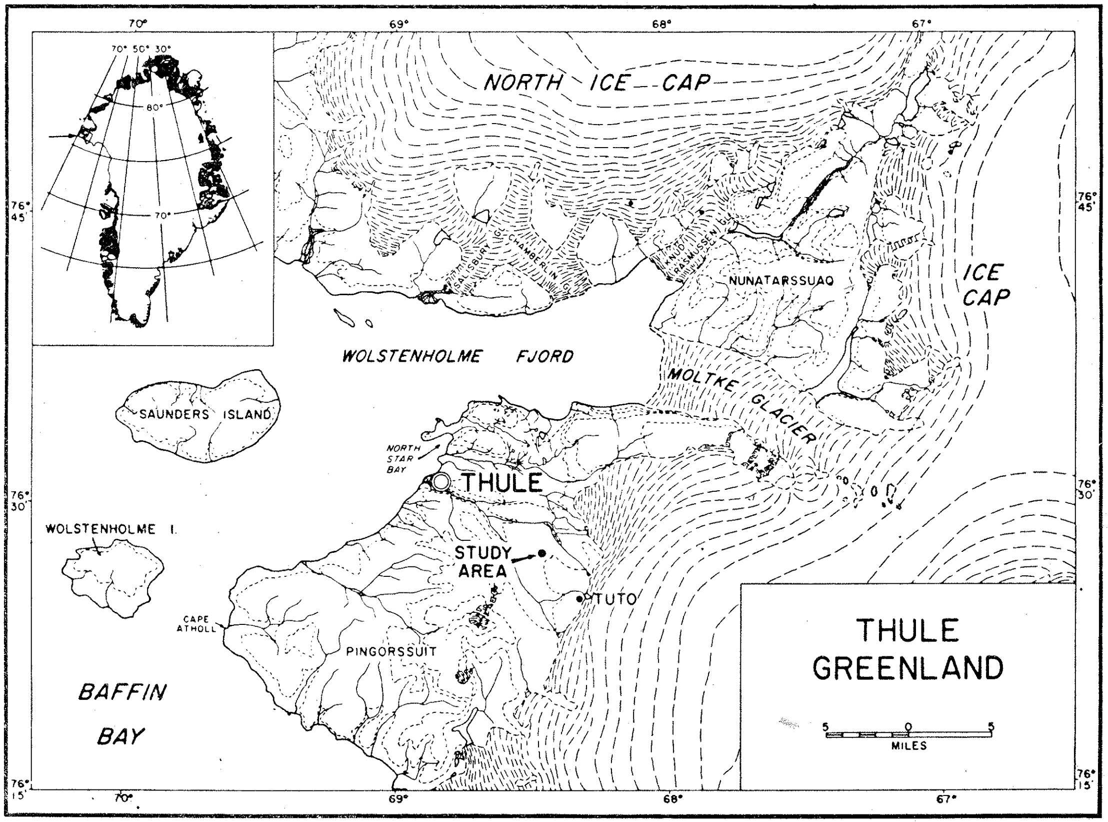

Fig. 1. Location map of study area near Thule, NW Greenland

During the summer of 1956 it was observed that, when the active layer was removed in areas of ice wedge polygons (type 2), the melting of the ice wedges in the permafrost produced a similar polygonal pattern. The removal of the active layer from pattern types 3 and 4 caused collapse of the permafrost to form very irregular mounds and depressions, indicating a permafrost rich in ice and suggesting that pattern types 3 and 4 might be related to type and/or quantity of ice in the permafrost. At the same time it was noted from an examination of airphotos that ice wedge troughs are poorly developed or end in the vicinity of types 1, 3 and 4 (pl. 1). It was not known whether only the troughs or both wedges and troughs disappeared.

Several trenches cut in the active layer of pattern types 3 and 4 in 1956 indicated that there was a vertical sorting with coarser material at the surface grading into finer material at the bottom of the active layer.

To investigate these aspects of the patterned ground problem, a large program of investigations was planned and carried out during the summer of 1957, the results of which are presented in this report.

The excavations made in each pattern are shown in plate 1, with a circle and a rectangle for type 1 and a series of interconnected trenches for types 2, 3 and 4. The study area is located a few miles from the border of the ice cap and about 16 miles from Thule, roughly halfway between the ice cap and the sea, and about 225 m above sea level. It is part of the outwash which has been deposited and worked by rivers emerging from the ice cap. The composition of the outwash varies considerably within short distances. In some places it is composed of a mixture of gravel, cobbles, boulders, and sand with no fines, whereas close by it may show a fairly high percentage of fines and a low concentration of the coarsest fraction.

Part 1 of the report deals with the physical characteristics of the surface pattern and the active layer and their relation to type and distribution of ground ice in the permafrost. Part 2 covers investigations into the physical characteristics and fabric of four kinds of ground ice.

In addition to the basic investigations of relationships between pattern, active layer, and ground ice, ecological studies on the plant life in the pattern areas were made by Dr. John W. Marr, Director of the Institute of Arctic and Alpine Research of the University of Colorado. Anthony D. Nicolaou of the University of Minnesota, attempted to use geophysical methods to locate ground ice in the permafrost. Brief discussions of their work are presented in an appendix.

Of the many factors which may affect the behavior of a soil under freeze—thaw action (Corte (1961), only three are considered in this

Fig. 2. Surface map of Area 1, Thule, Greenland

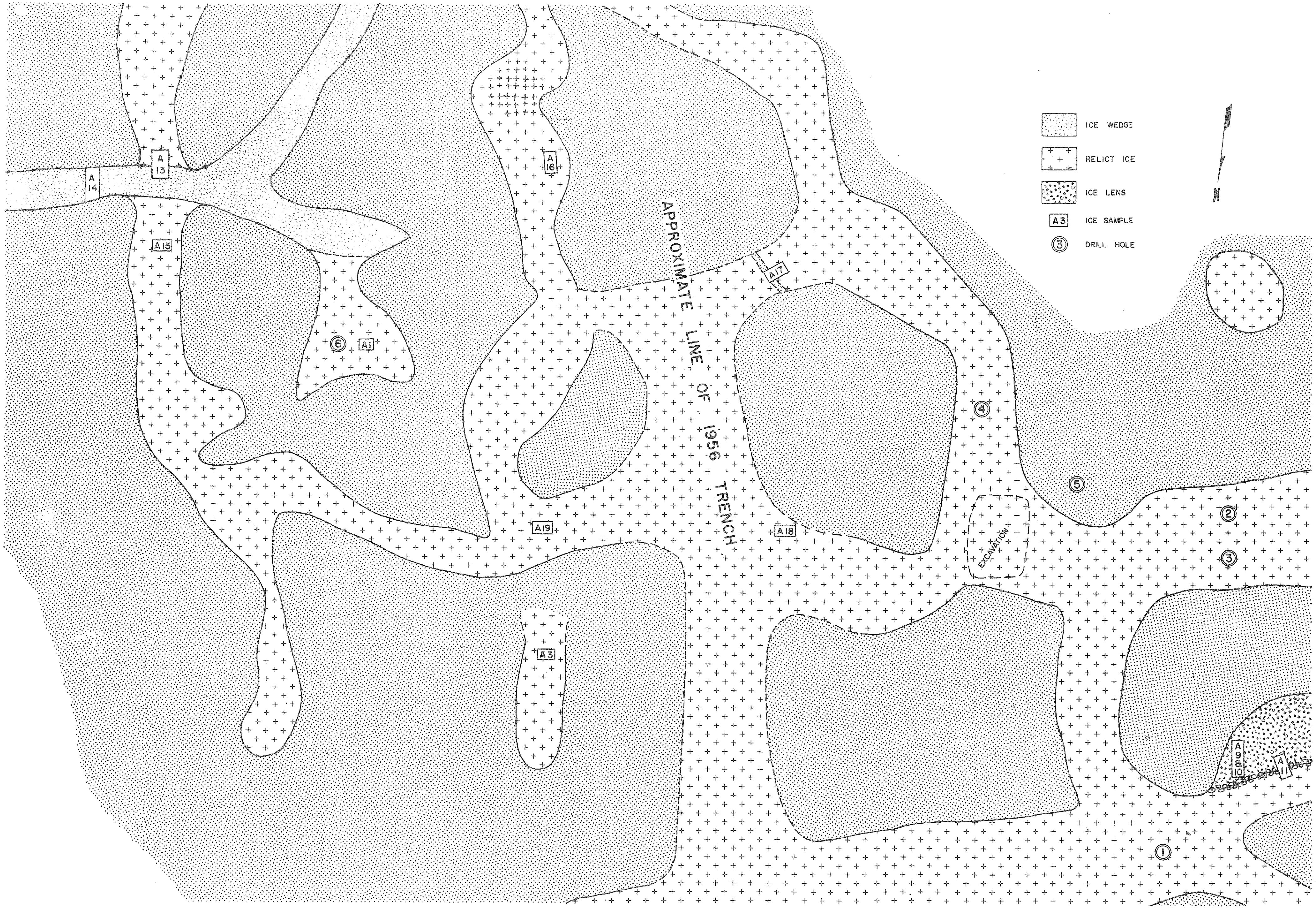

Fig. 3. Ground ice distribution in the permafrost, Area 1

report: grain size gradation, range of grain size, and percentage of the fraction finer than 0,074 mm in diameter (200 ASA mesh). Because of the small area in which these studies were conducted, such important factors as mineral composition of both the coarse and fine fractions were considered consistent throughout the area. Similarly, data on moisture content are not presented because the study areas were drained before the main trenches were cut and such data would therefore be misrepresentative.

The current Corps of Engineers criterion for frost susceptibility of a soil (Linell and Kaplar 1959) is based principally on the percentage by weight of the fraction finer than 0,02 mm in diameter, as early advanced by Casagrande (1934), Watkins *et al.* (1931), and Beskow (1934). The derivation of this criterion is related to the amount of heaving produced in soils by a specific rate of frost penetration. In the studies presented here, however, this criterion is not used and the terms *frost-susceptible* and *non-frost-susceptible* are used to differentiate between degrees of disturbance observed in the active layer. A direct correlation between the degree of disturbance and the percentage by weight of the soil fraction finer than 0,074 mm (200 ASA mesh) will be shown. It must, however, be assumed that the soils described as non-frost-susceptible are relatively dry and well-drained.

SURFACE PATTERN, STRUCTURE OF THE ACTIVE LAYER, AND TYPE AND DISTRIBUTION OF GROUND ICE IN THE PERMAFROST

PATTERN TYPE 1: CIRCULAR AND LINEAR DEPRESSIONS IN UNSORTED OUTWASH

Circular depressions, Area 1

An oblique airphoto (pl. 2) shows the approximate outline of the excavation and the important morphological characteristics of Area 1: an essentially flat surface broken by closely spaced circular depressions or kettles, and a longitudinal branching ice-wedge trough.

Depressions had a local relief of about 1 meter and were spaced 6 to 10 m apart in unsorted outwash consisting of cobbles and boulders in a matrix of sandy gravel (pl. 3). The average size of the larger fragments was from 10 to 20 cm. The surface displayed a complex network of cracks, with most junctions within depressions. Ice-wedge troughs in this area had a depth of about 30 cm (pl. 4). A surface map was made by plane table survey to record the features for reference after the area was excavated (fig. 2).

Structure of the active layer

During the summer of 1956 a trench was cut across one of the depressions in Area 1 (fig. 2, A—A′) using a bulldozer and explosives. This trench revealed a body of ice whose upper surface reached to the permafrost table beneath surface mounds and dipped beneath pockets of frozen gravel and sand under the depressions (pl. 5). A profile (fig. 6) was constructed to record the structure of the active layer and the location of soil and ice samples taken from the east [1] wall of the trench. The ice was overlain by well-sorted conformable beds of water-deposited sand and gravel. Grain size analyses of selected samples taken from the active layer and permafrost are shown in figures 4 and 5.

Two samples from the top and two from the middle of the active layer showed similar gradation, with less than 2% fines (*fines* is used in this report to indicate that fraction finer than 0,074 mm) and no vertical sorting in the active layer. Grain size analysis of samples from the permafrost (fig. 5) showed it to be composed of well graded sands and gravels with less than 2,5% fines. According to current engineering standards (U.S. Army Waterways Experiment Station 1957), inorganic soils containing less than 3% by weight of grains finer than 0,02 mm are generally non-frost-susceptible (not subject to frost heaving). Therefore the material constituting the active layer and permafrost in Area 1 would be classified as non-frost-susceptible and patterns must have been formed by a means other than frost heaving.

Soil particles from these samples were subangular to subrounded and no glacial striae were found — further indications that the material was a fluvial deposit.

In 1957 the entire active layer was removed from Area 1 by bulldozer to study the areal distribution of the ice and to take ice samples for fabric analysis. Since this was begun in early June, the active layer was not fully thawed and several scrapings were necessary, with intervening periods of melting, to expose the permafrost table. When the ground ice was exposed the active layer proved to be roughly 5 feet thick.

Ground ice and its relation to surface morphology

After removal of the active layer the ice exposed was mapped on the same scale as the surface map (fig. 2, 3). Ice exposed at the permafrost table was in the form of sinuous and interwoven bands under what had been elevations at the surface. Under surface depressions were pockets

[1] Compass directions are true unless otherwise indicated.

of frozen sand and gravel at the permafrost table. In the west corner of the area a branching ice wedge was exposed below the well-developed trough seen at the surface. It may also be noted that, as the main surface trough ends in the vicinity of the pattern of depressions, so also does the underlying ice wedge as it enters the area of *relict* ice (so-named for reasons described below). Another very small wedge was found by chance during the examination of a sample thought to be relict ice (sample A-17, fig. 3). This small wedge was apparently related to a fine crack at the surface. As this wedge was discovered by chance during fabric analysis of the relict ice sample in the laboratory after the field season, it was impossible to determine whether or not other fine wedges occur beneath the other surface crack.

Another type of ice was found in the northwest corner of the area, a lenticular body of transparent ice separated from a section of the relict ice by a wall of cobbles, most of which had their long axes oriented vertically along the contact (pl. 6). At the line contact with the relict ice the lens was about two feet thick, but it pinched out in lenticular shape at its south and east borders. The lens lay in a shallow basin lined with a layer of clean, washed cobbles (pl. 7). A few small pebbles were found suspended in the ice lens, the cryoconite holes refrozen and showing little vertical streamers of silt and fine air bubbles.

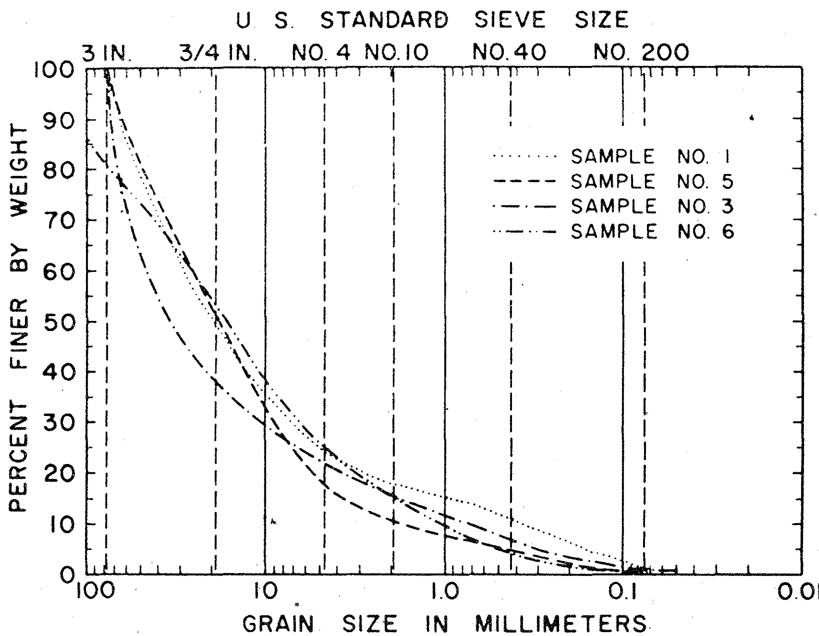

Fig. 4. Grain size of the active layer, Area 1 (see fig. 6 for sample location)

The ice lens was possibly the result of the freezing of a small slush pond and subsequent covering by fluvial deposits during a later stage of outwash deposition (see discussion under *Fabric analysis*, p. 40).

Unfortunately the lens was found outside of the surface area originally mapped so that the original topography at that point is unknown. However, an examination of the airphoto (pl. 2) of the area based on the relationships reported in this paper, indicates the likelihood that the active layer here contained a greater percentage of sand and exhibited no surface pattern.

A second profile of the active layer (fig. 7) was made in this corner of the area in order to determine the relationship between the two kinds of ground ice and the active layer above them. This profile curved around the north corner of the area, beginning at the middle of the right side of figures 2 and 3, cutting the first band of relict ice in figure 3, the ice lens and second band, and continuing around the corner of the map to cut the band a third time where it leads out of the corner of the area (pl. 8).

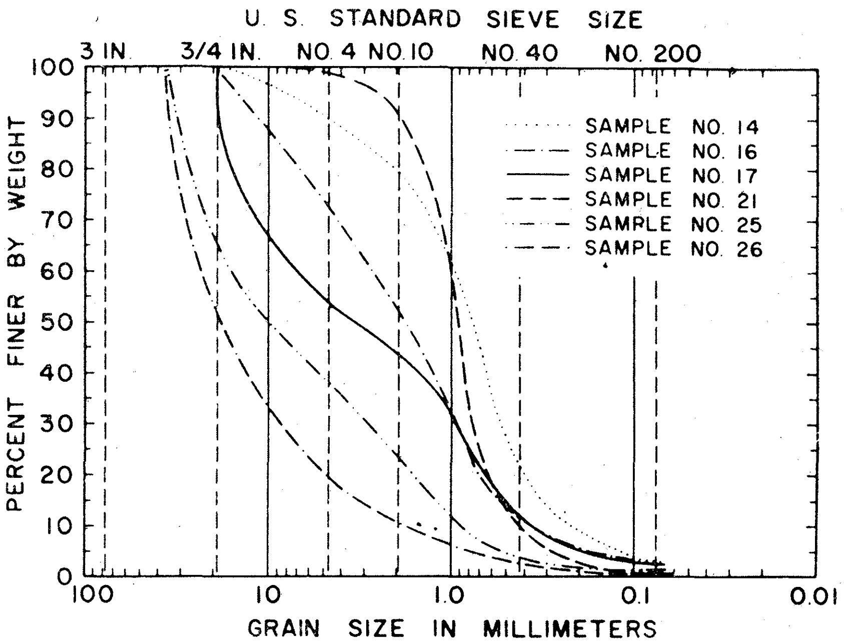

Fig. 5. Grain size of the permafrost, Area 1 (see fig. 6 for sample location)

At the left end of the profile the relict ice was covered by layers of clean undisturbed sand and gravel without fines which dip downward at the edges of the band, supporting the observations made in the trench that the sand and gravel layers are conformable to the ice surface. The actual ground surface at the line of the profile was disturbed by the passage of heavy equipment in 1956 and covered by material from the excavation in 1957. However, for construction of the profile, the approximate position of the original surface was determined from an indistinct layer of oxidestained rocks and fine grass rootlets. Since the relationship between the surface morphology and the ice was determined at other points in this area the loss of the accurate surface profile in the cross-section is of no great importance.

Continuing the profile to the right, the sand and gravel layers become more nearly horizontal as they come to the ice lens, which is overlain by a layer of fine, well-graded sand without fines. The layer of sand ends at the cobble wall between the ice lens and the relict ice band a thinner diagonal layer above is bent downward sharply and truncated at the ice surface. On the right side of the cobble wall, above the band of relict ice, similar steeply inclined truncated beds occur. The reason for this is unknown. Further to the right, at the edge of the band, the bedding in the active layer curves downward to conform with the ice surface as in the first profile. The conformable beds again ascend into the active layer at the edge of the band at the right end of the profile, but become disturbed and contorted above the relict ice. Plate 8 shows a general view of the right three-fourths of profile 1.2 (fig. 7) and the relationship between features in the active layer and those in the permafrost.

Relict ice is believed to be of glacial origin — a section of ice broken off from the retreating ice cap and covered by fluvial sediments from the outwash streams. Varying thicknesses of cover caused differential melting of the surface, producing humps and depressions covered by outwash. What are now ridges would originally have been meandering stream beds in which sediments were deposited preferentially, thereby resulting in greater insulation. Under these conditions the original topography would become reversed through differential melt. Continued or subsequent deposition of sediments would fill in the new depressions to a certain extent and an equilibrium would finally be reached when the ice surface melted down to the level of the permafrost table.

Such a process is going on today at the border of the ice cap. Plate 9 shows glacial ice being covered by stream borne deposits. The streams flowing over the ice remove material and redeposit it farther dwonslope where, owing to differential melting, elevations and depressions are produced. However, as the stream volume decreases and current becomes less, heavier deposits will be laid in the stream beds and differential melt will cause a reverse of the original features. Plate 10 shows a large mound of ice covered by outwash, of which a portion was removed to expose the ice. In the foreground a depression containing water is being filled with sand and coarser material rolling down from the elevated portions. Differential melt will lower this less insulated depression even more, causing more material to roll down from the slopes until coarse material from this source and finer particles carried in by the stream will create greater insulation in the depression and allow differential melt to reverse the topography. Another outstanding example of this process occurs 2 miles south of Tuto where outwash streams and rivers are covering several acres of glacier ice with outwash material.

Excavations and drillings were made in Area 1 in an effort to determine the thickness of the body of relict ice. The trench excavated in 1956 cut through approximately 7,5 feet of relict ice from the permafrost table down. A small excavation was then made by hand near the lowest point in the trench, and a plastic clayey soil was found at a depth of about 13 ft on the vertical scale in figure 6, indicating that the ice is about 18 in. thick at its thinnest point and about 8 ft thick beneath the band exposed at the permafrost table (Espach 1956). A 7-ft excavation was made in relict ice in 1957 (center right, fig. 3) without reaching the bottom. In addition, five holes drilled in bands of relict ice (fig. 3) consistently showed the bottom of the ice to be between 6 and 7 ft below the exposed surface. Slightly different thicknesses of ice may due to local variations in thickness and to lowering of the ice surface below the permafrost table through melting. Unfortunately cores were not obtained from the drillings and it was therefore impossible to determine what underlies the ice.

An examination of the active layer exposed in profiles 1.1 and 1.2 (fig. 6, 7) revealed two important and distinctive features: (1) an accumulation of fines on top (pl. 11) and clean-washed coarser particles without fines beneath large stones, and (2) a white deposit of evaporite on the underside of these stones (pl. 12). These features are considered to be the result of washing within the active layer, both during and after deposition. (The white deposit does not occur where more than 3% fines occur in the active layer, see page 22).

Vilborg (1955) has presented grain size analyses of the gravelly material beneath large stones in the moraine of the Kebnekajse area of Swedish Lapland. He compared these with grain sizes of the material in the surrounding soil, but further away from the stones rather than at the sides and tops. He does not state whether permafrost or patterned ground occur at the sites, nor does he mention any accumulation of fines on top of the stones. However, he did note a markedly different grain size curve for the coarser material beneath the stones.

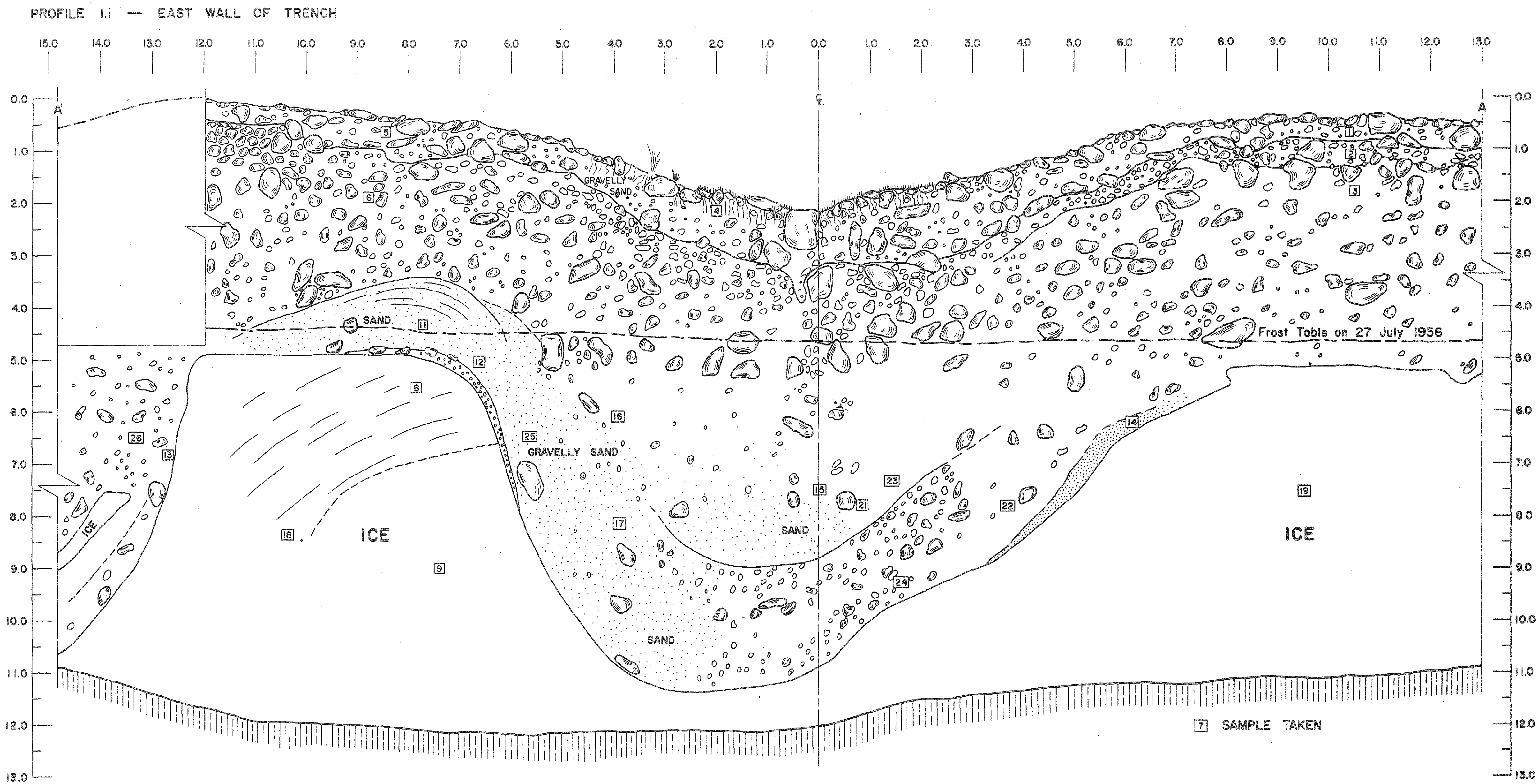

Fig. 6. The active layer and ground ice beneath pattern type, Area 1. Profile 1.1

A spectro-chemical analysis of the evaporite shows its composition to be 34,96% SiO_2, 57,69% $CaCO_3$, and 0,81% Fe. Major constituents are Na and Mg, with minor amounts of K, Cu, Pb, and Sn, with traces of Al, Mn, Ag, and B. Essentially then, the deposit is a siliceous calcareous evaporite. Since evaporation is a function of the amount of water available and the pore space present, the upper surface of stones with its deposit of fines does not provide sufficient pore space for evaporation and the material runs around to the underside where the washed sand provides pore space. This deposit is considered a feature of desertic or semi-desertic regions in which evaporation exceeds precipitation (Senstius 1958, p. 356). It occurs quite commonly in arctic and subarctic areas and has been seen by the author in the tundra of the Rocky Mountains at 11 500 ft and in the active layer on the coastal plain in northern Alaska.

Linear Depressions, Area 5

Area 5 was located about 100 yd east southeast (true) of Area 1 (pl. 1) and consisted of three parallel shallow valleys and a circular depression spaced 6 to 10 m apart. The crests between the valleys were at roughly the same elevation as the surrounding terrain, which sloped downward slightly, with the fall line at right angles to the axes of the troughs and ridges. A well-developed ice wedge trough entered the area from the south and faded to a crack running along the eastern ends of the depressions. Only two other cracks were found in the area, in sharp contrast to the well--developed system of cracks in Area 1.

The surface was an unsorted layer of cobbles, pebbles, some sand, and no fines except for two appearent eruptions of fine material at the northwest end of the area. Although Area 1 was a pattern of closed depressions or kettles and this one of linear depressions or valleys, the similarities between the two areas were striking, even to the disappearance of the ice wedge trough. It was therefore decided to trench Area 5 to check predictions on ground ice type and distribution and on the structures of the active layer, based on the work in Area 1. A surface map was made, therefore, and a trench cut normal to the axes of the valleys in such a position that it intersected the ice wedge trough (pl. 13) and bisected one of the eruptions of fines.

Structure of the active layer

The active layer, as seen in profile, was composed of unstratified sandy gravel without fines. Cobbles and pebbles were generally oriented with their long axes parallel to the ground surface (pl. 14). At the bottom of the active layer there was a thin layer of fine sand which could only be detected where it rested on ground ice.

The wall of the trench which cut through what had appeared from the surface to be an eruption of finer material exhibited an interesting profile. The cross-section appeared in the shape of a squat, flat-topped mushroom of fine material that flowed out over the ground surface. Fine flow lines in the material have the appearance of the upward flow.

Ground ice and its relation to surface morphology

Upon excavation of the trench the correlations noted between surface features and ice in the permafrost in Area 1 proved to apply in Area 5 as well. Bands of relict ice were exposed at the permafrost table beneath the surface crests and an ice wedge beneath the polygonal trough, with frozen sand and gravel between (pl. 14, 15; fig. 8). The ice wedge pinched out about 2 m inside the trench and was bounded on its southern side by relict ice, the band of which appeared to swing around the end of the wedge and join, within the confines of the trench, the band under the next crest.

It is apparent that the genesis of the surface pattern in Area 5 is the same as that of Area 1, i.e., a large mass of ice, probably of glacial origin, was buried by outwash deposits as the ice cap retreated and then subjected to differential melting. From the lack of obvious bedding in the active layer it appears that outwash deposition and differential melting occurred simultaneously and without interruption until the entire deposit was laid down (pl. 14, 15).

PATTERN TYPE 2 AND 3: POLYGONAL TROUGHS IN UNSORTED OUTWASH AND SORTED CIRCLES OR CENTERS OF FINES

Pattern type 2, ice wedge polygonal troughs (pl. 16), is the most completely studied and best known ground pattern of permafrost regions (Leffingwell 1919; Black 1951, 1952, 1954; Shumski 1956; Dostovalov 1958), and is the result of the filling of thermal contraction cracks with ground water or atmospheric moisture to from ice wedges. Development of an active layer results in slumping of material above the wedge and the formation of troughs filled with washed cobbles and boulders. The ground surface enclosed within the net of troughs is unsorted and consists of mixed boulders and cobbles in a matrix of sandy gravel.

Pattern type 3, centers of relatively fine material surrounded by coarser

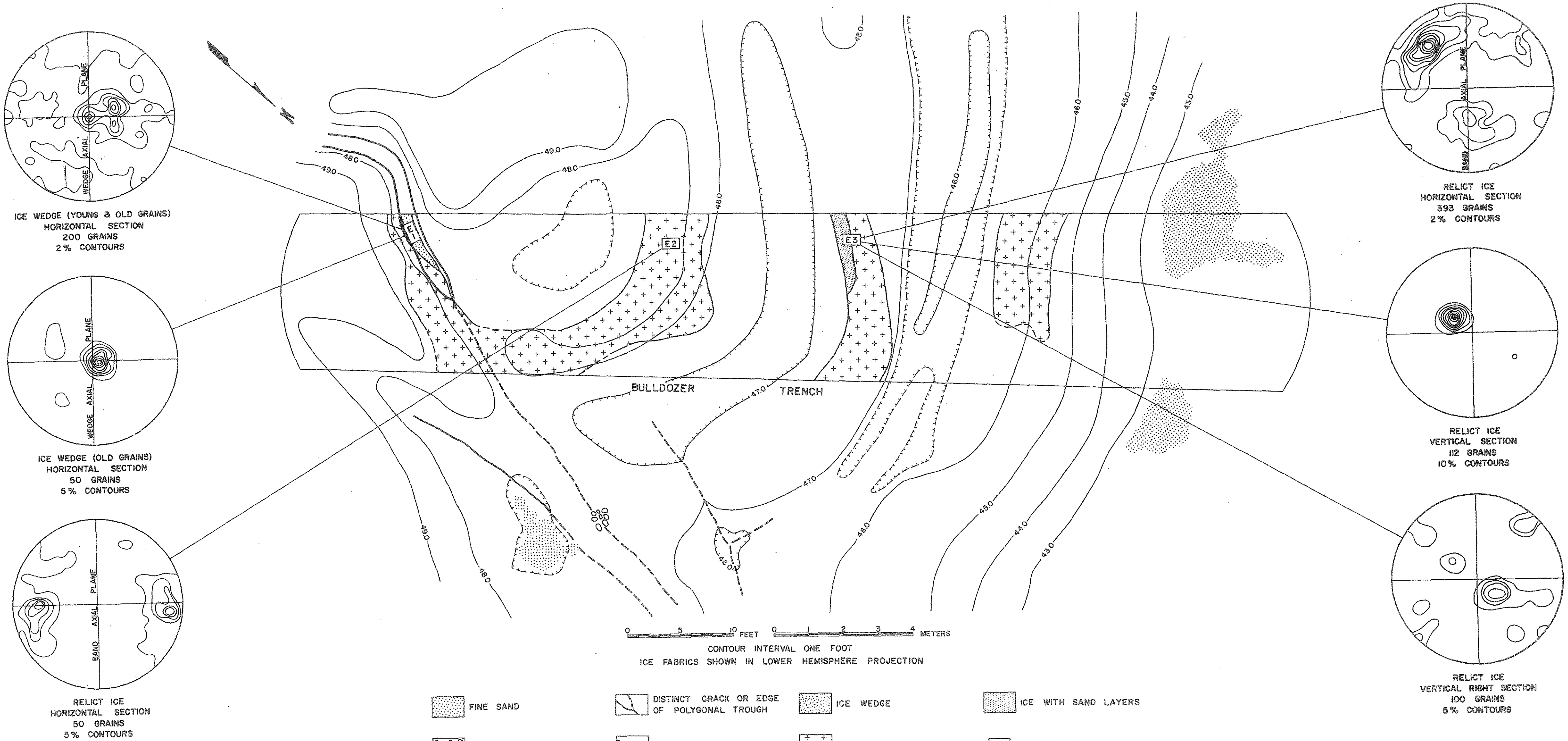

Fig. 8. Relationship of surface topography to ground ice in the permafrost, Area 5, Thule, Greenland

washed stones (called *sorted circles* by Washburn 1956), is also well known and has received extensive treatment in the literature, dealing with both its genesis and geographic distribution. Many theories have been advanced to explain the origin of this pattern, but none have met with general acceptance. These theories will not be discussed here, as summaries as well as the arguments for and against each have been published by Troll (1944), Cailleux and Taylor (1954) and Washburn (1956).

In the Thule outwash area many variations in centers of fines are encountered, from small centers a few centimeters in diameter to ones as large as four meters (pl. 17); some centers are raised (pl. 18) and others are depressed (pl. 19). They may be quite isolated or occur closely spaced in groups (pl. 20). (Some authors refer to these closely spaced centers of fines as *stone polygons*, but it is the opinion of this author that the term *polygon* should be reserved for thermal contraction and dessication features where a definite geometric polygonal form is present. In centers of fines a polygonal form is a secondary characteristic based solely on the spacing of the centers). Most are composed of sand and fines, either with or without included pebbles, but others are composed entirely of pebbles or small cobbles (pl. 21). They generally occur within bands or „streams" of washed cobbles and boulders.

The two patterns do not occur fully developed in the same location. As polygonal troughs enter an area of centers of fines they characteristically disappear or fade to mere cracks which may run through the centers (pl. 22, foreground and just above left center), a fact noted also by Colton and Holmes (1954, p. 36) in a similar area a few miles from Thule. For this reason it was considered that, as a research subject, the contact zone was as important as the individual patterns. Therefore two areas which contained good examples of both individual patterns and zones of pattern contact were selected for study.

Area 3

Area 3, the primary research area (pl. 1), was roughly 80 × 60 m in size and contained well-developed ice wedge polygons on its north and south sides and a sorted depressed area cutting diagonally arcoss it in east—west direction. The surface of the polygonal portion was a heterogeneous mixture of unsorted material ranging from sand to boulders, with cobbles of the average size. There was a sorting of cobbles and boulders into the troughs, the result of collapse over the ice and washing out of the finer fractions, but as this was very local to the trough, the active layer in general is considered unsorted.

The depressed area was apparently an old stream channel which contained washed cobbles and boulders surrounding scattered centers of fines ranging from a few centimeters in diameter to about 4 meters in the case of the one in plate 17, center. A large ice wedge trough, seen on both sides of the stone strea, faded to a small crack crossing this center, as seen in the figure.

Structure of the active layer

Area 3 was mapped by plane table to record the essential features of topography and relief, plus those of the patterns and grain sizes at the surface (fig. 9). An east—west trench was cut through a section of stones stream and into the finer material north of it, and a branch cut from the west end of this trench to provide drainage of melt water from the area. The main trench was then cut across the east end of the first trench to expose the permafrost beneath the main polygonal trough, the sections of the stone stream, and the large and complex centers of fines in the center of the area. The outlines of the excavation and the exposures of ground ice within it were mapped and are shown in figure 10, which may be overlain by figure 9 in order to relate surface features to those of the permafrost table.

After the trenches were made and ground ice mapped, profiles were made of the trench walls (see fig. 10 for location of profiles). Only selected profiles are presented here for illustrative purposes.

Profile 3.1 (fig. 11), running from the center of the area to the intersection of the trench wall with the ice wedge, presents a continuous cross--section of the active layer from a sorted area containing centers of fines into the unsorted active layer of the ice-wedge polygons. The active layer in the latter section shows the horizontal bedding of primary deposition and no vertical disturbance or sorting other than the concentration of coarse material in the trough above the ice wedge. The permafrost beneath the polygon is composed of frozen sands and gravels except for the ice wedge. The surface is unsorted and smooth.

Along the profile to the left and into the sorted area, however, several changes take place in the active layer. The horizontal bedding becomes disturbed and contorted, a new type of amorphous ice „mass" appears in the permafrost, the percentage of fines increases, and the surface becomes uneven and sorted. At the left end of the profile, beneath a surface composed of fine material, there is plug of finer materials. These plugs of fine material have been reported beneath sorted circles or centers of fines by other authors such as Washburn (1956, p. 836)

Fig. 9. Surface map of Area 3, Thule, Greenland

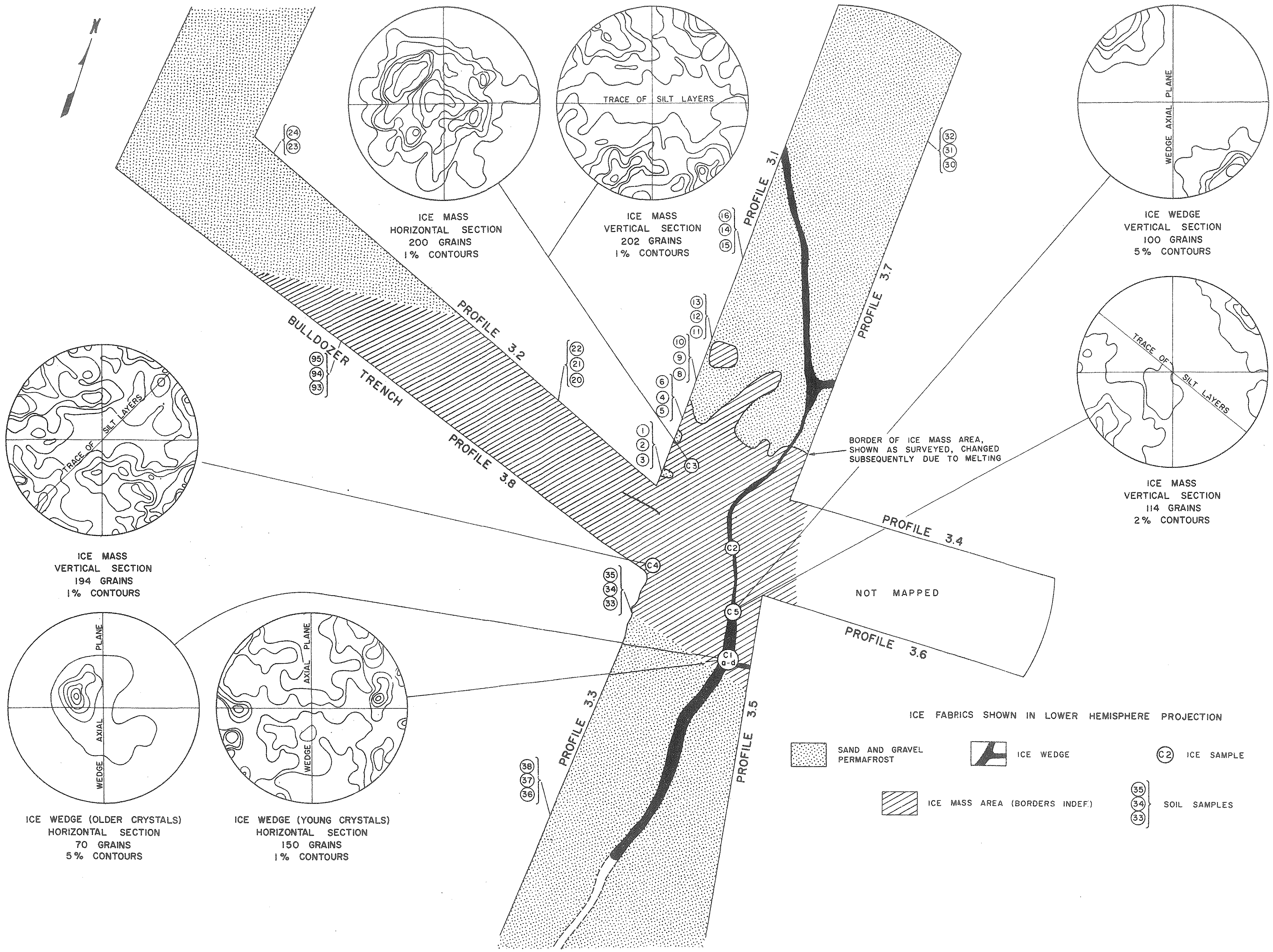

Fig. 10. Ground ice distribution in the permafrost, Area 3, Thule, Greenland

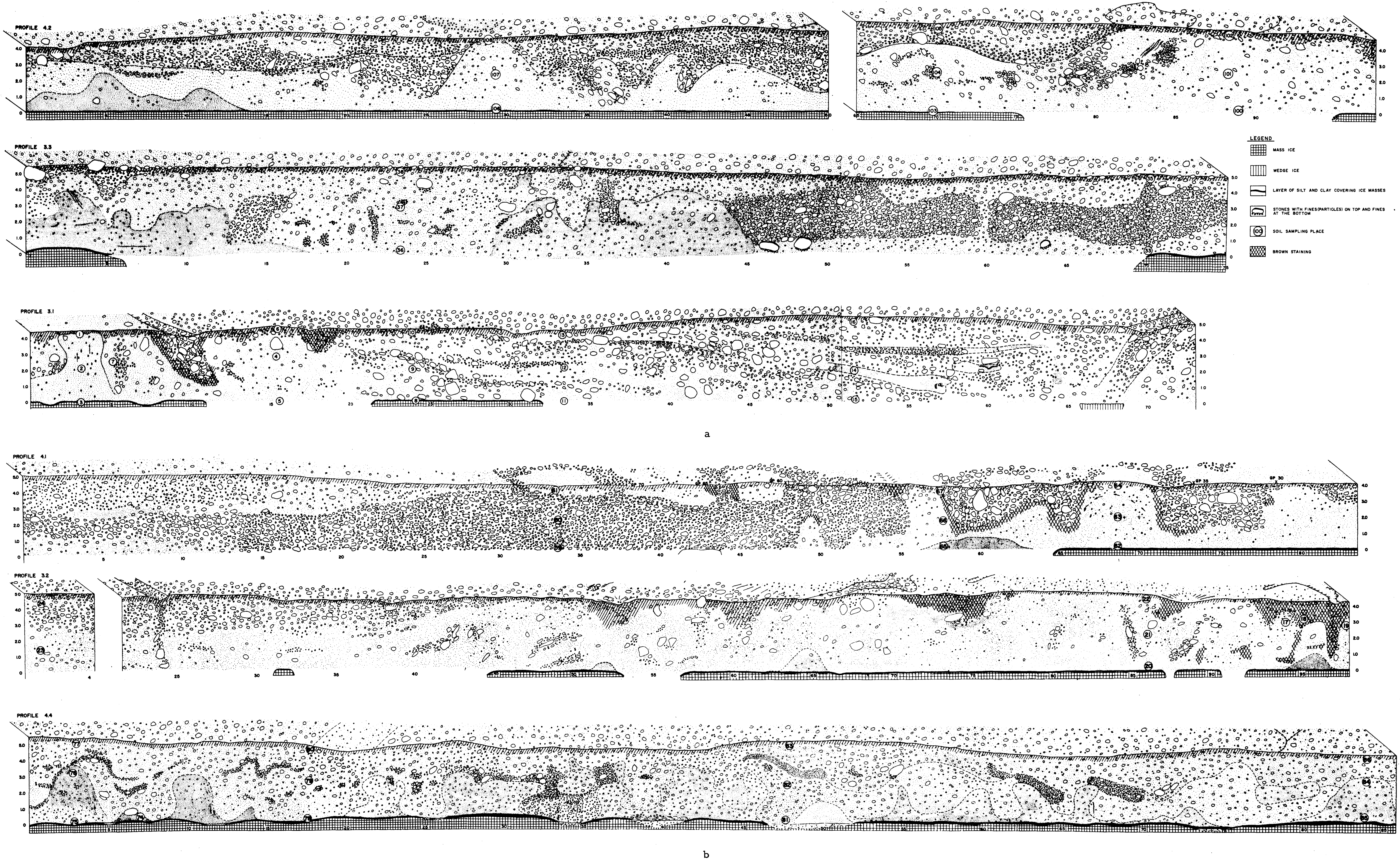

Fig. 11. Representative profiles of the active layer, Areas 3, 4 and 4 a

and MacKay (1953, p. 35), although limited equipment for excavating prevented them from making the observations possible with the aid of a bulldozer. The stones within this plug were oriented with their long axes vertical, as indicated by the arrows in the profile.

The permafrost beneath this disturbed active layer was composed in large part of ice masses containing layers of fine particles and scattered stones. The ice of these masses was clear and transparent except for the included soil particles.

At the bottom of the sorted active layer and resting directly upon the upper surface of the ice masses was an accumulated layer of fines, represented by a heavy black line in figure 11. This layer was not observed under the unsorted active layer of the polygons.

For purposes of comparative discussion, the active layer beneath a smooth unsorted surface will be termed *undisturbed* on the basis of the presence of undisturbed primary depositional features. The active layer beneath an uneven sorted surface will be termed *disturbed* on the basis of the contorted and broken condition of these features, while the transition zone between the two extreme types of active layer will be termed *slightly disturbed.* Further basis for this subdivision of the active layer will become apparent in the following pages.

Profile 3.2 (fig. 11) also illustrates the differences between, disturbed and undisturbed active layers. The left portion of this profile shows the unsorted surface and undisturbed active layer of an ice-wedge polygon where a smooth surface, undisturbed horizontal bedding, and a sand and gravel permafrost are present. Farther to the right the structure of the active layer becomes increasingly disturbed, the beds inclined and contorted, the texture becomes finer, the surface rougher and more irregular, while ice masses appear in the permafrost with a layer of fines resting upon them.

Soil samples were taken from various points along the trench walls for comparative analyses of the differences in grain size between the disturbed and undisturbed active layers. These samples were taken in groups of three, from the top, middle, and bottom of the active layer. Their locations in the trench walls are shown in figure 10 as well as in the profiles (fig. 11). Samples from the disturbed area were taken from the plugs of finer material alone as the material between them was too coarse for sampling with the containers and equipment available.

Average grain-size curves representing three groups of samples from the undisturbed and five from plugs in the disturbed active layers are presented in figure 12. Two distinct groups of curves are apparent. The lower group, representing the undisturbed type, shows it to have a larger average grain size throughout and no basic difference in grain size between the top, middle, and bottom, each of which averages less than 2% fines. The disturbed active layer, on the other hand, shows finer texture throughout and clear sorting of finer material toward the bottom, with an average of 5% fines at the top, 11% in the middle, and 14% at the bottom. This differential accumulation of fines and range of grain size in general in the disturbed active layer will be termed *vertical sorting* in this report. It is produced as a result of freezing, thawing, and washing of the active layer both during and after deposition of the material.

Another notable distinction between the two types of active layer is the presence of the siliceous calcareous evaporite deposit on the underside of large stones in the undisturbed active layer (as found in Area 1) and its absence from stones in the disturbed active layer.

The transition from undisturbed to disturbed active layer is not sharply defined, but rather occurs over a distance of 6 m or more in which depositional beds first become inclined, then bent and contorted, and finally broken or entirely absent. At the same time the surface changes from smooth to slightly uneven, then increasingly rougher until sorting occurs. Such a transitional zone, therefore, appears to be „slightly disturbed".

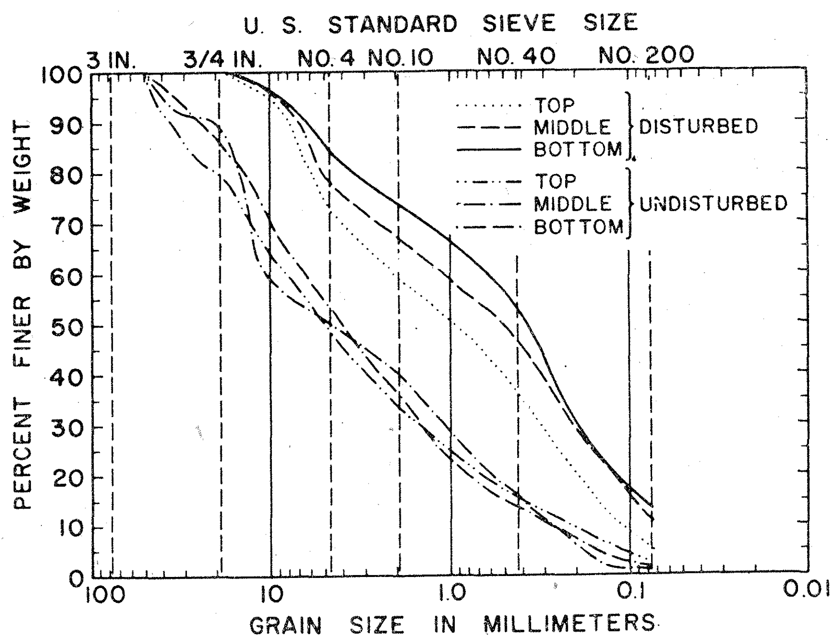

Fig. 12. Average grain size of top, middle and bottom of disturbed and undisturbed active layers, Area 3

Three series of soil samples from such slightly disturbed sections of the active layer were analyzed and showed an average of 4% fines at the top, 2,5% in the middle, and 8% at the bottom (fig. 13), thereby indicating that the slightly disturbed zone is also transitional with respect to the percentage of included fines. The average percentages of fines for the three types of active layer in Area 3 (fig. 14) therefore have a direct relationship to the amount of disturbance: 2% fines in the undisturbed, 5% in the slightly disturbed, and 10% in the disturbed.

Profiles 3.1, 3.2 and 4.1 (fig. 11) indicate that average depth of the disturbed active layer is less than that of the undisturbed. The average depth of the disturbed active layer in these profiles is 51 in. while that of the undisturbed is 62 in. This difference is believed due to the finer grain size in the disturbed active layer which allows it to hold more moisture. This in turn means greater loss of heat by evaporation and therefore shallower penetration of thaw and less collapse. There is some misrepresentation in the profiles in this respect, since, for their construction, a straight line on graph paper was assumed for the permafrost table. In actual fact the permafrost table is an undulating surface rather than a horizontal plane.

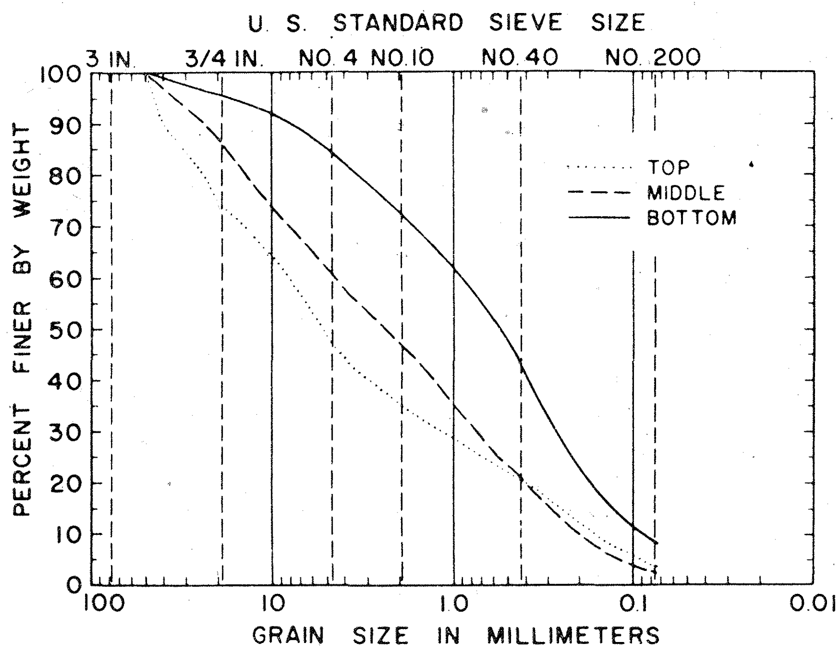

Fig. 13. Average grain size of top, middle and bottom of slightly disturbed active layer, Area 3

Before coming to any conclusions regarding the cause of pattern formation or of any of the features which occur in conjunction with them, we must know whether the materials in sorted and unsorted adjacent areas were deposited under the same conditions and at the same time. For this reason two samples from the middle of the active layer of an unsorted area and two from a sorted area were analyzed to determine their indices of roundness and sphericity, using Wadell's (1932) methods. The coefficient of shape (sphericity) is determined using the formula: $\frac{d_c}{D_c} = \varnothing$, where d_c is the diameter of a circle equal in area to the area obtained by planimeter measurement of the projection of the grain when the grain rests on its largest face, D_c is the diameter of the smallest circle circumscribing the projection, and $\varnothing$ is the shape value. The index of roundness is expressed by the formula $\frac{\Sigma \frac{r}{R}}{N} = P$, where r is the radius of curvature of the corner, R is the radius of the maximum inscribed circle, N is the

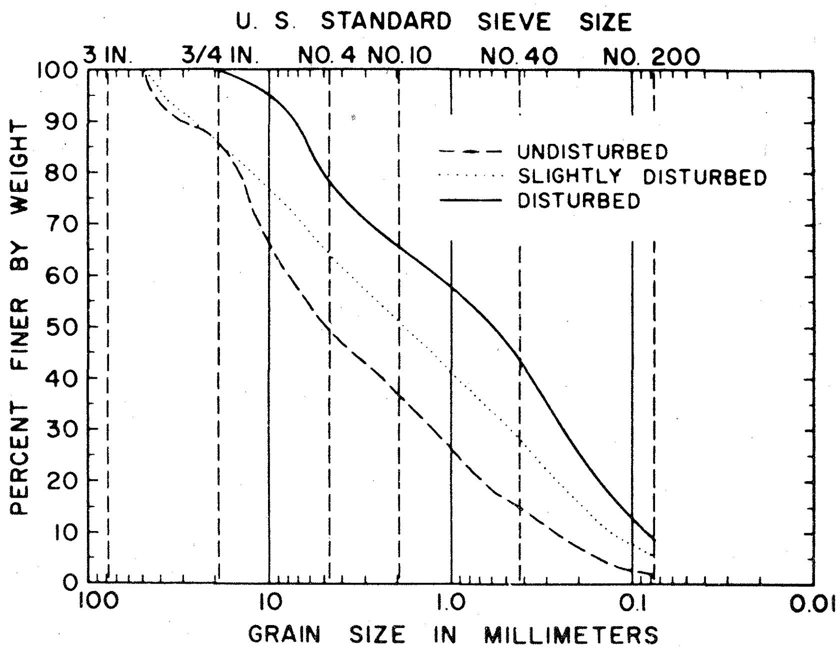

Fig. 14. Average grain size in disturbed, undisturbed and slightly disturbed active layers, Area 3

number of corners, and P is the total degree of roundness [2]. The maximum value for sphericity and roundness determined by these formulae is 1.

Values were determined for pebbles in two size groups, having diameters in the ranges of 4,68 to 9,52 mm and 9,52 to 19,2 mm. The results are presented in table I.

Table I

Indices of sphericity and roundness of disturbed and undisturbed active layers, Area 3

Pattern type	Sample No	Sphericity				Roundness			
		Grain diameter in mm							
		4.68—9.52	Avg	9.52.—19.1	Avg	4.68—9.52	Avg	9.52—19.1	Avg
3	2	0.79		0.81		0.28		0.42	
disturbed			0.79		0.80		0.33		0.43
	4	0.80		0.79		0.38		0.44	
2	31	0.80		0.78		0.39		0.50	
undisturbed			0.79		0.81		0.39		
	14	0.78		0.84		0.40		0.42	0.46

It is apparent from these values that the material in both the sorted and unsorted sections of Area 3 was deposited at the same time and from a common source. Unfortunately this analysis is a very time consuming operation and the results did not seem to justify expenditure of the time required for a valid statistical analysis. It would, however, be interesting to see whether the effects of frost action and sorting could be analyzed by these methods and presented in statistical form.

It is evident that the formation of centers of fines in Area 3 is the result of local conditions of morphology, washing, differential deposition of fines or other such factors rather than of differences in history of deposition or source of material.

Ground ice and its relation to surface morphology

Excavation to the permafrost table revealed two distinct types of ground ice in the permafrost. The first was the expected ice wedges located roughly beneath the surface troughs as described in Area 1 (page 13). Plate 23 shows the bubbly ice of the wedge entering the trench at the north end

[2] Discussion of these and other methods may be found in Krumbein and Pettijohn 1938.

of profile 3.5 (fig. 10). As the wedge entered what had been a sorted area of the ground surface (compare fig. 9, 10) it narrowed sharply to a few centimeters in width. On the surface at this point the well-developed trough ended and a small but distinct crack ran from the end of the trough across the centers of fines to join a polygonal trough at the opposite side of the sorted area (fig. 9). After narrowing to a few centimeters the ice wedge followed along beneath this crack and again broadened out to nearly a meter in width beneath the trough on the other side.

The small north—south trough running through the stone stream near the center of the area pinched out to a crack which crossed the large center of fines at nearly right angles to the crack mentioned above. A tiny wedge was found in the permafrost beneath a portion of this, but could not be traced the full length of the trough and crack because of drainage problems in the trench. The larger trough entering the drainage trench at right angles near its northern end could not be related to a wedge in the permafrost at all, but that section of the excavation was not studied with as much detail as the more central area. Since the trough ended near the trench wall it is also entirely possible that the wedge had already pinched out before reaching the trench.

The second type of ice encountered in this excavation was a series of large, amorphous and discontinuous bodies of transparent ice (pl. 24) containing folded layers and scattered particles of sediments (pl. 25, 26). These ice masses were of very irregular shape and began to appear at roughly the same point where the ice wedge decreased in width, that is, at the border of the sorted area. Attempts to map the position of individual ice masses proved pointless since the outline changed continuously as the ice melted. Such an attempt was made in the north arm of the trench to illustrate the irregular form and border of the ice mass area (fig. 10), but should not be considered as a definite border. The important fact to be noted is that the ice mass area corresponds to that of the centers of fines at the surface and to the increased percentage of fines in the active layer (pp. 20—21). Conversely, where polygonal troughs are most fully developed, the ice wedges are large and the active layer contains a very low percentage of fines.

The explanation for the abrupt decrease in size of the ice wedges when entering an area of finer material is not known, but it is possible that three variables are involved: (1) the fines areas have a higher tensile strength than the coarser areas, (2) the fines areas, having a greater moisture content, will be less affected by temperature changes, i.e., will cool more slowly than coarser dryer areas, and (3) the presence of sorting may produce variations in tensile strength distribution within the sorted areas.

For comparative purposes, the principal features of pattern types 2 and 3 are presented in table II.

Table II

Comparative features of pattern types 2 and 3

	Pattern type 2 Ice wedge polygons	Pattern type 3 Centers of fines
Surface	Smooth, unsorted; patterned with network of polygonal troughs	Uneven, sorted, patterned with centers of fines in coarse washed material
Active layer	Primary depositional bedding	No primary depositional bedding
	No plugs of fine material	Plugs of fine material erupt to surface
	No vertical sorting Percentage of fines: top — 2%; middle — < 2%; bottom — < 2%	Vertical sorting Percentage of fines: top — 5%; middle — 11%; bottom — 14%
	No accumulation of fines at the permafrost table	Accumulation of fines at the permafrost table
	Siliceous calcareous evaporite on under surface of stones	No siliceous calcareous evaporite on under surface of stones
Ground ice	Well-developed ice wedges — up to 1 m wide	Few or no ice wedges — maximum of a few cm wide
	No ice masses	Ice masses

The engineering applications of the relationships discussed above are obvious and very important when considering a site for construction or a source of non-frost-susceptible building material. Determination of surface characteristics, i.e., roughness, presence or absence of sorting or ice-wedge troughs, will provide a valuable and ready key to the frost-susceptibility of the underlying active layer and to the presence and type of ground ice in the permafrost.

Area 4

Area 4 (pl. 1), selected as a control area adjoining Area 3, contained a diagonal zone in the center composed of fairly densely-grouped centers of fines separated by accumulations of clean cobbles and boulders (pl. 27).

In most of the sorted section of Area 4 and in contrast to that of Area 3, the centers of fines appeared to be the dominant feature rather than the stone stream. In much of the pattern the coarse material gave the appearance of filling in pockets or depressions in the fine material, which often graded evenly into the coarser heterogeneous material of the unsorted area without the surrounding border of cobbles and boulders (see the northeastern portion of the sorted pattern in figure 15).

A well-developed ice wedge trough cut across the eastern end of the sorted zone, where it narrowed considerably, though remaining an obvious trough. A three-pronged section of trough occurred at one side of the centers of fines and faded through distinct to indistinct cracks as the prongs approached sorted areas. The troughs of Area 4, though well-developed, were narrower and shallower than those of Area 3 and in general might be described as „fragments" of troughs since they did not join to form complete polygonal features.

Small cracks occurred commonly in the centers of fines. One distinct crack can be traced in figure 15, running from the end of the eastern ice--wedge trough, across unsorted ground and into the sorted area in the center of the figure. There it becomes indistinct and continues into the center of the sorted area.

Structure of the active layer

After being mapped, Area 4 was cut with a T-shaped trench, the stem of which connected to the drainage channel from Area 3 to provide drainage of melt water (fig. 16). This excavation cut across both sorted and unsorted surfaces and across the ice-wedge trough in the eastern part of the area. Ground ice in the permafrost was mapped within the outlines of the excavation, and profiles were constructed of the active layer along the trench walls.

A representative profile presented in figure 11, profile 4.1, shows a cross--section of the active layer ranging from undisturbed at the left, through slightly disturbed in the center, to disturbed at the right. As in Area 3, a close relationship is apparent between the structure of the active layer and the pattern formation at the surface. A thick gravel bed at the bottom of the active layer runs from left to right with a fairly level upper boundary until it nears the area of surface sorting, where it rises to the ground surface. Very shortly thereafter, where it reaches the sorted area, the gravel is underlain by an irregular body of finer material which appears to force its way through the gravel to the surface to form centers of fines.

Soil samples for grain size analysis were taken from the top, middle

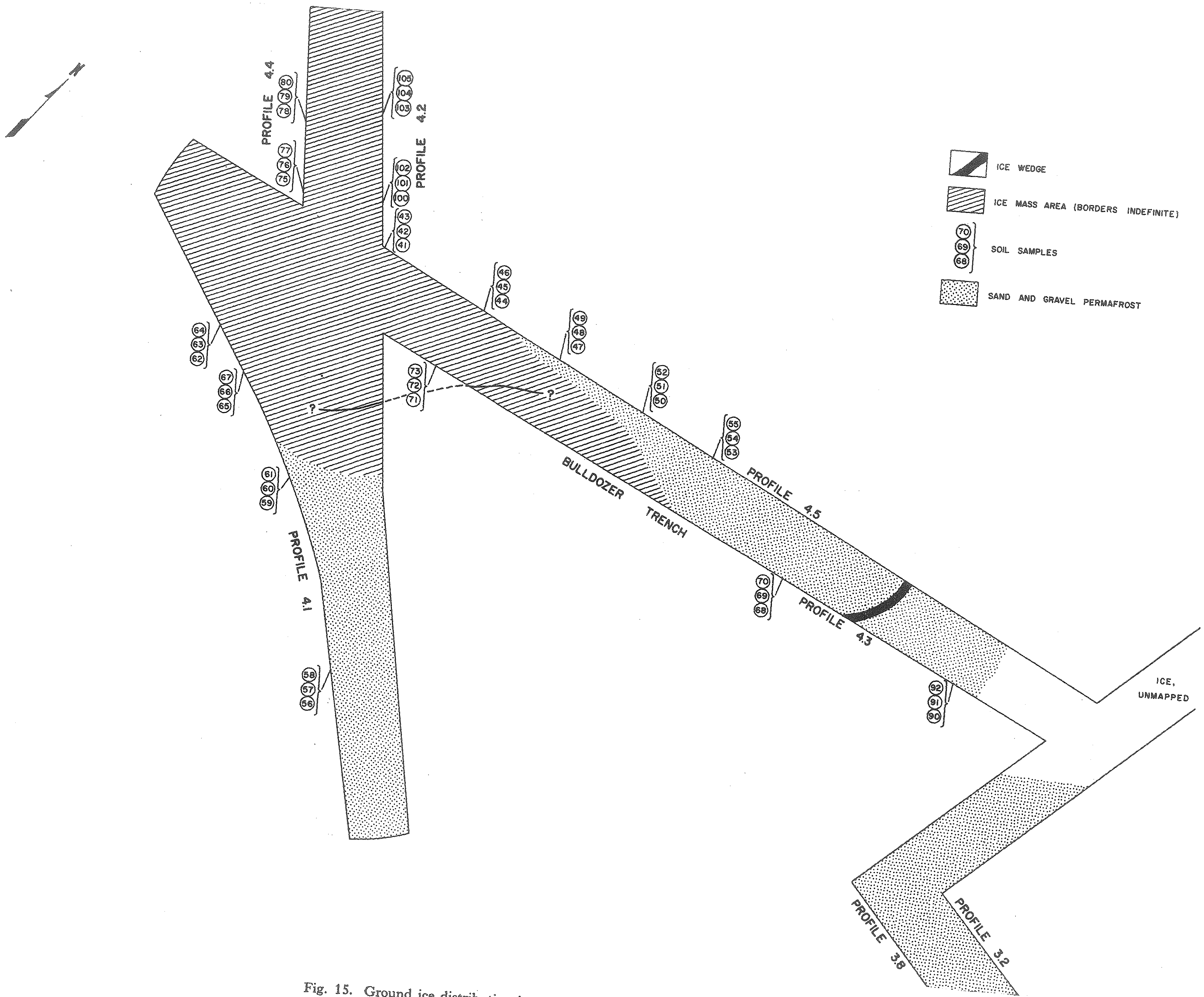

Fig. 15. Ground ice distribution in the permafrost, Area 4, Thule, Greenland

Fig. 16. Surface map of Area 4

and bottom of each type of active layer. Average grain size curves for disturbed and undisturbed active layers are presented in figure 17 (sample numbers and locations are shown in figure 16). The results are very similar to those obtained in Area 3 (fig. 12) and show clearly developed vertical sorting in the disturbed active layer beneath centers of fines where the amount of fines ranged from 3% at the top to 6% at the bottom, with curves showing a remarkably parallel gradation in all grain sizes. (Samples from the disturbed area were taken from plugs only, because the material between plugs was too coarse to allow accurate sampling).

The undisturbed active layer of the polygonal areas shows an inversion with the greatest amount of fines at the surface and the least in the middle of the active layer. With a maximum of 2% fines at the surface, the entire undisturbed active layer is considered non-frost-susceptible. An analysis was also made of samples from the intermediate or slightly disturbed active layer where traces of primary depositional features were still present, but where finer material appeared at the bottom and plugs formed but did not reach the surface (fig. 18). Vertical sorting was well developed but still incomplete in the median sand range. The percentage of fines ranged from 3,5 at the bottom to 0 at the top, thereby placing this active layer just within the frost-susceptible limits.

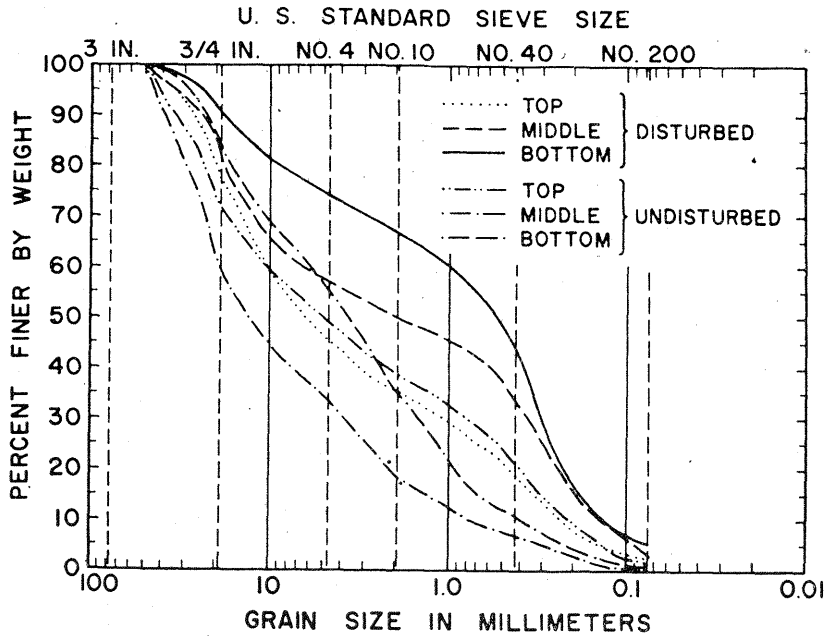

Fig. 17. Average grain size of top, middle and bottom of disturbed and undisturbed active layers, Area 4

Average grain size curves for the three types of active layer are shown in figure 19. The disturbed active layer averaged 4% fines, the slightly disturbed 2%, and the undisturbed just over 1%. The curves for the undisturbed and slightly disturbed layers show a slight inversion in grain sizes between 2 and 50 mm.

Sphericity and roundness analyses were made on particles with grain sizes ranging from 4,68 to 9,52 mm and 9,52 to 19,1 mm for comparison with the results obtained in Area 3.

The average indices obtained from this area are almost exactly the same as those from Area 3 for the same grain sizes (tabl. I, III) and indicate simultaneous deposition from the same source in both areas. The greatest variation in values occurred between the indices of roundness in the disturbed and undisturbed active layers in Area 4. This difference is only 12% of the roundness scale and is based on only one sample from the undisturbed active layer. Since both values indicate that the particles are sub-angular to sub-rounded, analysis of more samples from the undisturbed active layer is necessary before any statistical reliance can be placed on the value obtained for that type.

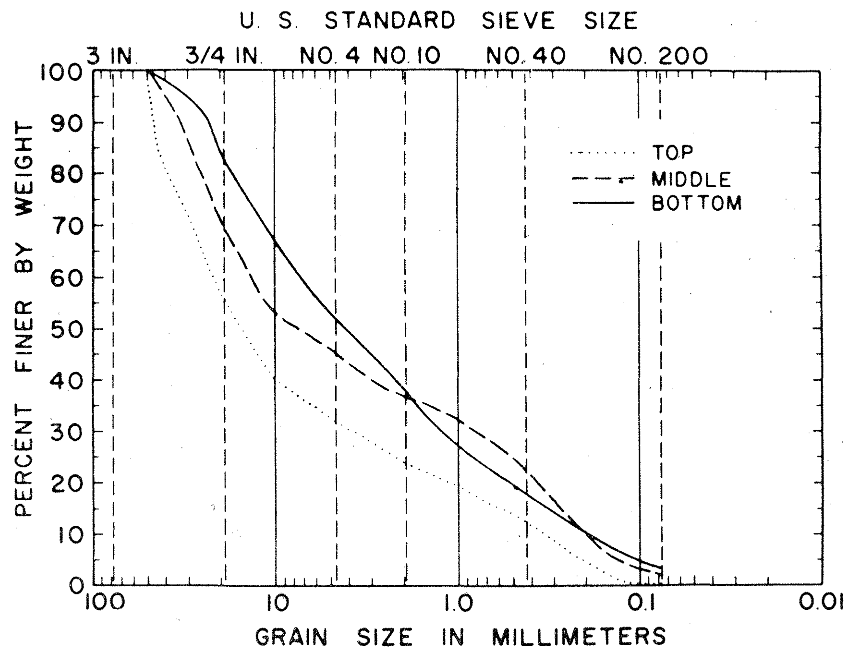

Fig. 18. Average grain size of top, middle and bottom of slightly disturbed active layer, Area 4

Table III

Indices of sphericity and roundness of disturbed and undisturbed active layers, Area 4

Pattern Type	Sample No	Sphericity				Roundness			
		Grain diameter in mm							
		4.68—9.52	Avg	9.52—19.1	Avg	4.68—9.52	Avg	9.52—19.1	Avg
	63	0.77		0.80		0.29		0.44	
3	42	0.80	0.78	0.80	0.80	0.33	0.32	0.42	0.41
(disturbed)	66	0.77		0.80		0.33		0.38	
2 (undisturbed)	57	0.78	0.78	0.81	0.81	0.44	0.44	0.49	0.49

Ground ice and its relation to surface morphology

Comparison of figures 15 and 16 shows that the relationship of type and distribution of ground ice to surface patterns is the same as that found in Area 3. A smooth unsorted surface is underlain by frozen sand and gravel without distinct ice bodies, the polygonal trough by an ice wedge, and the sorted surface by an area of ice masses whose borders conform quite closely to those of the surface pattern.

A very small wedge a few centimeters in width was found cutting through the ice masses in both sections of the trench. Although no surface crack was noted, the orientation of the wedge indicates that it might perhaps be associated with a small surface crack which appeared to stop upon reaching the sorted area. However, no conclusive relationship could be found between this wedge and a surface feature.

No ground ice samples were taken in Area 4 because of advance in the season and the consequent increased severity of the weather.

It may therefore be said, based on a comparison of observed features in Area 3 and 4, that the division of the active layer into three types, based on the amount of disturbance, is valid and that a close relationship exists between surface pattern, type of active layer, and composition of the permafrost, with all three factors apparently dependet upon the percentage of fines in the active layer.

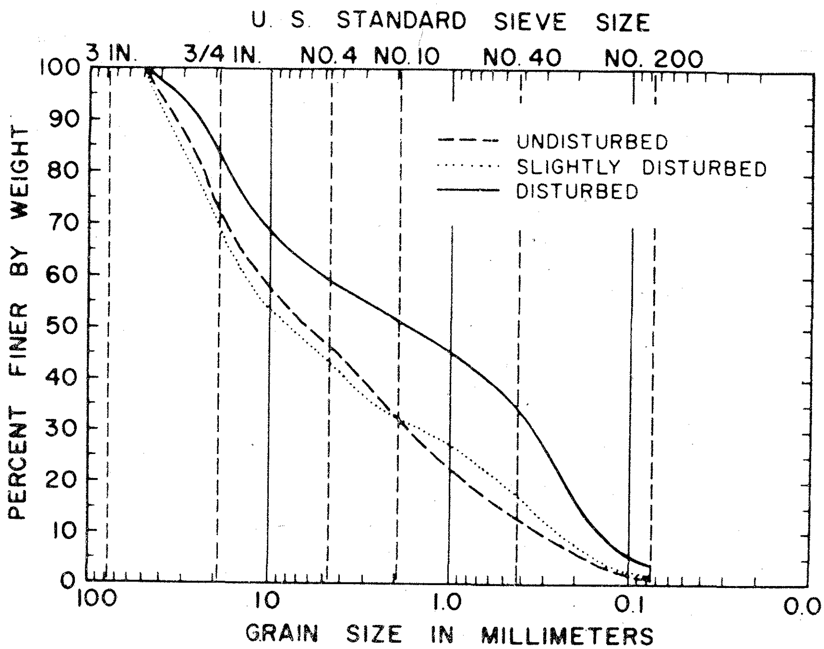

Fig. 19. Average grain size of disturbed, slightly disturbed and undisturbed active layers, Area 4

PATTERN TYPE 4: MOUNDS AND DEPRESSIONS OF LOW RELIEF IN UNSORTED OUTWASH

Area 4a

Area 4a, actually an extended portion of Area 4, was characterized by low mounds and depressions with a relief of 0,15 to 0,45 m (pl. 28). The features were quite irregular and of lower relief than those of Areas 1 and 5. In addition, the ground surface was composed of finer material, with much sand and pebbles. Because of this finer material and consequent higher moisture content, grasses and sedges were relatively more common, particularly in the depressions. No sorting was evident at the surface except for one center of fines which was rather poorly defined because of the generally fine texture of the surrounding soil.

As in sorted areas, ice-wedge troughs disappeared upon reaching the edge of this area (note the numbered troughs at the left edge of the area in plate 29). Few surface cracks occurred, the most distinct of which was an extension from the end of an ice-wedge trough which just entered the southwest side of the area.

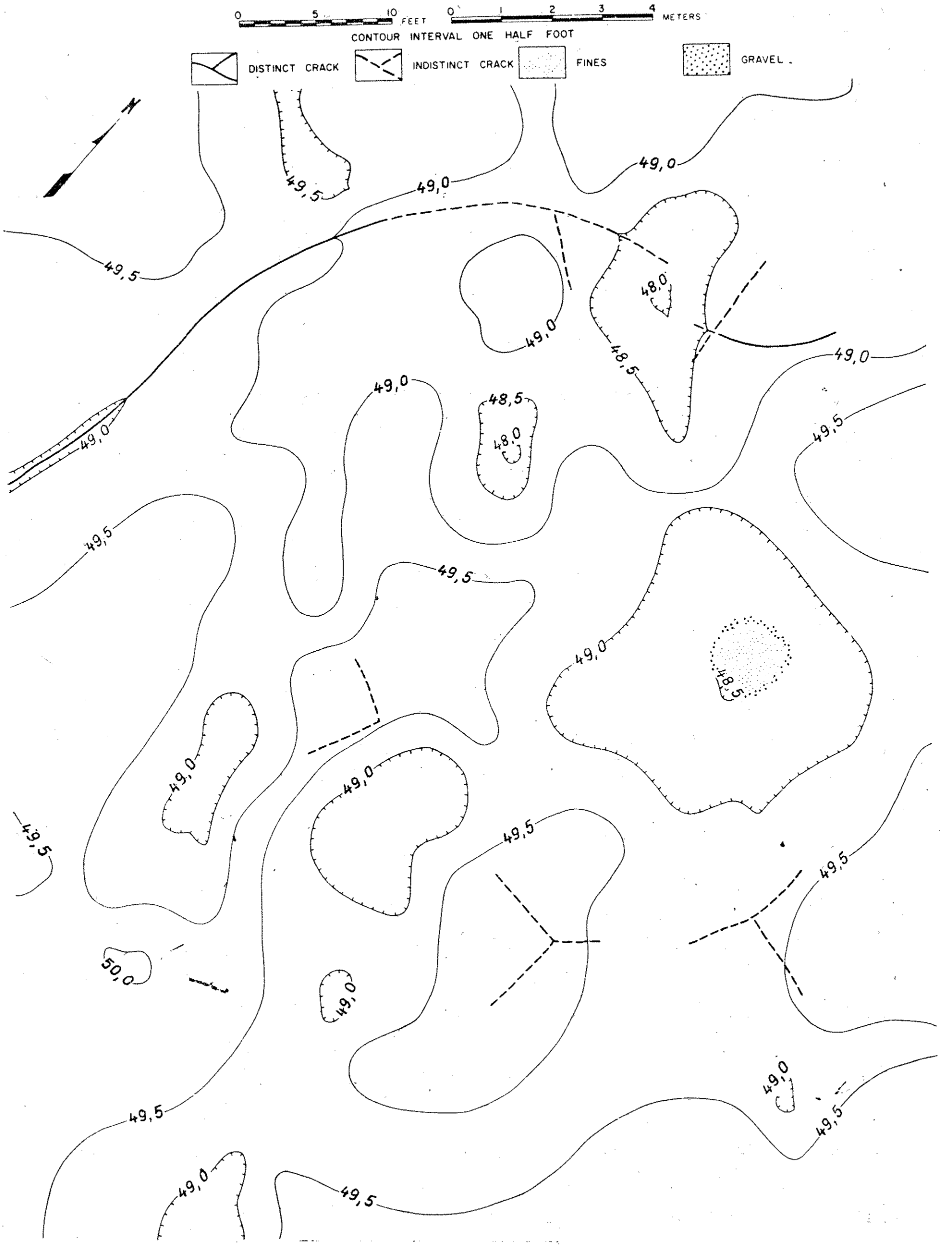

Fig. 20. Surface map of Area 4a

Because of the lateness of the season and increasingly severe weather conditions, little time could be spent on this area and a comprehensive investigation was not feasible. However, after the surface was mapped (fig. 20) the main trench from Area 4 was extended into this area (fig. 21) to provide a continuous trench and line of profiles from the polygonal trough pattern in the eastern portion of Area 4 trough the disturbed and sorted section in the center, and into the finer material of the Area 4a pattern.

Structure of the active layer

Profiles 4.4 of the west and 4.2 of the east wall of the trench are presented in fig. 11. The limits of these profiles are indicated by the locations of foil samples from the trench wall (fig. 11, 16, 21). Both profiles, but particularly 4.4, show the highly disturbed structure of this active layer. Beds were very contorted and discontinuous and plugs of fine material numerous, although as mentioned above, only one plug reached the surface.

Soil samples were taken at the top, middle and bottom levels of the active layer, both from within plugs and between them. Because of the relatively finer grain size of the active layer and the lack of large cobbles and boulders, these samples may be considered more truly representative of the entire grain size of the active layer than the samples taken in other areas.

Analysis of these samples (fig. 22) reveals a very high percentage of fines for the area. Samples from the tops of plugs averaged 5% fines, those from the middle 12% and those from the bottom 28% — by far the highest percentages found in any of the area studied. Samples from the disturbed active layer between plugs averaged 2% fines at the top, 1% in the middle, and 3% at the bottom, or roughly the same as a slightly disturbed active layer as a whole. These values give an average of 8,5% fines for Area 4a as a whole. The curves show a marked vertical sorting both within and between the plugs and also the relative accumulation of larger stones in the top and middle levels of the active layer between plugs. An appreciable lateral sorting is evident between plugs, which average almost 15% fines, and the areas between them which average a mere 2%.

Although the only plug to reach the surface did so in a depression, no specific relationship was apparent between plugs and the surface topography.

The profiles and grain size curves from Areas 4 and 4a present an interesting problem. The south-east side of Area 4 is an unsorted area

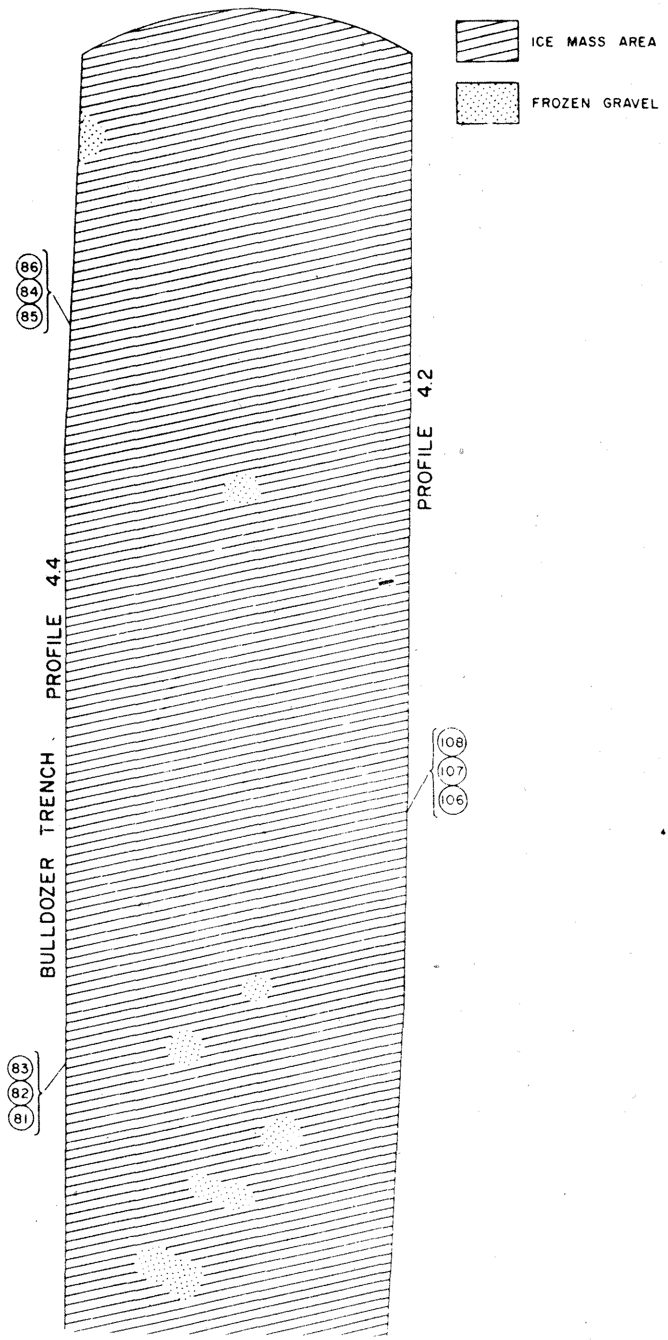

Fig. 21. Ground ice distribution in the permafrost, Area 4a

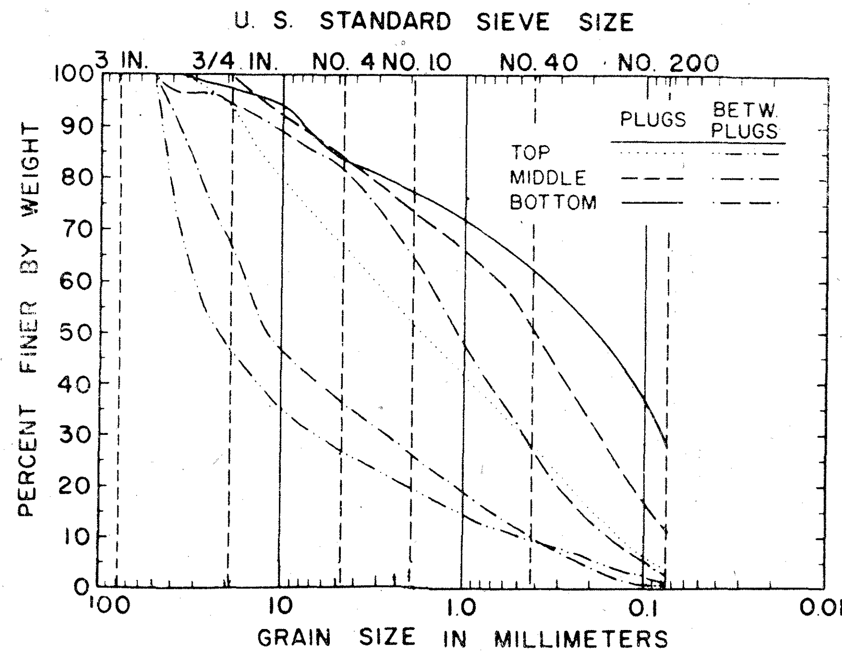

Fig. 22. Average grain size from top, middle and bottom of disturbed active layer, Area 4a
Curves for plugs represent samples 100, 101, 102, 106, 107 and 108. Curves for the areas between plugs represent samples 78 through 83 (see fig. 11, profiles 4.2 and 4.4)

with a non-frost-susceptible and therefore undisturbed active layer (less than 1% fines). The central portion is sorted at the surface and has a disturbed frost-susceptible active layer averaging 4% fines. Area 4a, on the other hand, is unsorted and has a highly disturbed frost-susceptible active layer averaging 8,5% fines.

The explanation for this seemingly ambiguous situation is uncertain, but it is possibly a matter of densities. In the sorted areas studied the soil samples had to be taken within plugs where the coarser fractions were absent. According to a theory by Jahn (1940—1946), these coarser fractions would be concentrated near the surface by washing down of the finer fractions. In this manner a density diference would be greater between the coarse material at the surface and the finer material beneath. The finer material, because of its grain size and greater pore space, would be more fluid and therefore forced upward along paths of least resistance by the overlying weight of coarse material, to be extruded at the surface as centers of fines. In Area 4a, where the plugs of fines do not generally reach the surface, the explanation is perhaps that sufficient coarse material is not available to cause extrusion of the fines at the surface. Another

Table IV

Indices of sphericity and roundness from the disturbed active layer of Area 4a

Pattern Type	Sample No	Sphericity				Roundness			
		Grain size in mm							
		4.68—9.52	Avg	9.52—19.1	Avg	4.68—9.52	Avg	9.52—19.1	Avg
4	101	0.79		0.79		0.33		0.35	
(disturbed)	104	0.80	0.80	0.81	0.80	0.36	0.36	0.38	0.38
	107	0.80		0.81		0.39		0.41	

possible explanation for the extrusion of fines, once they have been washed down to the permafrost table, lies in the difference in thermal properties between pockets of fines and the surrounding coarser material. The author has observed the extrusion of originally flat and domed layers of silt through coarse sand in laboratory experiments on saturated samples after 20 freeze—thaw cycles. This was apparently the effect of side freezing resulting from high thermal conductivity in the sample containers. In nature the side freezing effect might come through more rapid cold penetration to depth through coarse material and its lateral effect on pockets of fines. However, laboratory as well as field work is necessary to investigate these and other possibilities before definite conclusions on the mechanics of this sorting are possible.

Sphericity and roundness indices were determined for two grain sizes from three soil samples from Area 4a for comparison with the values obtained in Areas 3 and 4. As the entire active layer of this area was disturbed, it was impossible to analyze an undisturbed sample for comparison. The results of the analysis are presented in table IV.

As found in Areas 3 and 4, particles in these size ranges are sub-angular to sub-rounded, indicating a smiliar history of transportation and deposition for all three areas (compare tables I, III and IV).

Ground ice and its relation to surface morphology

For all practical considerations, the entire portion of the permafrost table exposed by the Area 4a trench was composed of ice masses (fig. 21). A few small spots of frozen sand occurred, but were unrelated to any element in the surface topography and may very well have been chance pockets within the ice masses. Although the ice masses could not be directly related to any specific surface or active layer feature, the close relationship between ice masses and a high percentage of fines in a disturbed active layer is readily apparent.

GROUND ICE STUDIES

Samples of four different types of ground ice — wedge, relict, mass, and lens — were taken, as well as samples from the contacts of different types of ice. In all, 27 samples were taken in three areas; analysis of 16 of the most representative of these is presented here.

Gross samples were numbered in the order collected from a study area, preceded by a letter to indicate the area. Therefore A-9 indicates the ninth sample taken in Area 1, C-4 the fourth taken in Area 3, etc. Thin sections and fabric diagrams were identified by the sample number followed by "V" or "H" to indicate whether cut from the vertical or horizontal plane, a second letter to show from which face of the sample it came („L" for left, „R" for right, „F" for front, „T" for top, „B" for back or bottom), and a number to indicate the number of the slide made from that face. Thus A9-HT-1-2-3 means a fabric diagram made from three thin sections from the horizontal top surface of sample A-9, and A11-VB1-2, means one made from two vertical thin section from the back surface of sample A-11. A number in parenthesis following a fabric diagram number indicates the number of grains measured in preparation of the diagram. The number labeling a thin section photograph is the actual number of the thin section made.

Fabric analysis of thin sections was done on a Rigsby stage, an adaptation of the universal stage used in petrofabric work, and plotted on a Schmidt net, an equel area stereographic projection using the lower hemisphere [3]. Thin sections were photographed under a 1 cm plastic grid for scale purposes.

The data and discussion on ground ice fabrics are considered a preliminary survey and statement of the problems, designed to serve as a general outline for use in future studies on the origin and physic of different types of ground ice.

AREA 1

Lens ice

History

The only direct reference to the fabric of an ice lens found in the literature was that made by Black (1954, pp. 487—490), who refers to such a transparent body of ice as a lens, sheet, or mass, and gives its origin

[3] A discussion and explanation of the techniques and equipment used may be found in Langway (1958).

as a frozen and buried beaver pond. In terms of general description and nomenclature, Taber (1930, 1943) and Nakaya and Magono (1944), refer to the segregated ice formed both in nature and in laboratory experiments on soil subjected to freezing under controlled conditions simply as „ice layers". Others, such as Osterberg and Fead (1955) in a review of moisture migration in soils, refer to this segregated ice as lenses. However, as is readily apparent, there is no standard nomenclature for either this type of segregated ice or any other ground ice with the exception of ice wedges.

The term *ice lens* is used for the ice discussed here because of its transparency and lenticular shape. The term *mass* is applied specifically to an amorphous body of transparent ice containing layers of filt. It is apparent, from the multitude of terms used in the literature by different authors for various types of ground ice, that an international agreement on ground ice terminology is greatly needed. A recent Russian publication [4], gives a table for genetic classification of ground ice by type, but does not really provide a nomenclature to differentiate between the various forms of ice discussed in this paper. It is the present author's opinion that more detailed work is needed on the fabrics of both natural and experimentally produced ice and the relationship of fabrics to environment before a sound basis for such a nomenclature is established.

Appearance of the ice

The ice lens found in Area 1 was about 40 cm thick at the contact with the band of relict ice and pinched out to the permafrost table at its other borders (pl. 6). It was extremely clear and transparent, although a few pebbles were suspended within it just above the bottoms of former cryoconite holes which had refrozen, trapping little streamers of silt and bubbles (pl. 7). The bed in which the lens lay was formed of cobbles and coarse gravel which appeared to be fairly well washed. A few of the cobbles were frost-shattered, with the fragments spread slightly from the center of density and suspended in the ice.

During the uncovering of the ice and the cutting of samples the ice was shielded from direct radiation by canvas tarpaulins to delay the development of internal melting (Tyndall figures). The transparency of such an ice lens is due to the lack of both internal melting figures and air bubbles.

---

[4] „Osnovy Geokriologii" (1959), p. 283.

Fabric analysis

Two samples were obtained for fabric study. Sample A-9 was cut one meter from the stone wall which separated the lens and relict ice, A-11 was cut next to, the stone wall and included a section of it. (fig. 3). The samples were about 40 by 40 cm and 30 cm thick, and both were oriented in relation to the stone wall. In A-9 the horizontal sections were cut normal to the stone wall and the vertical were oriented with the vertical plane 45° to the horizontal axis of the stone wall. In sample A-11, horizontal and vertical sections are both oriented parallel to the plane of the stone wall. In all, 41 thin sections were prepared from the two samples, althouhg only the most representative will be discussed here.

Sample A-9. Vertical and horizontal thin sections (pl. 30 and 31 respectively) prepared from sample A-9 show that grain size in an ice lens varies as a function of the presence of sand and dirt particles, ranging from a minimum of 1/4 cm^2 in the vicinity of soil particles to a maximum of 80 cm^2 in clean ice. Grain shape is irregular in both planes and no preferred grain elongation is apparent. The few Tyndall figures present in the lens ice are fairly evenly distributed. These appear as shining plates in plan view and rod-like structures in cross section (pl. 30—1). They lie with their planar surfaces normal to the *c*-axis of the crystal and therefore in the basal plane. A comparison of plates 30 and 31 with plate 47 will illustrate the scarcity of Tyndall figures in lens ice as compared with relict ice. They are caused by melting around dust and dirt particles included in the ice and therefore suggest that the lens was at one time exposed to insolation and later covered by outwash deposits. The fact that the lens was composed of very clean ice and was not exposed to radiation during the cutting of the samples explains in part the lack of Tyndall figures. The presence of some Tyndall figures, plus the cryoconites in the lens point strongly to the possibility that it was formed from a small slush pond which froze solid and was later covered by outwash.

The dark spots in the large grains in plates 30 and 31 are air bubbles trapped during the mounting of the thin sections on glass plates, and the feather-like crystals in the upper left portions of thin sections 3 and 5 are crystals formed between the thin section and the slide at the same time.

A characteristic of the lens ice samples examined was the presence of groups of grains in which the individual grains extinguished in close succession with rotations of the A_1 axis on the order of 1 to 5°, such as those in plate 31. In the fabric studies in this report each such unit is considered an individual grain which appears to have a disctinct extinction position.

Fabric diagrams of *c*-axis orientation in A-9, vertical and horizontal sections, are presented in figure 23. Diagram I represents the *c*-axis distribution in 200 grains from eight horizontal thin sections from the top plane of the sample. In these sections there is an obvious tendency for the *c*-axis to be inclined about 45° from the vertical with no truly equatorial or polar grains. Diagram II, of five vertical front thin sections, shows the *c*-axis concentrated in fairly strong isolated maxima at low angles with a minimum around the pole. Diagrams IV and V show the *c*-axis distribution in three vertical back and five vertical left sections respectively in clean ice. Strong maxima inclined 45° to the vertical occur in planes across the diagrams, with minima across the middle of the projection. For diagrams IV and V, 93 and 172 grains were measured in three and five sections respectively, indicating that each glass plate of 120 cm^2 contained between 30 and 35 grains averaging about 4 cm^2 per grain.

Diagram III (fig. 23) shows the *c*-axis orientation in a thin section cut diagonally across the upper right corner of the sample. In this part of the sample the ice contained layers of fine sand and small stones with streamers of silt. The grain size in this section is 2 cm^2, compared with an average size of 4 cm^2 in ice without soil particles. *C*-axis orientation is again characterized by isolated maxima, now occurring closer to the pole. It is possible that soil streamers cause this shift in location. The maxima are in planes approximately normal to the trace of the streamers (not shown in the diagram). Comparing the diagrams (fig. 23) it is apparent that the *c*-axes in clean lens ice lie at about 45° to the vertical, but are shifted slightly more toward the horizontal in the presence of dirt layers and streamers.

Sample A-11 was a block 30 cm square and 20 cm thick cut from the lens at the stone wall. It included part of the wall, but no relict ice. Thin sections were analyzed from all faces of the block, which was arbitrarily divided down the center in a plane parallel to the stone wall for the purpose of analyzing the influence of the wall on the crystal size and structure. Sections considered „close to" the stone wall were separated from those considered „away from" the wall by only a few centimeters and therefore any differences noted occur over a range of about 25 cm at most.

A comparison of grain sizes in the two groups of thin sections reveals a range of approximately 1/4 to 7 cm^2 in both, but a slightly higher percentage of small grains close to the stone wall and therefore a slightly smaller average grain size (pl. 32, 33). Spicules and tiny grains at the borders and along cracks in plate 32 (especially in section 3) were formed during the mounting of the thin sections.

Figure 24 shows the *c*-axis distribution in horizontal sections close to

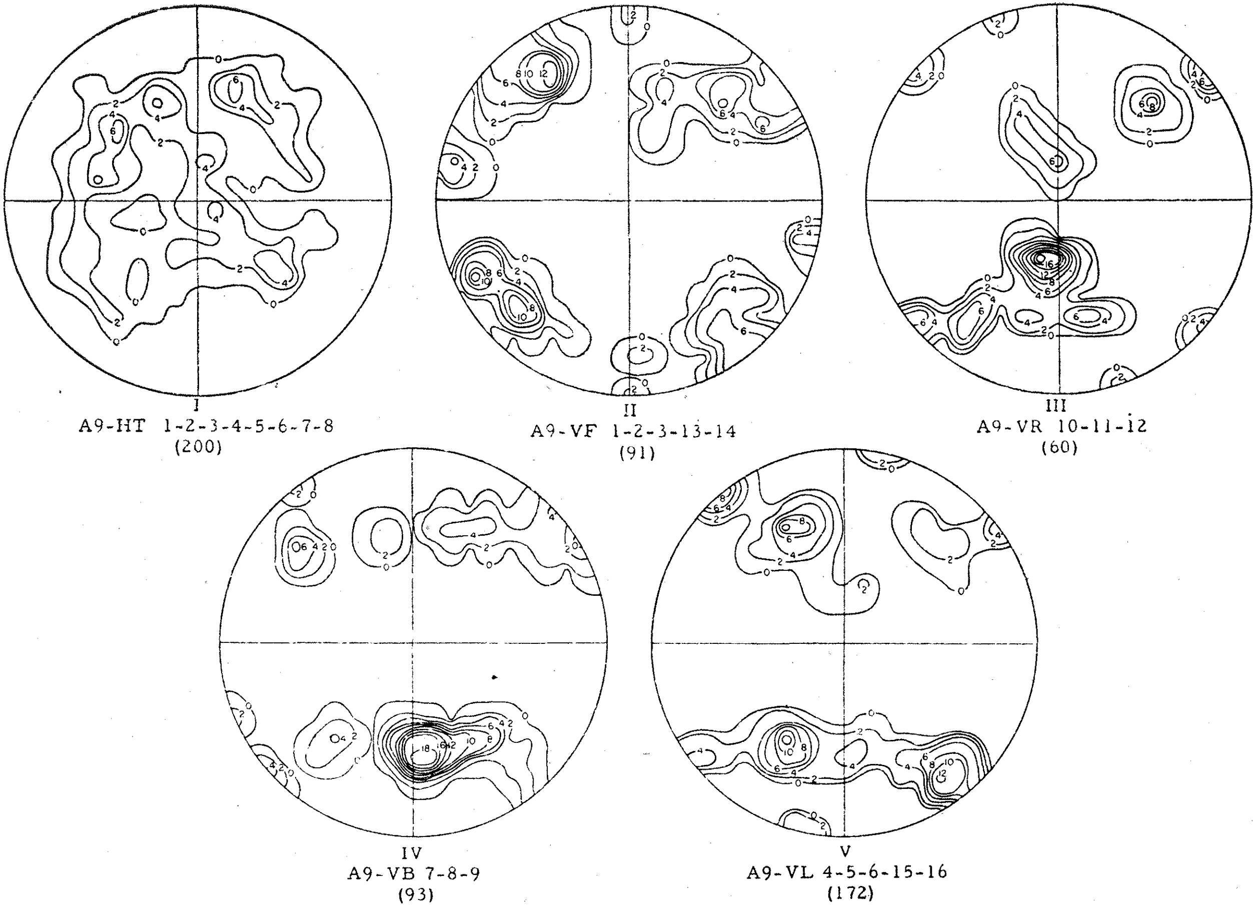

Fig. 23. Fabric diagrams, lens-ice sample A-9

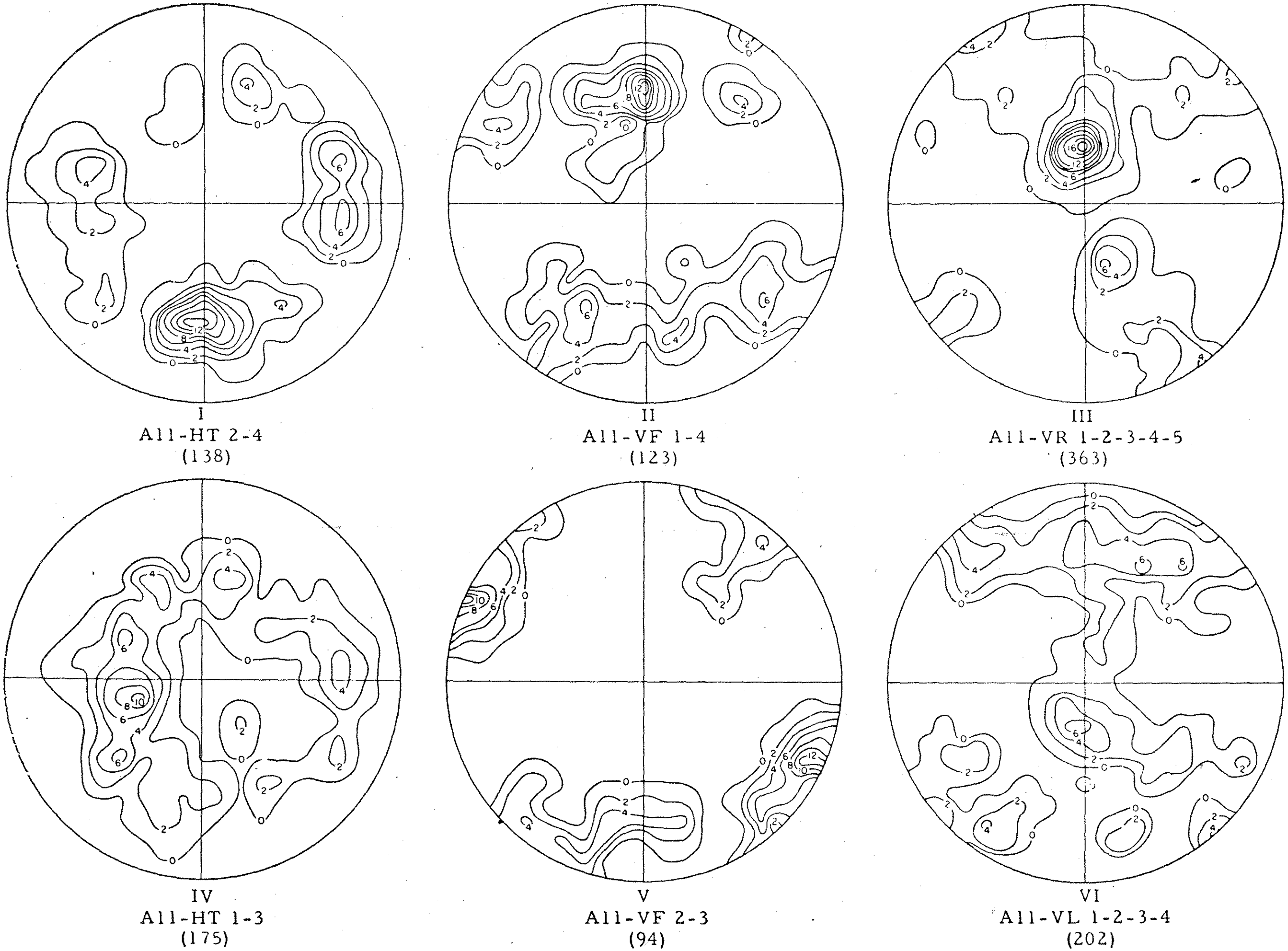

Fig. 24. Fabric diagrams, lens-ice sample A-11

I — close to stone wall; II — close to stone wall; III — close to stone wall; IV — away from stone wall; V — away from stone wall; VI — away from stone wal (diagram I) and further away (diagram IV) from the stone wall[5]. As in sample A-9, it is apparent that *c*-axes are inclined about 45° to the vertical, though variations occur in both diagrams. In diagram I there is a 12% concentration in a plane parallel to the stone wall and small maxima of 4 and 6% in a plane normal to the wall. This fact is well supported by the fabric of the front vertical sections close to the wall (fig. 24-II) which shows a maximum of 12% in a plane parallel to the stone wall, although the 4 and 6% maxima appear in planes about 40° off normall to the wall.

Further away from the stone wall a shift in position of maxima is apparent (fig. 24: diag. IV, V). In the horizontal sections, maxima of 10 and 4% lie in a plane normal to the wall and only 4% in the parallel plane. In the front vertical sections a strong maximum of 12% falls in a plane 20° off normal to the wall and a weak maximum of 4% slightly off a plane parallel to the wall.

As in sample A-9, there was a pronounced tendency toward groups of grains in which individuals tend to be extinguished upon slight rotation of the A_1 axis of the stage. Grain shape is irregular in all thin section Pl. 32, 33), but the vertical sections cut farthest from the wall show a pronounced vertical elongation not seen in the closer sections. *C*-axes are oriented approximately normal to the direction of elongation.

Vertical sections were cut from the left and right faces of the sample parallel to the stone wall and may, therofore, be analyzed respectively as „away from" and „close to" the stone wall. It is apparent from pl. 34 that the crystals close to the wall are smaller than those in the vertical section of sample A-9 cut 1 m away from the stone wall (pl. 30). The fabric diagram of five vertical thin sections cut close to the wall is presented in diagram III (fig. 24). In this diagram a 16% maximum of *c*-axis orientation occurs in a plane almost normal to the stone wall, in sharp contrast to the orientation found in the horizontal and front vertical sections. It can only be assumed that there is a strong but very local effect from the stone wall. Thin sections cut from the opposite face of the sample show a more random crystal orientation, supporting in general the pattern seen in the horizontal top and vertical front sections (fig. 24: diag. IV, V). It may be noted by comparing diagrams that there is a similarity of pattern in vertical sections from samples A-9, and A-11, in all of which the low in *c*-axis distribution occurs along the east—west axis of the projection. Horizontal sections from the bottom of A-11 show the same pattern of *c*-axis distribution seen in the top sections, except that the maxima are generally shifted further toward the horizontal.

[5] The axis of the stone wall lies parallel to the north—south axis of diagrams I, II, IV and V.

Table V is presented to facilitate comparison of the more significant features discussed above in sections cut close to the stone wall and those cut further away. *C*-axis concentration is generally stonger near the wall and is oriented in a plane roughly parallel to it except in the sections made right at the contact, where the orientation is nearly normal. On the other side of the sample the concentration is weaker and the orientation more nearly normal to the wall.

Table V

Effect of included stone wall on ice lens fabric, sample A—11

Thin section location	Plane of thin section	No of crystals measured	Crystal shape	*C*-axis orientation related to the vertical	Figure No	Concentration of orientation max. in rel. to stone wall	
						Normal	Parallel
Close to stone wall	Horizontal top	138	irreg.	50°	45, 47—I	4 & 6%	12%
	Vertical front *	123	irreg.	45°	46, 47—II	*	12%
	Vertical right	363	irreg.	65°	47—III	16 & 6%	none
Away from stone wall	Horizontal top	175	irreg. vert.	30 to 50°	45, 47—IV	10 & 4%	4%
	Vertical front	94	elong. vert.	80°	46, 47—V	+	+
	Vertical left **	202	elong.	65 & 25°	47—VI	6%	none

* 4 & 6% random distribution; + 12% max. at 20° off norm. to wall. *C*—axis norm. to gr. elong.;
** much random distribution.

Wedge ice

History

The ice wedge is the only type of ground ice hitherto studied in detail. In this country Leffingwell (1919) is considered the pioneer of the thermal contraction theory of formation. Because of contradictions brought up by Taber's laboratory experiments (1930), Black (1951, 1952, 1954) undertook extensive field work in Alaska which eventually supported the thermal contraction theory. Russian scientists have generally considered that ice wedges are produced by thermal contraction processes (Shumski 1955, p. 110—111), although Popov (1955) and Shvecov (1956) indicated that there are still conflicting opinions on genesis there also.

As may be observed in plate 5, only one large ice wedge occurred in Area 1. This entered the southeast corner of the area, cut through a band of relict ice, and branched. The smaller branch left the area directly while the main branch continued into the area for about five meters and then pinched out. Little time was spent studying the structure of the wedge itself owing to the extensive work done by others, but some effort was made to study the contact with other kinds of ground ice.

Appearance of the ice

Ice wedges may be distinguished from other kinds of ground ice by their form, bubble content, grain size, and the presence and structure of inclusions. In a plan view at the permafrost table, wedges appear as interconnected belts of ice underlying the troughs which occur at the ground surface. They range in width from a few centimeters beneath small polygonal cracks to as much as 1 meter beneath large troughs. In cross section they are generally V-shaped, although a 60 cm excavation in the wedge in Area 1 showed it to have vertical sides to that depth (pl. 35).

In general it was observed that the center of a wedge is milky in appearance owing to the inclusion of air bubbles and that it grades out to more nearly transparent with fewer air bubbles at the borders (pl. 35, 36). Parallel layers of bubbly ice and sand can be distinguished at the borders of the wedge, a typical feature of this type of ice (Shumski 1955, p. 111).

Fabric analysis

Sample A-14 was taken of pure wedge ice in Area 1 (fig. 3).

A careful examination of thin sections from A-14 revealed a fine vertical cracks, parallel to the wedge axis. A section 2 to 4 mm thick made across this crack (pl. 37) shows only large crystals 0,5 to 3 cm^2 in size. If, however, the section is thinned to 1 mm (pl. 38), fine crystals of 1 to 3 mm^2 are observed in this crack. The smaller grains are those formed recently in a thermal contraction crack, while those at each side are older grains formed by recrystallization from small ones.

The high bubble content which accounts for the milky appearance of wedge ice may be seen readily in plates 37 and 38. Although other

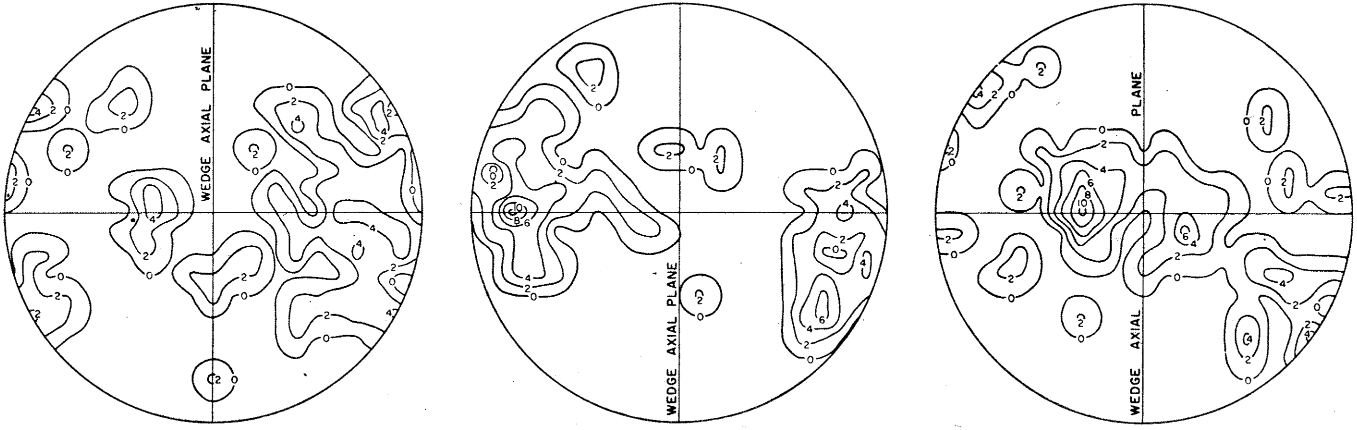

I
A14-HT
(Large grains at left)
(98)

II
A14-HT
(Small grains in center)
(92)

III
A14-HT
(Large grains at right)
(89)

Fig. 25. Fabric diagrams, ice-wedge sample A-14

I — large grains left of contraction crack; II — small grains in contraction crack; III — large grains right of contraction crack kinds of ground ice contain bubbles, wedges contain the greatest concentration and are readily identifiable by this characteristic.

Three horizontal fabric diagrams were prepared from sample A-14 in order to investigate the characteristics of the small grains and compare them to the larger grains. Diagram I (fig. 25) was made on the basis of 98 grains located to the left of the vein of fine crystals. Diagram II shows the *c*-axis distributions in 92 fine crystals from the central vein, and diagram III the fabric of 89 larger grains at the right of the vein. In the fine grains there is a strong tendency toward horizontal orientation, normal to the axial plane of the wedge. The fabric diagram of the grains in the right side of the section shows a fairly strong concentration maximum of 10% of the *c*-axes dipping toward the axial plane at an angle of about 65°. Smaller scattered maxima of 6% and 4% dip in the opposite direction (fig. 25: diag. III). The fabric of the crystals to the left of the small vein shows a less well-defined concentration dipping in the opposite direction and at a greater angle to the vertical (diagram I). Considering the number of grains on each side of the vertical axis of each diagram, diagram I shows 64% of the *c*-axes dipping toward the wedge axial plane from the left and diagram III shows 56% dipping toward the axial plane from the right. This indicates that ice wedge crystals, when first formed, are small and have a horizontal optical orientation, but, through stress-strain, a recrystallization occurs which reorients the grains at an angle to the axial plane of the wedge. It is obvious that future work on ice wedges should take this fact into consideration and that care should be taken to relate the position of the sample taken to the small crack or cracks in the center of the wedge.

Relict ice

History

No references were found in the literature regarding large bodies of ice underlying ridge-and-valley or hummocked ground surfaces, ice occurring at the permafrost table in the form of bands or belts, either interwoven or separated, or ice in any form which might be what the author terms *relict ice*. A list of periglacial forms published by the Commission on Periglacial Morphology (1952, p. 24) of the International Geographical Union omits mention of any such pattern or ice type. It would therefore appear that this is the second relationship between surface pattern, structure of the active layer, and ice in the permafrost to be described. The first was that described by Leffingwell in 1919, which dealt with ice wedges and their surface troughs.

Appearance of the ice

As seen in fiaure 3, a large proportion of the ground ice uncovered in the excawation of Area 1 consisted of bands of reliect ice. The trench made in 1956 revealed the likelihood that these bands were actually connected laterally with depth beneath pockets of frozen gravel to form a single large body of buried ice (pl. 5; fig. 6). When the entire area was excavated in 1957, care was taken to note other factors in relationship to this hypothesis.

Heat from the sun caused melting of the permafrost while the ice was being mapped, ice samples taken, and the profile made. Figure 3, therefore, represents the ice exposure within about one foot of the actual permafrost table except where the 1956 trench was made, in which location the permafrost table may have been lowered much more. However, during this period of mapping and sampling it was noticed that sections of the ice bands originally exposed as isolated sections surrounded by garvel melted down and increased the ammount of ice exposed, in some cases joining isolated sections into continuous bands. Plate 39 shows two of these sections which, upon further melting and removal of the intervening gravel, proved to be a continuous ice band wider than the original sections uncovered. It was also noticed that the surface of the relict band was convex in many cases, dipping down to the centers of frozen gravel (pl. 40).

The explanation that relict ice is actually glacial ice covered by outwash sediments and subjected to thermal erosion (p. 12, 13) is supported by the fact that the surface of the ice undulated below the permafrost table, and also by small cryoconites Jound in the ice. Plate 41 shows a linc of small stones frozen in the ice, leading to a small patch of elear ice with some included fines. These stones were apparently cryoconites which absorbed radiation and sank into tche ice until a balance in heat flow was achieved. Plate 42 shows another type of inclussion; a depression filled with concentric and conformal layers of frozen sand, apparently a primary alluvial deposit. These features would indicate that the body of ice was once exposed or very nearly exposed to the sun's radiation, and then covered by outwash deposits of sufficient thickness to insulate it.

In general, relict ice is mikly in appearance when uncovered owing to the inclusion of air bubbles and perhaps also to disturbance by the bulldozer although it is somewhat clearer than wedge ice. The presence of Tyndall figures also adds to its milky appearance. However, local variation in the form of more transparent ice was noted, ranging from slightly cloudy to almost the transparency of an ice lens. In instances where clear ice was uncovered it very soon became clouded by Tyndall figures developed as a result of radiation. The figures developed in vertical planes, giving the ice a banded appearance alternating clear and cloudy layers (pl. 43). The ice in the right foreground of plate 44 was transparent immediately after being uncovered, but became cloudy after a few moments exposure to the sun. In some sections of cloudy ice small portions of clearer ice were observed (pl. 45). Although most of the relict ice observed was milky in appearance immediately after being uncovered, it is not known whether this is the natural state or the result of radiation received through a thin insulating cover before being completely exposed, disturbance created by the bulldozer, or some other factor. It is apparent, however, that more care must be exercised in future work involving the excavation and sampling of ground ice. Suggestions are presented in Appendix C for obtaining samples of ground ice with minimum disturbance.

Fabric analysis

Sample A-1 was taken about two feet from the contact between the relict ice and the frozen gravel (fig. 3) and contained some sand and pebbles 1 to 5 cm in diameter. Crystal size of the ice averaged about 2 to 3 cm^2. Internal melting figures occurred frequently in the crystal lattice.

Horizontal top, vertical right and vertical front fabric diagrams were prepared, using 50 grains for each. The diagram of the horizontal sections shows a strong concentration of 14% in a plane perpendicular to the axial plane of the band (fig. 28). The front vertical fabric exhibited four maxima located at 90° to each other. The strongest maxima, of 14%, are about 20° off the axial plane of the band, or 20° off vertical. The other two maxima, of 10%, are oriented about 20° to the horizontal. The right vertical diagram shows a single maximum of 14% oriented about 40° to the horizontal, dipping from left to right in the diagram.

Sample A-15 was cut from a band of relict ice near the southeast corner of the area, about two meters from the contact between the band and the ice wedge (fig. 3). Two horizontal thin sections were prepared from the sample: section 1 (pl. 46—1) from the center of the band and section 2 (pl. 46—2) 15 cm closer to the border of the band. Cracks in the thin sections are the result of the mounting process. Crystal size ranged from about 0,5 to 4,0 cm^2. Thin section A15-HT-1 shows a maximum of 25% of the *c*-axes in a plane normal to the band axis and a 15% maximum parallel to it (see fabric diagram in fig. 28). Thin section 2, taken closer to the border of the band, shows maxima of 20% and 25% in a plane parallel to the band axial plane.

Samples A-18 and A-19 were taken from the ice in the wall of the trench cut in the area in 1956 (fig. 3, center), but unfortunately were not oriented. Blocks 30 by 30 cm and 20 cm deep were cut from cloudy ice and four horizontal top thin sections were made from each. Fabric diagrams were prepared for each thin section and one composite diagram for the four sections from each sample to determine the consistency of *c*-axis orientation and concentration from section to section and to determine the number of crystals necessary for a representative diagram. Grain size in all sections from both samples ranged from 0,5 to 3 cm^2 with the grains similar in shape and occurring in groups in which individuals tend reach extinction position upon very slight rotation of the A_1 axis (pl. 47—3, 4; pl. 48—1). Tyndall figures appear as shining disks or plates.

The sections from A-18 showed two orientation maxima, one normally stronger than the other with concentrations varying from section to section, but in constant position. One maximum ranged from 5 to 20% and the other from 11 to 35%, with one decreasing as the other increased. Each diagram was based upon 80 to 100 grains. The composite diagram of 375 grains (fig. 28) shows maxima of 8 and 16% in the same positions as the maxima in the individual diagrams.

Thin sections from A-19 showed a similar pattern of consistency. Although there was one maximum of 12 to 35% located in constant position, the other was less well developed, was not located in opposite positions on the diagram, showed some variation in position, and ranged from 6 to 11%. In this sample the strongest concentration remained in one position. The composite diagram of 351 grains (fig. 28) shows a maximum concentration of 20% in this position and a less well-defined maximum of 4%.

It is apparent from these two samples that *c*-axes in relict ice show definitely preferred orientation consistent from section to section, and that a fairly accurate picture of the fabric may be obtained from an analysis of from 80 to 100 grains.

Contact between ice wedge and relict ice

The contact of an ice wedge with relict ice is well-defined by the differences in appearance between the two types of ice (pl. 44), the former being much milkier or whiter because of a higher air bubble content. A detailed study was made on the contact to determine the crystal pattern at the intersection and in an effort to learn something about the relative ages of the two types of ice.

Sample A-13 was cut at the contact of the wedge and relict band in the southeastern corner of the area (fig. 3) and consisted of a rectangular block of ice 65 cm long, 30 cm wide, and 25 cm thick. Eight thin sections were prepared, four along the top axis of the block and four in lateral series from the front vertical plane so that each series included wedge, contact, and relict ice. The corresponding sections are shown through crossed polaroids in plate 49. The first two horizontal and vertical sections are shown through a single polaroid in plate 50. The wedge ice (HT-1 and VF-1) is composed of small crystals 1 mm^2 to 3 cm^2 in size, irregular in shape in horizontal section, but elongated vertically. Fine cracks in the ice are filled with small new crystals. Bubbles are numerous, particularly in the cracks containing the fine grains. Bubbly, fine-grained wedge ice continues into section HT-2 where another fine crack appears, but then gives way to relict ice with a crystal size slightly larger than that of the wedge and containing fewer air bubbles. This zone is considered the contact and is composed of a mixture of wedge and relict crystals. Relict ice crystals in section VF-2 still show vertical elongation. However, moving further away from the zone of contact into the relict ice (Sections HT-3 and 4 and VF-3 and 4; pl. 49) the number of bubbles descreaes even more while crystal size increases up to 8 cm^2 and vertical elongation disappears until typical relict ice crystals appear. The smaller relict crystals in sections HT-2 and VF-2 are considered the result of pressure from the ice wedge.

The milky appearance of the ice wedge is due primarily to the presence of air bubbles, but also to internal melting figures formed around fine dirt particles when the ice was exposed to radiation during excavation. Dirt particles occur occassionally in wedge ice without the development of Tyndall figures. Plate 51 shows dirt particles as opaque bodies located primarily at the crystal boundaries. Air bubbles are worm-like and contorted for the most part, and Tyndall figures are the geometric, primarily hexagonal plates shown here in a section normal to the *c*-axis of the crystal.

Eight fabric diagrams were prepared from sample A-13, four horizontal and four vertical, corresponding to four horizontal and four vertical thin sections (fig. 26). The first horizontal and vertical diagrams therefore present the fabric of the ice wedge, the second pair that of the contact between wedge and relict ice, and the last two pairs — the fabric of the relict ice successively farther away from the contact. Only the larger wedge crystals in the left side of sections HT-1 and VF-1 were measured (diag. I, V) to avoid the zone of contact and thereby obtain a fabric diagram representative of the wedge alone. Owing to their very strong orientation, only fifty grains were measured; *c*-axis orientation was almost vertical and about 15° from the direction of crystal elongation. Both horizontal and vertical diagrams show maxima located along the axial plane of the wedge. Ice at the contact zone (diag. II, VI) shows a strong vertical orientation, although there is a shift of the maximum into the northeast quadrant of the projection. The relict crystals close to the contact (diag. III, VII) show further inclination of the *c*-axes and a split into a strong maximum of 8% and a weaker one of 4% in the horizontal section, and a very strong maximum of 40% in the vertical sections. Still farther from the contact (IV, VIII) there is approximately the same distribution of *c*-axes, with maxima of 12 and 2% located normal to the band axial plane and at 45° to the vertical, a situation fairly typical of relict ice. There is, therefore, a shift from vertical *c*-axis orientation in a wedge to a less well developed orientation at about 45° to the vertical and normal to the band axial plane in relict ice.

Sample A-17, a block 70 cm long, 30 cm wide, and 20 cm deep, was obtained from the west wall of the 1956 trench just after its excavation, and was oriented with respect to the surface map made that year. The sample was not oriented with respect to the large ice body from which it came because the horizontal configuration of the ice was unknown at that time. Field examination revealed dense vertical streamers of bubbles in the left two-thirds of the sample and a sharp decrease in bubble content with complete lack of vertical streamers in the right third.

Five horizontal top and six vertical front thin section were prepared in the laboratory. Examination of these under crossed polaroids revealed a small vertical crack at the left end of the sample, the axis of which fell under a small crack mapped at the ground surface. This crack in the ice was filled with fine grains from 0,5 to 5 mm² in size, oriented horizontally, normal to the axial plane of the crack. Crystal size increased gradually with distance from the crack, ranging from 0,3 to 3 cm². These larger grains were oriented roughly vertically and showed grain elongation along this axis. These factors indicated that a small ice wedge was present in the sample and that the crack was a thermal contraction crack filled with new wedge crystals. The axis of this small crack was therefore selected for orientation of the thin sections and fabric diagrams for comparison with the fabric of sample A-13.

Vertical elongation of grains ceased and preferred orientation opened out to 60° where the bubble streamers ended in the righthand section of the sample. Grains became irregular in shape and had a maximum size of about 4 cm². Based upon the criteria established in sample D-13, the boundary between the wedge and relict ice would be in thin section VF-5 and between HT-4 and HT-5 where the bubble streamers stopped and grain elongation ceased. However, the boundary was not as clearly defined as it was in A-13.

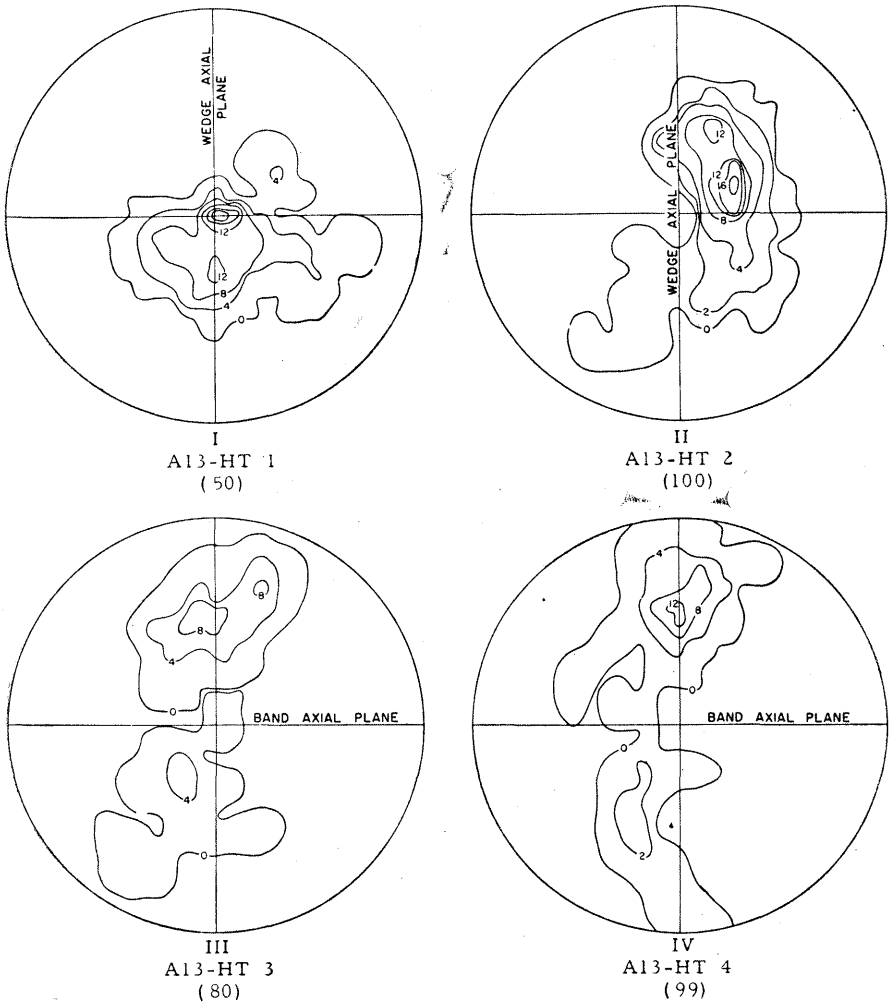

Fig. 26. Fabric diagrams of contact between
I — wedge ice; II — contact between wedge and relict
VI — contact; VII —

Microscopic examination of the young ice wedge crystals (pl. 52) revealed that air bubbles occur as worm-like structures located along crystal interfaces and elongated normal to the sides of the crack, a feature also recorded in Alaskan ice wedges by Black (1954). Fine dust and dirt particles are also concentrated along a recent crack which has now closed to form a linear series of crystal interfaces. The fact that the crack formed along crystal interfaces rather than breaking through crystals

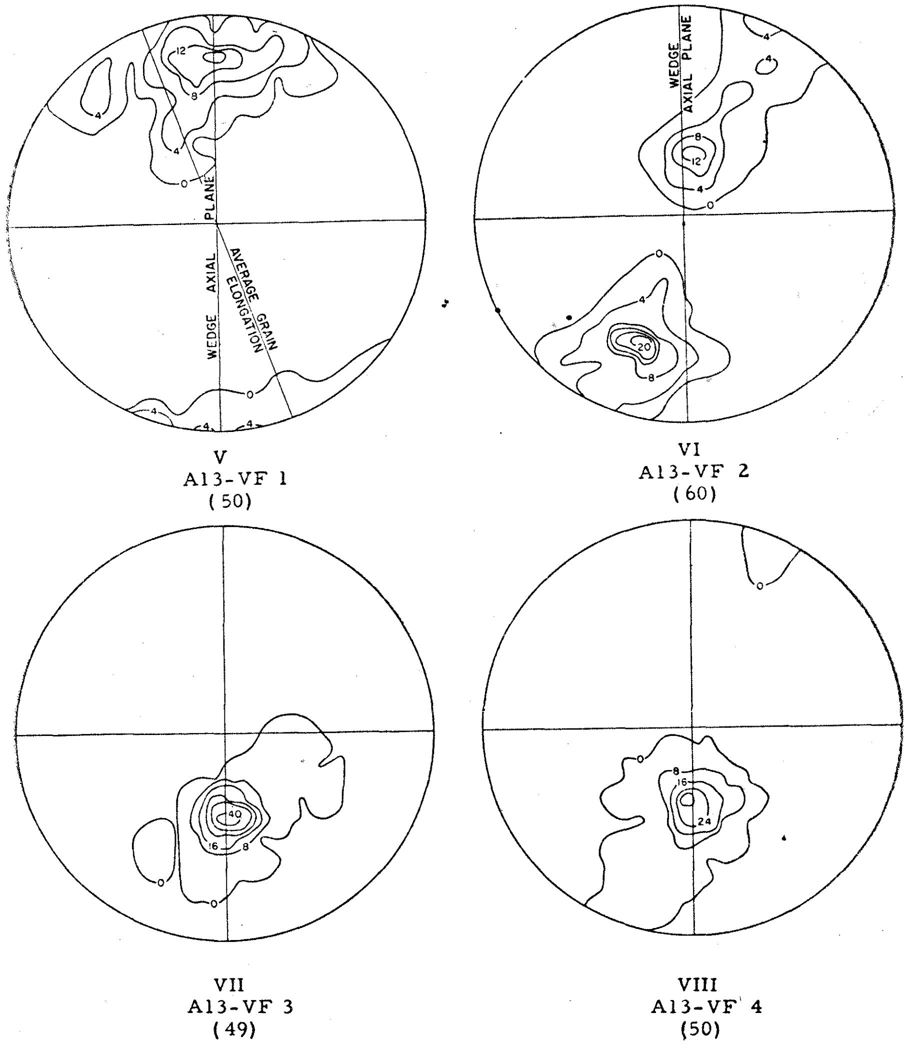

an ice wedge and relict ice, sample A-13
ice; III — relict ice; IV — relict ice; V — wedge ice;
relict ice; VIII — relict ice

indicates that it was a natural phenomenon and not the result of the mounting process and washing in of fine particles.

The dirt particles also appear to be located primarily at crystal interfaces. Numerous air bubbles formed around dirt particles during mounting of the section when dirt particles absorbed more heat and caused local melting. These bubbles appear as large transparent figures of irregular shape and the dirt particles as opaque bodies within the bubbles.

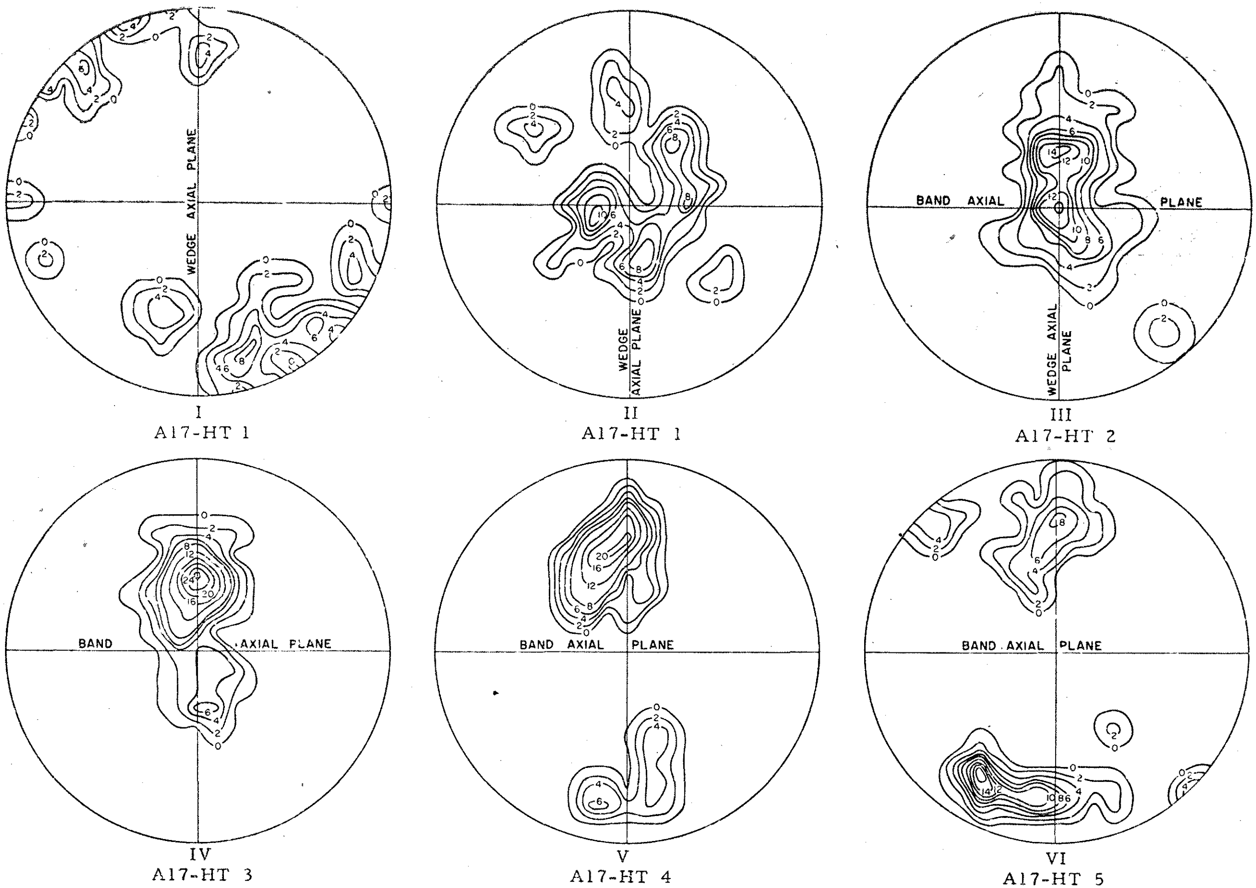

Fig. 27. Fabric diagrams of contact between an ice wedge and relict ice, sample A-17

I — wedge (young crystals, many bubbles); II — wedge (small, vertically elongated crystals); III — wedge (small, vertically elongated crystals); IV — contact; V — relict ice, still influenced by contact; VI — relict ice (few bubbles, larger crystals)

Fabric diagrams of the five horizontal top thin sections are shown in figure 27. The new and older wedge grains in thin section HT-1 were diagrammed separately to show the major change in orientation from horizontal to nearly vertical respectively (diagrams I and II). Crystals remained fairly small in both sections HT-2 and 3 and the orientation maximum increased to 14% and then 24%. Further away from the fine wedge grains the maximum decreased to 20% and then 8%, while a secondary maximum developed in the opposite hemisphere, increasing in strength from 6 to 16%. These maxima occurred in a plane normal to the axial plane of the band and moved away from the vertical to about 60° in the last thin section (diagram VI). The last diagram is considered to be of fairly pure relict ice, in which grain shape is irregular, vertical elongation is slight, and grain size has increased to 4 cm^2.

Ice sockets

In addition to the three major types of ground ice found in Area 1, a fourth kind occurred with some frequency. Sockets of clear ice were found under stones in the permafrost. After the active layer was removed these stones absorbed heat and loosened in their sockets so that they could be removed (pl. 53).

One thin section was prepared from this ice and revealed an absence of air bubbles and an average grain size of 0,5 cm^2. The number of grains in the thin section was insufficient to prepare a reliable fabric diagram.

Representative fabric diagrams of the three major ice types and of the contacts between them in Area 1 are shown in figure 28. In general it may be said that new ice wedge grains are strongly oriented in a horizontal plane roughly normal to the wedge axial plane while the older grains assume a strongly vertical orientation. Relict ice is characterized by one or two fairly strong maxima oriented 30° to 60° to the vertical and in a plane normal to the band axial plane. (The axial plane of the band was used for the vertical axis of the diagrams unless otherwise noted). Lens ice has a weaker grain orientation, roughly 45° to the vertical, with minor concentrations ringing the vertical pole and minima in both horizontal and vertical planes.

Where an ice wedge cut through a band of relict ice it reoriented the adjacent relict crystals to nearly vertical, but this effect was lost within 30 cm of the wedge.

The contact zone between relict ice and a lens was not clearly defined as in the wedge contact, but in general *c*-axis concentration was stronger near the contact and was oriented roughly parallel to it. Further away the concentration was weaker and the orientation tended to be more nearly normal to the contact. Since only one sample was studied at such a contact it is not possible to say whether these characteristics are a result of the contact itself or caused merely by the stones included in the ice at the contact.

AREA 5

Wedge ice

Fabric analysis

Sample E-1. Where the wedge entered the west side of the trench, it was about 0,5 m wide and contained many vertical bands or streamers of sand along its right side, parallel to the edge (pl. 54). A sample 30 cm long, 20 cm wide, and 40 cm deep, was taken from the ice and sand layers and included none of the relict ice in contact with the „front" face (pl. 32). (For purposes of sample orientation, the „front" of the sample was considered to be the left vertical face of the sample as seen in plate 32). Three vertical left and three horizontal top thin sections were made at 10 cm intervals and analyzed in the laboratory.

Under crossed polaroids a typical wedge structure was seen, with a vein of fine crystals in a recent thermal contraction crack along the axial plane of the wedge (pl. 55 — 1). Crystal size in this vein was a fraction of square centimeter and shape was irregular. In vertical section (pl. 55 — 2) the vein of fine grains appeared as a line of irregularly shaped grains down the center of the section. The grains on either side were larger and showed vertical elongation, dipping steeply toward the wedge axial plane. With increased distance from the vein the grains retained an irregular shape in horizontal section, but size increased to a maximum of about 3,4 cm^2 at a distance of 30 cm from the vein (pl. 56).

An enlarged portion of thin section VL-3 is shown in plate 57 and reveals Tyndall figures as rod-shaped structures normal to the plane of crystal elongation. Air bubbles appear as larger structures of irregular shape. In plan view normal to the *c*-axis (horizontal thin section) Tyndall figures appear as hexagonal or polyhedral plates (pl. 58) about 1 mm in diameter. These figures occur within the basal plane of the grain lattice and are, therefore, perpendicular to the *c*-axis [6].

Fabric diagrams (fig. 29) represent a typical ice wedge fabric of ver-

[6] An excellent reference on Tyndall figures is Nakaya's work (1956).

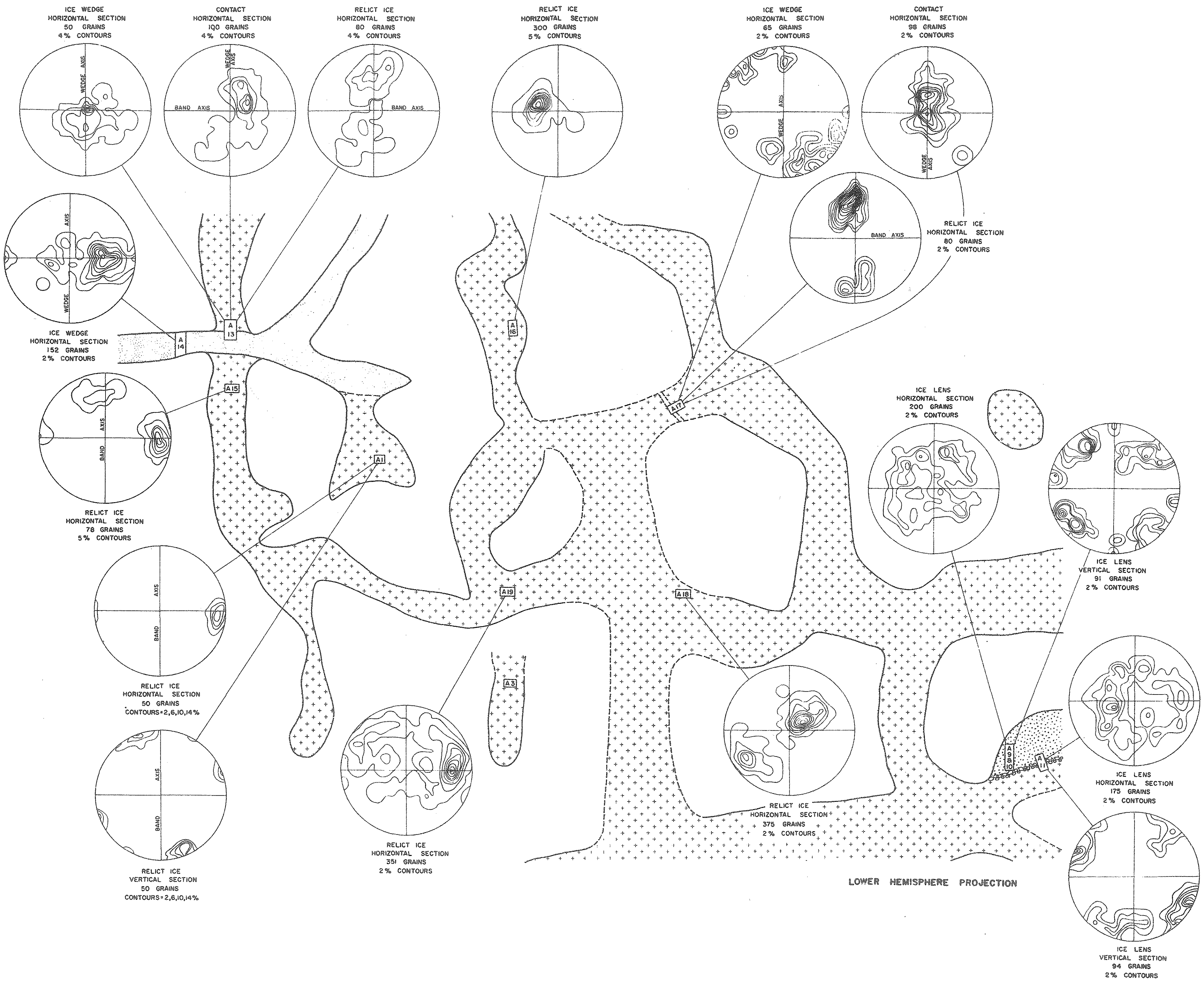

Fig. 28. Ground ice fabric, Area 1

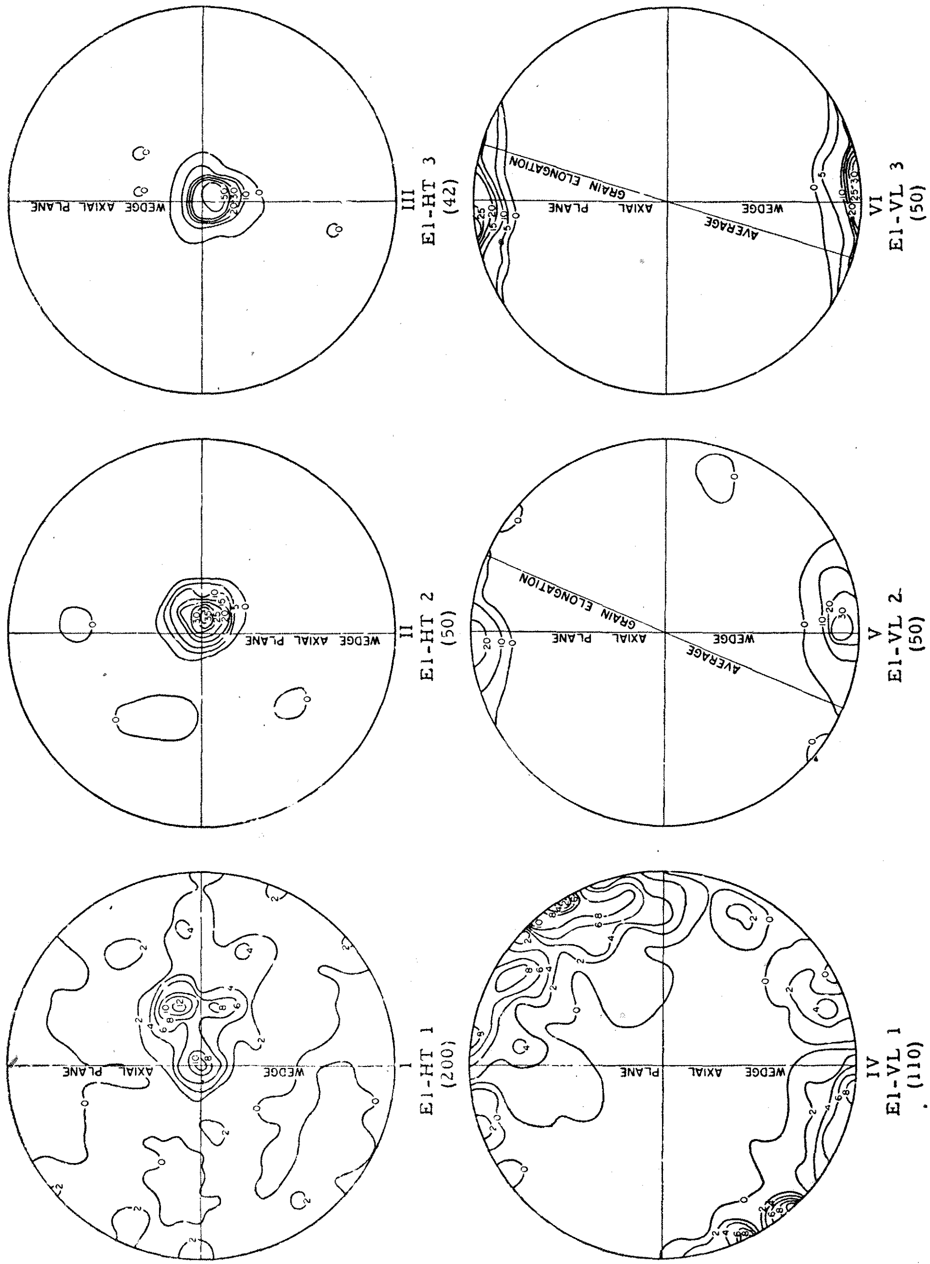

Fig. 29. Fabric diagrams of wedge ice, sample E-1

tically oriented grains except for the first horizontal diagram (diagram I), in which a small percentage of horizontally oriented grains from a recent thermal contraction crack are represented as well as the older vertically oriented grains from the left side of the crack.

From the fabric of the vertical thin sections (diagrams V, VI) it may be seen that the axis of grain elongation was roughly 25° off the plane of maximum *c*-axis concentration.

Relict ice

Fabric analysis

The relict ice uncovered in Area 5 exhibited the same characteristics as that found in Area 1: bands 1 to 2 m wide at the permafrost table and cloudy ice which was relatively clean except at the edges where the ice dipped beneath pockets of frozen sand and gravel. Some sand layers alternating with layers of relatively transparent ice occurred at the contacts between the ice bands and the pockets of gravel. A 7-ft excavation made in this band failed to reach the bottom of the ice; binding of the drill prevented deeper drilling.

Sample E-2 was cut from the center of an exposed band (fig. 8) and consisted of typical relict ice with a grain size ranging from 0,5 to 6 cm^2 (pl. 59). Grain shape was irregular. Air bubbles and Tyndall figures, though present, were much less numerous than in wedge ice.

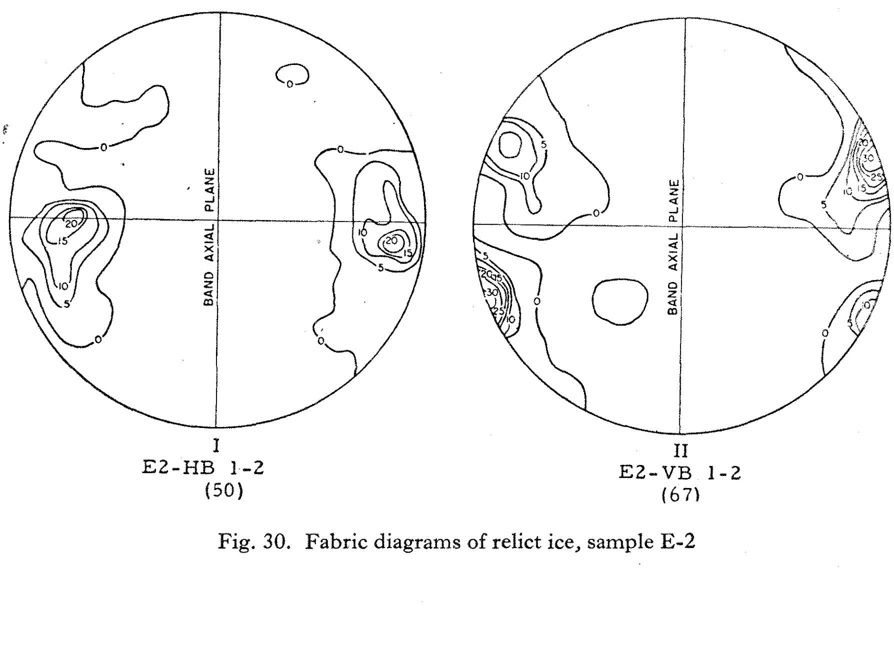

Fig. 30. Fabric diagrams of relict ice, sample E-2

The fabric diagrams (fig. 30) are typical of relict ice and show strong horizontal concentrations in a plane normal to the axial plane of the relict band.

Sample E-3 was cut from the edge of another band of relict ice, (fig. 8) and included alternating layers of sand and clear ice (pl. 60). Excavation of the sample revealed that these layers sloped down and outward from the edge of the band, apparently following the bottom contour of the gravel pocket. Crystal size ranged from 0,3 to 4 cm², and was therefore slightly smaller than in sample E-2.

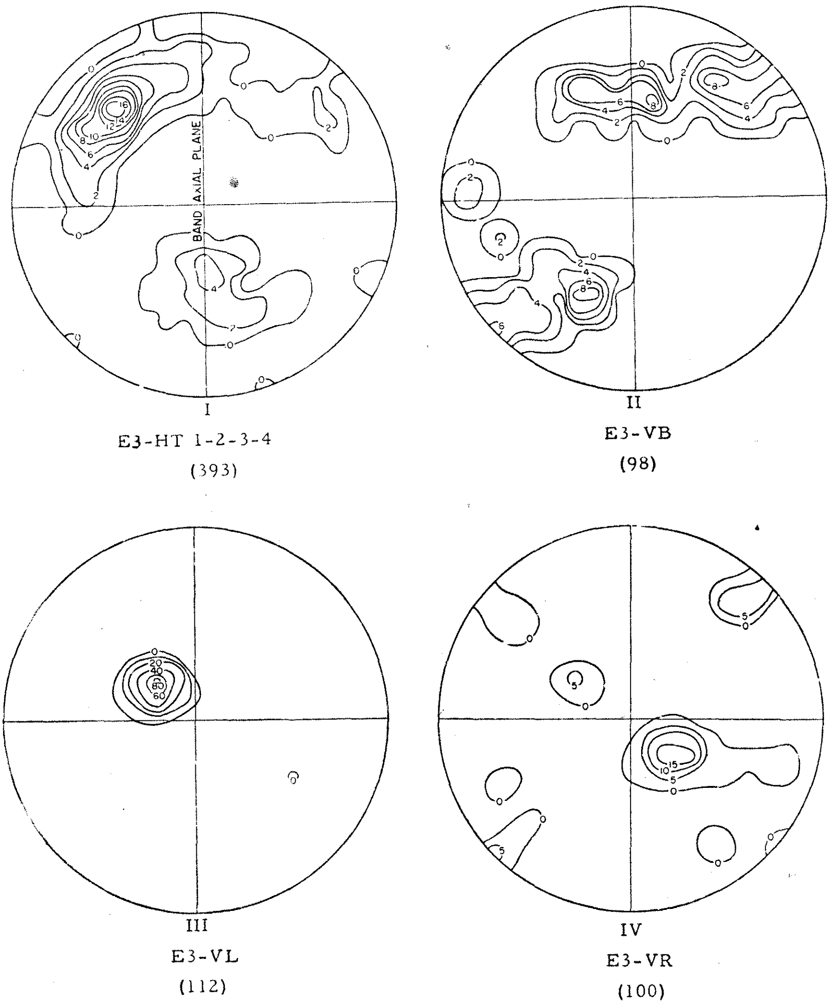

Fig. 31. Fabric diagrams of relict ice showing effect of sand layers on *c*-axis orientation, sample E-3

Fabric analysis was done to compare thin sections close to the sand layers with those 10 cm away toward the axis of the band. The individual diagrams of horizontal thin sections from the ice at the contact with sand layers showed strong concentrations of 40% and 25% of the *c*-axes in a plane oriented about 45° to the band axial plane. These concentrations were at an angle of about 30° to the horizontal. Ten centimeters farther into the band the concentrations were weaker and more random. All four horizontal top thin sections were plotted together in figure 31, diagram I. The strong concentrations in the sections close to the sand layers are apparent, but are considerably weakened by the addition of the random grains from the sections farther away. The differences in concentration are best seen in vertical sections. Diagram III (fig. 31) shows an 80% concentration of *c*-axes dipping toward the sand layers at an angle of about 20° from the horizontal. This is the strongest concentration found in any of the types of ground ice studied. On the other side of the sample, 10 cm away from the sand layers, a more random distribution is apparent, although there is still a 15% concentration in the same position as in diagram III (diagram IV, shown in superimposed position, without rotation).

AREA 3

Ice mass

History

The type of ground ice here referred to as an „ice mass" (p. 26) has been described by various authors, such as Taylor (1956), who investigated the center of fines pattern as well as those dealing with ground ice in general. Nothing has been done heretofore on the fabric and type of the ice body and its relationship to surface pattern and structure of the active layer. Some authors (Taber 1943; Nakaya and Magono 1944) have used the term *ice layers* to denote ice bodies segregated in soils by the freezing process, but this name would seem to fall short of describing some ice bodies in which there are no actual layers, but only randomly scattered mineral particles, as in plate 26. Neither would it seem to allow for the completely amorphous shape of the ice bodies referred to in this report. The term *ice mass* is therefore proposed for this type and defined as follows: An ice mass in an amorphous body of transparent bubble-free ice formed below the permafrost table, which contains varying amounts of clay, silt, fine sand, and pebbles in layers or randomly distributed.

Appearance of the ice

As noted above, ice masses are composed of transparent ice without air bubbles. The included soil particles most commonly occur in roughly parallel layers which may have any inclination or be thoroughly contorted. Plate 25 shows a cross-section of an ice mass (sample C-4) containing inclined layers of material in the upper left and lower right corners, with more randomly distributed material between. The horizontal configuration of a typical ice mass is shown in figure 32, with variations in the angle of inclination of the dirt layers indicated by dip symbols.

Fabric analysis

Two samples from the ice masses, C-3 and C-4 (fig. 10), were analyzed for basic ice mass fabric in an attempt to determine whether or not any differences exist between masses containing fine material in layers and those in which it is randomly distributed. However, C-3, which appeared to be unlayered at the surface (pl. 61), proved to have discontinuous layered inclusions oriented 0° to 20° to the horizontal when viewed from the side (pl. 62). These appeared at the top as randomly distributed pockets of soil. However, since the layers in sample C-4 were oriented at 45°, these two samples still provided a means for analysing the effect the soil layers on crystal orientation.

S a m p l e s C-3 and C-4. Crystal size to both samples was generally quite large — up to 10 cm^2 — but tiny crystals less than 1 millimeter in diameter were observed close to individual or groups of soil particles. A few of these may be distinguished in thin section 1, plate 63, but for the most part, only the larger crystal sizes are apparent there and in plate 64.

Groups of crystals with very close extinction positions were fairly common in both samples, such as the one in thin section 4 (pl. 64). This phenomenon was also noted in relict and lens ice in Area 1 and has been found by C. L a n g w a y (personal communication) in glacier ice subjected to strain.

Crystals were irregular in shape and did not appear to be influenced in this respect by proximity to dirt particles, although in one section from C-4 examined under 10x magnification showed a slight tendency for small grains to be elongated parallel to the boundaries of dirt particles.

The horizontal thin sections from C-3 showed orientation of the *c*-axes roughly 45° to the vertical (fig. 33, diagram I), with concentration minima in both vertical and horizontal planes. Concentrations were generally weak and scattered, with a maximum of 5%. The vertical right and back

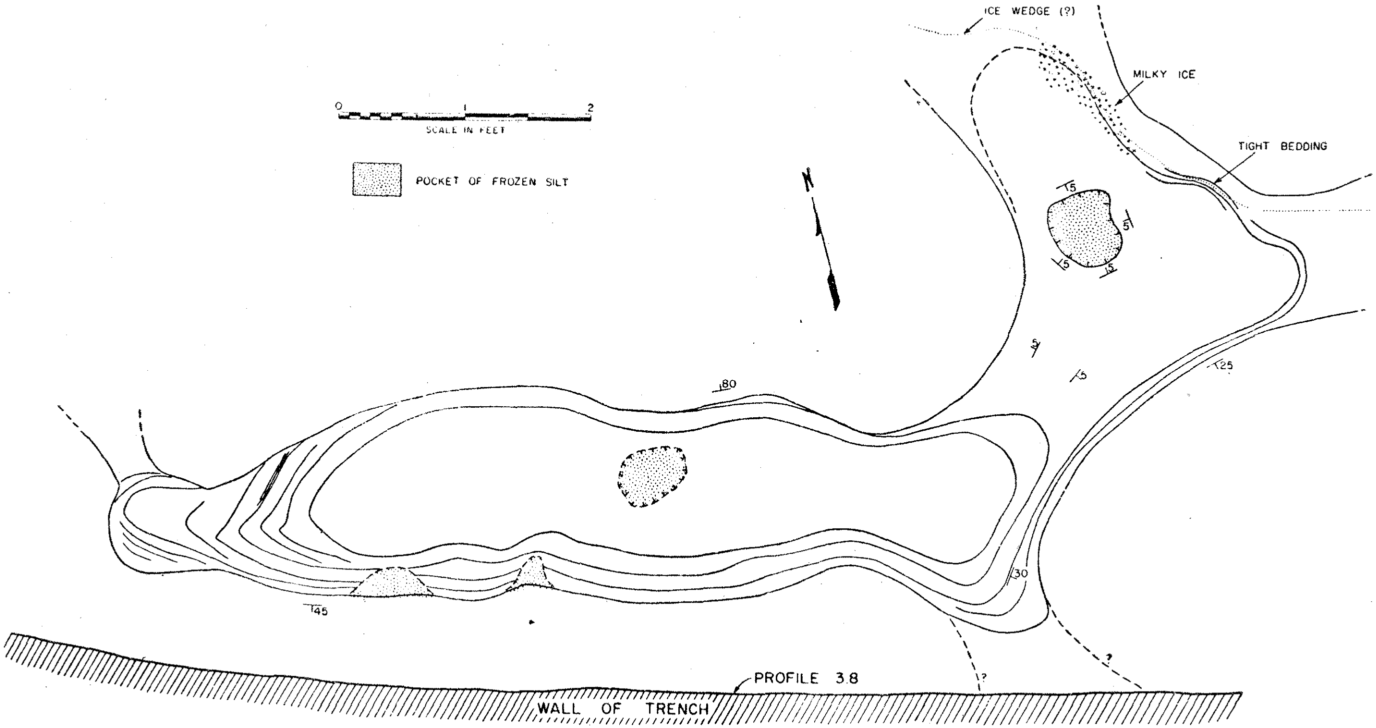

Fig. 32. Structure of layered ice mass in the permafrost, Area 3

Dip symbols show inclination of sand layers (see pl. 24)

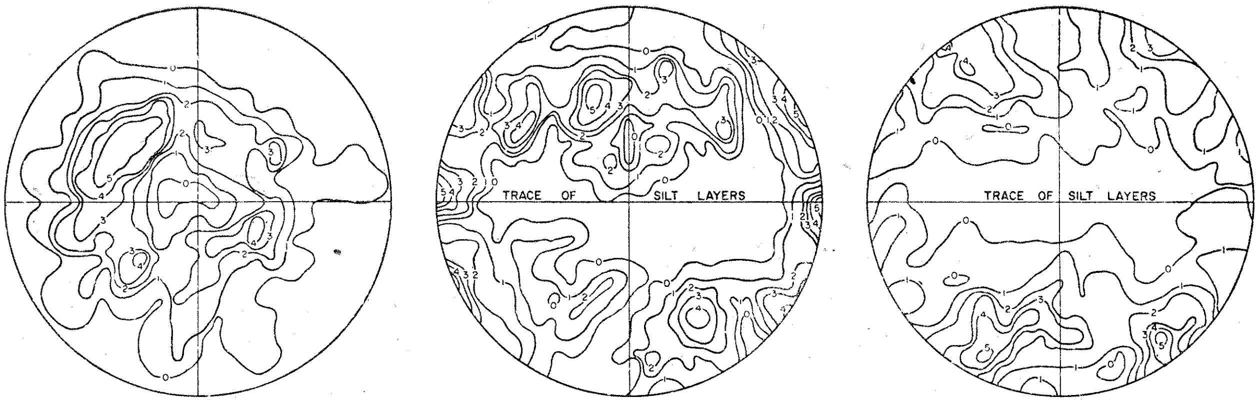

I. C3-HT 1-2-3-4-5 (200) II. C3-VR 1-2 (102) III. C3-VB 1-2 (202)

Fig. 33. Fabric diagrams of ice mass C-3 containing discontinuous layered inclusions oriented 0° to 20° to the horizontal

sections indicate this too (diagram II, III), with a linear concentration minimum in the plane of the silt layers, which, for practical purposes, was considered a straight line.

Vertical sections from C-4 were cut along two different silt layers for comparison of fabric patterns. One layer was well-defined (sections 1 and 4; pl. 63), but the other was more diffuse and particles were more randomly distributed (sections 2 and 5). Diagrams of both (II and III; fig. 34) show concentration minima oriented 45° to the trace of the silt layer, again occurring in the horizontal plane, as in C-3. This would indicate, at least in samples C-3 and C-4, that *c*-axis orientation was independent of the included silt layers.

A fabric diagram of four horizontal thin sections from C-4 (fig. 34-I) shows a tendency toward horizontal orientation with maxima scattered around the edge of the diagram. A fairly strong maximum of 10% occurs 30° from the horizontal in the southwest quadrant and another small maximum of 4% at the center. A well defined minimum arcs between the north and south poles, crossing the eastern axis at about 45°.

Comparison of this diagram with that of horizontal sections of sample C-3 shows little or no similarity. If, however, the C-4 diagram (a lower hemisphere projection) is rotated 45° on its north—south axis to depress the west side and elevate the east, a diagram very similar to that of C-3 would result. With orientation of the horizontal thin sections in the direction indicated by the arrow in plate 25, rotation of the fabric diagram would, in effect, rotate the plane of the silt layers to horizontal as it was in C-3.

The silt layers in the portion of sample C-4 remaining after the vertical sections were cut, were too dense to allow good fabric analysis. Therefore, the horizontal sections were cut in cleaner ice a bit to the side of the main silt layers and about 2 cm above the point where the other layers disappeared. Under these circumstances it would appear that the silt layers may have some effect on the ice near them.

There is, then, an apparent inconsistency between the fabrics of the horizontal and vertical sections of C-4. The horizontal fabric diagram seems to indicate some effect from the silt layers inasmuch as the fabric appears to be rotated 45°, a direct result of the 45° inclination of the silt layers. The fabrics of the vertical sections, on the other hand, present a pattern very similar to that of the vertical sections of C-3, with the exception that the trace of the silt layers occurs at an angle of 45° to the line of minimum concentration. This would, in contrast, indicate that the silt layers have little or no effect on *c*-axis orientation.

These analyses of ice mass fabrics are only a preliminary survey of

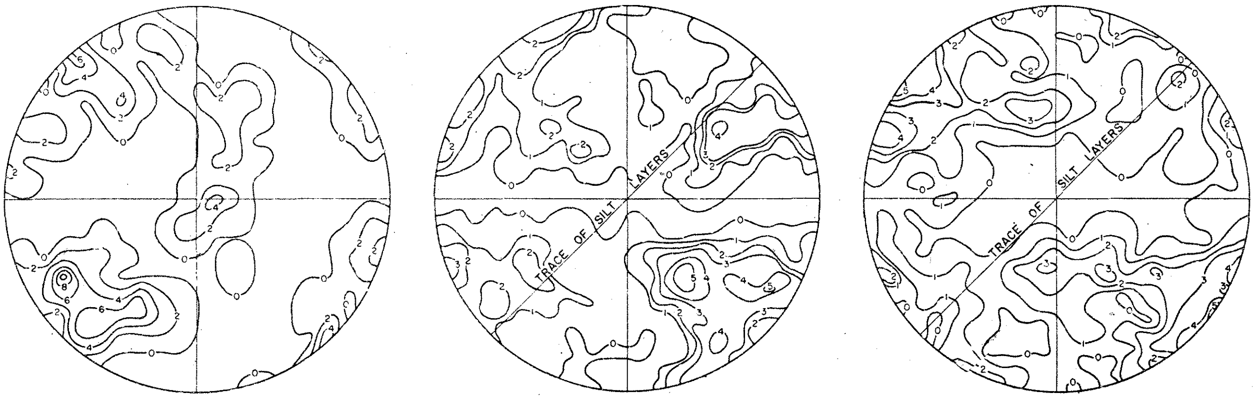

I. C4-HT 1-2-4-5 (177) II. C4-VF 2-3-5 (208) III. C4-VF 1-4-6 (194)

Fig. 34. Fabric diagrams of ice-mass C-4 containing layered inclusions of sediments oriented at an average angle of 45°

this interesting type of ice and much more work must be done in analysis of fabrics and of the stresses created by the included silt layers before the apparent inconsistency noted above can be explained or any conclusions presented on the genesis of ice masses.

Ice wedge

Fabric analysis

A fabric study of a single sample of wedge ice was made for comparison with wedge fabrics obtained in Areas 1 and 5. Sample C-1 was cut from a 3-pronged junction of ice wedges in the main trench, southwest of the junction of the trenches (fig. 10, pl. 65). A vein of clear ice occurred in the axial plane of each branch of the wedge. This was also found in samples of wedge ice studied in the other two areas, and is considered to result from recent thermal contraction cracks filled with melt water.

Separate fabric diagrams were made for the fine-grained ice and for the larger grained ice around the cracks (fig. 10). As in other wedge samples, the crack proved to be filled by small horizontal crystals with normal orientation to the axial plane of the wedge, while the larger and older grains on either side of the small vein were oriented about 20° to the vertical, dipping in toward the wedge axial plane. Only the crystals on the right side of the small vein are shown in the diagram of older crystals, represented, by the concentration in the left side of the diagram. It is of interest to note the strength of this concentration in contrast to the rather weak and random concentration found in sample A-14 from Area 1.

Contact between ice mass and wedge

Appearance of the ice

Where the ice wedge passes through the area characterized by ice masses there is almost continuous contact between these two types of ice (fig. 10). Study of the contact was deemed important as the relative age of the two types, determined through fabric studies, would prove useful to an understanding of the history and process of pattern formation.

The contact between an ice mass and a wedge is clearly defined by the different visual characteristics of the ice (pl. 66). An ice wedge is characterized by clean, dirt-free ice containing many air bubbles. These factors make wedge ice a milky white (the dirty appearance of the wedge in plate 66 is due to surface dirt from the excavation and melt water), whereas mass ice — clear, bubble-free ice containing scattered or layered silt particles — is dark and dirty.

Where silt layers occur in an ice mass close to a wedge they are generally oriented parallel to the edge of the wedge and may be vertical or dip steeply toward or away from the axial plane of the wedge. However, clear layering may be entirely absent close to the wedge, as in the mass in plate 67.

Fabric analysis

Sample C-5 (fig. 10) was cut from a wedge-mass contact and included ice of both kinds as well as the contact. Plate 68 shows the comparative features of the ice types, from the clean bubbly ice of the wedge through the more transparent ice containing scattered soil particles of the contact zone, to the clear transparent ice containing inclined layers of silt in the mass. Thin sections were prepared and analyzed from the top, back and front of the sample.

The wedge portion of the sample revealed typical elongated older crystals dipping toward the wedge axial plane at an angle of 20° to 30°. (The finer horizontal grains of new ice veins were not measured). As in other samples of wedge ice, the direction of average grain elongation varied from that of strongest *c*-axis orientation, in this case by about 25° (fig. 35—IV). Maxima of *c*-axis concentration in all the wedges studied were fairly well-defined and strong, and in this case ran as high as 20% concentration in 1% of the diagram area.

For fabric studies the ice mass crystals in this sample were divided into two groups: the larger, more equant grains located in the clean ice between silt layers, and the small (maximum grain size 0,5 cm^2), slightly elongate grains within and surrounding the silt layers. A diagram of the small grains (fig. 35—I), shows a *c*-axis orientation of 45° with maxima of 18% in a plane normal to the trace of the silt layers. This was the strongest concentration found in an ice mass.

The fabric diagram of the larger grains further away from the silt layers (fig. 35—II), and, incidentally, closer to the contact zone, shows weaker maxima of 8% in the same position, plus new secondary maxima of 6% in a plane roughly 90° to the first, or in approximately the same plane as the trace of the silt layers in the first diagram. In general this diagram shows more scattered orientation of *c*-axes than the diagram of small crystals.

In the zone of contact, the fabric diagram (fig. 35—III) shows a streng-

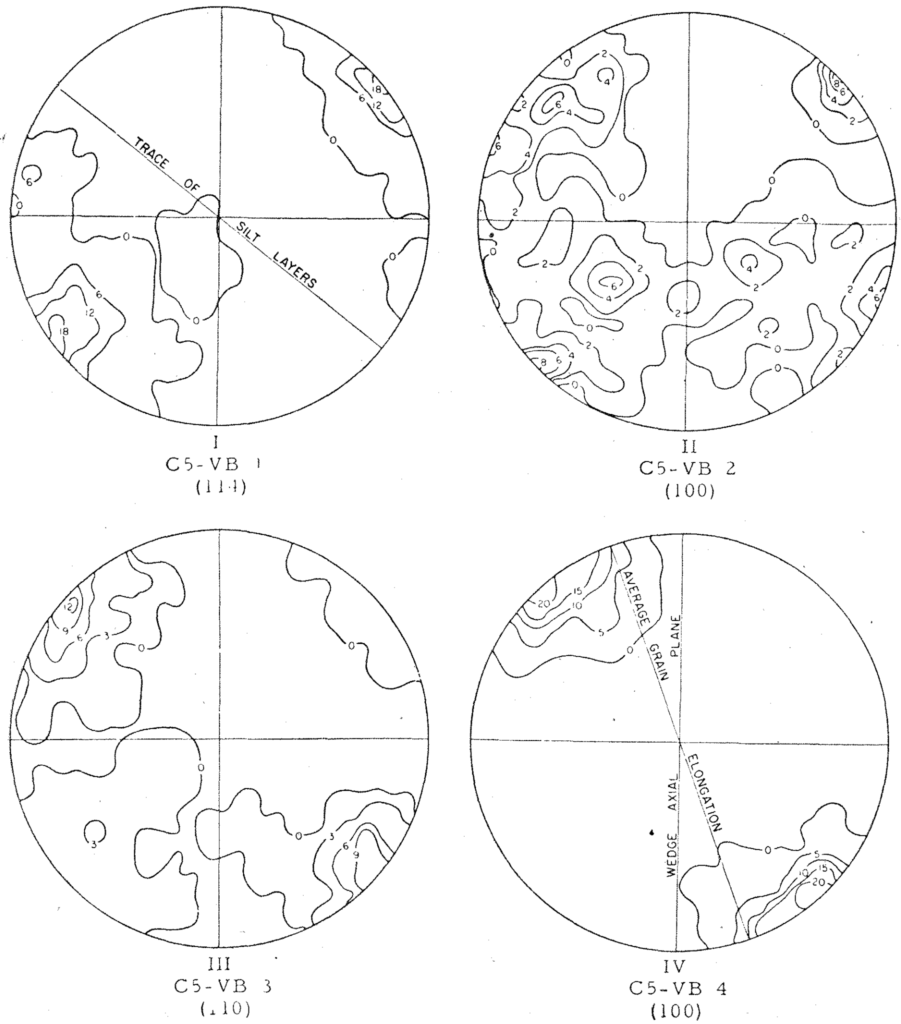

Fig. 35. Fabric diagrams of the contact between ice wedge and mass
I — mass — fine crystals along dirt layers; II — mass — large crystals away from dirt layers; III — contact; IV — wedge — large crystals

thening of the secondary maxima to 12% and a marked weakening of the first to less than 3%, except for one very small area. This diagram is very similar to that of the wedge, though it still shows a fairly strong influence from the ice mass.

Analysis of the ice-mass part of this sample would indicate that *c*-axis orientation is strongly affected by the silt layers within a relatively small area around the layers, but not to a distance of about 5 cm. Here the orientation becomes more random and, in this case, seems to be influenced by proximity to the ice wedge. The contact zone is apparently a mixture of wedge and mass crystals, or at least both ice bodies show influence on *c*-axis orientation, particularly the wedge. This relationship is very similar to that found in the contact between ice wedges and relict ice in Area 1, except that the influence of the wedge is not apparent at such a distance from its border as it was in the relict ice.

The highest concentration of *c*-axes found in an ice mass occurred in crystals near the contact with a wedge and is probably the result of stress created by growth of the wedge. These crystals, although not close to silt layers or particles, were smaller than those commonly found in clean mass ice, a condition which may also, in all probability, be ascribed to proximity to the wedge and to the stresses created by its intrusion into the mass. The development of a strongly preferred orientation close to a contact was also demonstrated in Area 5, where a maximum of 50% occurred in wedge crystals at the contact with relict ice (fig. 29, thin section E1-HT-3), and again in relict ice (fig. 31, sample E-3, VL) where a concentration of 80% occurred at its contact with sand layers. These were the highest concentrations found in any of the ground ice studied.

The problems of analyzing the fabrics of ground ice in general, and more particularly those of the contacts between different types of ice and of ice containing silt and stone particles will be greatly facilitated by laboratory experiments to determine the effects of stress and strain on determined ice fabrics at different temperatures. Rigsby (1958, p. 356) conducted laboratory experiments on polycrystalline ice from a tunnel in the edge of the Greenland Ice Cap (the ice was therefore subjected to pressure) and found that the grains tended to increase in size when kept in an annealing tank for two months. It is apparent, however, that much more work is necessary before a comprehensive analysis of the history and structural changes in ground ice can be attempted.

SUMMARY AND CONCLUSIONS

PATTERN TYPE 1: LINEAR AND CIRCULAR DEPRESSIONS IN UNSORTED OUTWASH

This pattern, described and investigated for the first time, was studied in two variant forms in Areas 1 and 5. In Area 1 the pattern was one of closely spaced, more or less circular depressions or kettles with centers spaced 6 to 10 meters apart and a local relief of about 1 meter. The surface was unsorted coarse sandy gravel with cobbles up to 20 cm in diameter.

The pattern in Area 5 was modified to form linear valleys 15 to 20 meters long, but otherwise the same description applies to both areas. Ice wedge troughs entering the two areas pinched out abruptly upon coming in contact with the pattern of depressions.

The active layer beneath this pattern was characterized by a lack of sorting at the surface and no vertical sorting of particle sizes other than the remnants of primary depositional beds. These were relatively horizontal in some instances, but often inclined and, in some cases, markedly broken and contorted. No depositional bedding was observed in Area 5, but the larger stones were oriented with their long axes conformable to the ground and ice surface contours. Fines averaged less than 1% in both the active layer and permafrost, making them not susceptible to frost heaving.

A layer of fine particles on top of the larger stones and coarser washed material beneath occurred in both the active layer and permafrost as the result of washing. A very thin layer of fines on top of the ice in the permafrost was deposited by the same process. A thin coating of siliceous calcareous evaporite on the under surface of the stones in the active layer was the result of washing and evaporation and indicates an arid or semi-arid climate during its deposition.

Removal of the active layer exposed sinuous and interwoven bands of fairly clean and bubbly ice beneath what had been elevations at the surface, and pockets of frozen sand and gravel permafrost under the depressions. Trenching the permafrost revealed that the bands extended laterally with depth to join beneath the pockets of gravel and that, therefore, the entire area was underlain by a large body of ice whose upper surface is believed to have been sculptured by thermal and aqueous erosion. This ice, apparently not discribed previously, is termed *relict ice* based on the belief that it originated as a fragment (or fragments) of glacial ice which was insulated and preserved by deposits of outwash material as the ice cap retreated. It is therefore a relict of another environment and was not formed *in situ* as ground ice.

Ice wedges entering the areas cut into the bands of relict ice but then pinched out abruptly, as did their troughs at the surface. A fine wedge found in a sample of relict ice in Area 1 appeared to be related to a small crack in the ground surface.

Fabric studies of relict ice showed it to have irregularly shaped crystals ranging in size from 0,5 to 6 cm². The ice generally contained many air bubbles and Tyndall figures which gave it a milky appearance, but in some cases it appeared relatively clear. Dirt particles and stones occurred at the edges of frozen gravel pockets and, in some cases, in cracks or slight depressions in the surface. In samples far from contact with other kinds of ice *c*-axis orientation tended to be nearly horizontal, with concentration maxima strong and oriented normal to the axial plane of the band of ice as exposed at the permafrost table.

Ice wedges were found to have fine cracks along their axes filled with very small horizontally oriented crystals. Outside these cracks the crystals were larger, elongated and reoriented so that *c*-axes and axes of elongation dipped steeply toward the axial plane of the wedge.

Relict ice crystals in the zone of contact with a wedge were generally smaller in size and showed elongation and reorientation to nearly vertical, as in older wedge crystals. Further from the contact, grain size increased, vertical elongation became less pronounced, and concentration maxima tended to become weaker and more horizontal until a typical relict ice fabric was found about 30 cm from the contact. In general, the strongest concentrations of *c*-axes, in both relict ice and ice masses, were found in the zone of contact with ice wedges.

A lens of clear transparent ice found in one corner of Area 1 appeared to be unrelated to any element of surface pattern, although airphotos indicate the possibility that the active layer in that spot contained a greater percentage of sand and exhibited no surface pattern. The ice was clean although a few frost-shattered rocks were suspended just above the bottom of the lens. Tyndall figures were relatively few and evenly distributed through the ice, and air bubbles were almost entirely absent. Crystal size ranged from 0,25 cm^2 in the vicinity of some soil particles to a maximum of 80 cm^2 in clean ice, with an average size of about 4 cm^2. *C*-axis orientation was generally inclined at about 45° and appeared to be affected locally by proximity to dirt and stone particles, although the amount of data available makes generalization of the effect liable to great inaccuracy. Although the origin of the lens is unknown, it is possible that it was formed by the freezing of a small slush pond during a later period of outwash deposition.

Many stones in the permafrost were found embedded in sockets of clean, transparent and bubble-free ice whose crystal sizes averaged about 0,5 cm^2.

Although much evidence points to the conclusion that relict ice is a buried segment of glacial ice eroded by heat and/or water-borne sediments, such a hypothesis does not appear to explain the horizontal orientation of *c*-axes into one or two maxima in a plane normal to the axial plane of the bands exposed at the permafrost table. If pressures within the permafrost were responsible, *c*-axes should be vertical as they are in ice wedges or in other types of ground ice affected by the lateral pressure of wedge growth.

Since the outwash in which this pattern of depressions was studied was almost free of fines (non-frost-susceptible), it would be interesting to investigate such glacial ice covered by materials containing a higher percentage of fines to see what type of pattern is formed.

PATTERN TYPE 2: POLYGONAL TROUGHS FORMED IN UNSORTED OUTWASH

Polygonal troughs, the best known form of arctic ground pattern, occurred in all areas studied, either in fully developed form or as fragments which ended upon contact with another pattern type. Easily recognized from the air, these polygons ranged in size from 3 to 30 m in diameter and appeared to be most fully developed in well-drained, somewhat elevated, areas.

The active layer associated with this pattern is characterized by a lack of sorting at the surface (cobbles are concentrated within the troughs, but the polygons themselves are unsorted), no vertical sorting of fines and coarse material within the active layer, more or less continuous primary depositional bedding, and an average of less than 1% fines. For descriptive and comparative purposes, an active layer with these characteristics is designated as „undisturbed". Deposition of fines on the tops and siliceous calcareous evaporite on the under surfaces of stones in the active layer, plus accumulations of coarse sand beneath them, are features of washing and evaporation.

The permafrost, composed of the same materials as the active layer, contains ice wedges beneath the surficial troughs. In the areas studied, both troughs and wedges decreased markedly in size, and in most cases pinched out entirely, upon contact with other pattern types and other kinds of ice in the permafrost. In some cases the wedge continued through the other type of ice in very decreased size until it again reached the undisturbed non-frost-susceptible active layer, where it increased to fully developed size. Where the wedge decreased to a few centimeters in width, its surface trough decreased to a small, and in some cases discontinuous, crack.

Fabric studies revealed recent thermal contraction cracks along the axial plane of the wedge filled with small horizontally oriented crystals 1 to 3 mm^2 in size. On both sides of these cracks the older wedge crystals were vertically elongated to 2 to 3 cm and had a strong vertical orientation, dipping steeply toward the wedge axial plane. A variation of about 20° was found between the directions of orientation and grain elongation in several wedge ice samples, with the direction of orientation falling on either side of the direction of elongation. The stresses involved in wedge growth are most likely horizontal and would therefore account for the growth and re-orientation of the older grains at a normal or slightly acute angle to the horizontal.

The fact that ice wedges are wider and more fully developed in coarse, non-frost-susceptible material than in fine material containing ice masses belies the physical principle suggested by Black (1951) that an increase in the coefficient of expansion is to be expected when there is an increase in the ice content of the soil. This apparent contradiction and the disappearance of ice wedges in areas of fines may perhaps be explained in terms of a higher tensile strength in soils containing fines and of the rate of temperature change which causes thermal contraction. Temperature changes would be slower in an area of fines because the soil would hold more moisture than a coarser area. Unequal distribution of stresses because of the presence of pockets of coarse material may also be a factor in a sorted active layer.

PATTERN TYPE 3: SORTED CIRCLES OR CENTERS OF FINES

Sorted circles are most obvious and commonly found in slightly depressed areas where the surface is otherwise composed of washed cobbles and boulders. The centers may be isolated or closely spaced, a few centimeters up to 4 meters in diameter, and the surfaces raised, level, or depressed.

The center of fines is caused by plugs of fine material within the active layer which break through to the surface. The active layer in such areas is vertically sorted as a result of washing, grading from coarse at the top to fine at the bottom. Fines are deposited on top of stones and on the permafrost table, and washed out from beneath the larger stones to leave an accumulation of coarse sand and gravel. No evaporite deposits were found on the underside of stones, an indication of the moisture-retaining quality of an active layer rich in fines.

Only fragmentary sedimentary bedding was found, the layers broken, inclined, and contorted. Plugs averaging 4% fines contained fragmentary and contorted sand and silt beds. In light of the above characteristics, this frost-susceptible active layer is described as ,,disturbed''.

Roundness and sphericity indices determined for soil samples of two different grain sizes from both the undisturbed and disturbed active layer of pattern type 2 and the disturbed active layer of pattern type 3 indicate that the materials of both kinds of active layer were derived from a common source and have a common history of transportation and deposition.

The permafrost beneath centers of fines is characterized by more or less continuous amorphous ice masses containing symmetrical or contorted layers of fines. Ice wedges, if present, are considerably reduced in size.

Mass ice is transparent and large-grained, with crystals up to 10 cm^2 in size where unaffected by silt layers. Fine crystals of a fraction of a square millimeter occur between sand and silt grains and along dirt layers, a direct and local effect of the dirt inclusions. Grain shape is irregular in general, but tends to be slightly elongate along silt bands at the contact with an ice wedge.

C-axes tend to be oriented at angles of 25 to 45° to the vertical, with a slight concentration in a plane normal to the trace of the silt layers as seen in a diagram of vertical thin sections. One fabric diagram did show a horizontal concentration in the same plane as the trace, but this was not found in other diagrams. Vertical diagrams show a concentration minimum in the horizontal plane regardless of the orientation of the silt layers, but analysis of more thin sections is necessary before it is safe to make generalizations concerning the relationship between *c*-axis orientation and the orientation of silt layers.

At the contact between an ice mass and a wedge, mass grains are smaller in size with a strongly preferred orientation parallel to wedge crystal *c*-axes, apparently a direct result of the intrusion of the younger ice wedge. Within 10 cm of the contact, however, its influence is lost and a typical mass fabric is found.

The formation of centers of fines is possibly the result of down-washing of fines through the active layer, concentration at the permafrost table and then extrusion caused by differences in density and/or thermal properties between the coarse material at the surface and the fines beneath. Laboratory experiments are necessary, however, before any definite conclusions can be drawn. Sorted circles have been produced in experiments conducted by the author in a layer of gravel of varying thickness overlying an ice sheet (Corte 1959). In this case the sandy gravel was non-frost-susceptible and sorting was produced mechanically by differential melting of the ice and collapse of the gravel layer. Although somewhat similar patterns were formed, mechanical sorting would seem to play a minor part, if any, in the formation of centers of fines produced in a frost-susceptible active layer where vertical sorting, a difference in thermal properties and/or specific gravity, and frost-heaving apparently play the significant roles. Recently Corte (1961) have demonstrated horizontal and vertical sorting by changing the orientation of the freezing plane.

The transition zone between pattern types 2 and 3 exhibits characteristics of both disturbed and undisturbed active layers. Sedimentary beds are inclined or slightly disturbed, the surface is somewhat rough and uneven

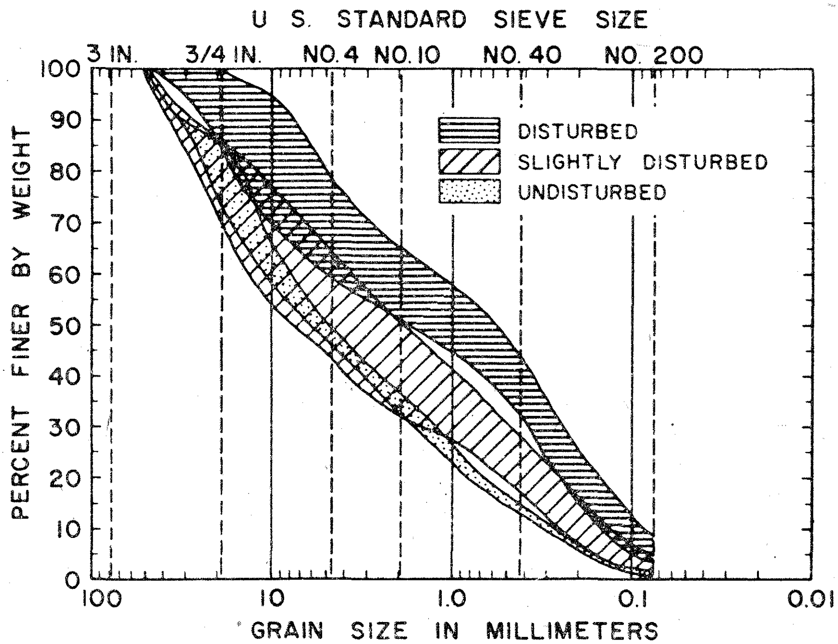

Fig. 36. Grain size range of disturbed, slightly disturbed and undisturbed active layers of Area 3 and 4

Curves for the disturbed type are based upon analysis of plugs only

although unsorted, the percentage of fines in the active layer varies from 2 to 5%, and scattered ice masses occur in the permafrost. Vertical sorting is evident but usually incomplete, and plugs of fines begin to appear in the active layer but do not reach the surface.

Plotting average grain size curves for the three types of active layers analyzed in Areas 3 and 4 provides the range of grain sizes for each type (fig. 36). The finer limit of each range occurred in Area 3 and the coarser in Area 4. Although there is some over-lapping of ranges in the coarser fractions, particularly in the undisturbed and slightly disturbed active layers, the separation is almost complete in the fractions finer than medium sand (no. 10 sieve size). It is apparent from figure 36 that disturbance due to frost action may begin to appear in an active layer averaging only 2% fines. Recent studies by other researchers have also pointed out the advisability of lowering the frost-susceptibility limit under certain conditions to less than 2% of the fraction finer than 0,02 mm (Dücker 1958).

PATTERN TYPE 4: MOUNDS AND DEPRESSIONS OF LOW RELIEF IN FINE-GRAINED UNSORTED OUTWASH

Although the surface was unsorted in this pattern, vertical sorting was well-developed, both within plugs and between them, runnig as high as 28% fines at the bottom of plugs and 5% at the top. The active layer was highly distrubed, with traces of depositional beds present only between plugs where soil material averaged only 2% fines. Where the percentage of fines was higher, as in plugs, these beds were obliterated.

The permafrost beneath this pattern was composed almost entirely of ice masses, with just a few small isolated pockets of frozen sand and gravel. A layer of fines occurred regularly on top of the ice masses.

No relationship was apparent between features of either the active layer or the permafrost and the surface pattern of low mounds and depressions. The one plug of fines which reached the surface did so in a depression, but others reaching to just beneath the surface showed no relationship to surface features. Inasmuch as the active layer was disturbed and vertically sorted to the surface by frost action and washing, the surface pattern must also be considered the result of frost action. Failure of the surface

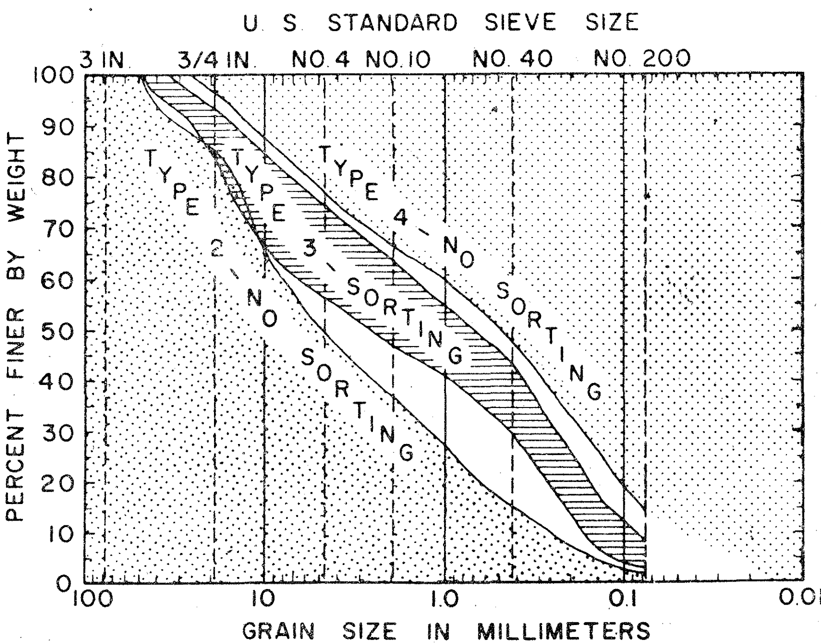

Fig. 37. Sorting in outwash as a function of grain size, based upon studies near Thule, Greenland. Presumably further studies would result in more clearly defined borders between sorting and no sorting in the finer grain sizes

Table VI

Comparative features of four pattern types

	Pattern Type 1	Pattern Type 2	Pattern Type 3	Pattern Type 4
Surface	Unsorted; patterned with network of circular or linear depressions up to 1 m deep	Smooth, unsorted, patterned with network of polygonal troughs	Uneven, sorted, patterned with centers of fines in coarse washed material	Largely unsorted. Few large cobbles or boulders. Pattern of low irregular mounds and depressions with relief of up to 30 cm
Active layer	Primary depositional bedding	Primary depositional bedding	No primary depositional bedding	No primary depositional bedding
	No plugs of fine material	No plugs of fine material	Plugs of fine material errupt to surface	Plugs of fine material. Do not generally reach the surface
	No vertical sorting Percent of fines: top — < 2%; mid. — < 2%; bot. — < 2%	No vertical sorting Percent of fines: top — 2%; mid. — < 2%; bot. — < 2%	Vertical sorting Percent of fines: top — 5%; mid. — 11%; bot. — 14%	Vertical sorting Percent of fines: Plugs: top — 5%; mid. — 12%; bot. — 28% Between plugs: top — 2%; mid. — 1%; bot. — 3%
	Very slight accum. of fines at permafrost table	No accum. of fines at permafrost	Accum. of fines at permafrost table	Large accum. of fines at permafrost table
	Siliceous calcareous evaporite on under surface of stones	Siliceous calcareous evaporite on under surface of stones	No siliceous calcareous evaporite on under surface of stones	No siliceous calcareous evaporite on under surface of stones
Ground ice	Wedges usually pinch out upon contact with relict ice	Well-developed ice wedges — up to 1 m wide	Few or no ice wedges — maximum of a few cm wide	Few or no wedges (none observed) — pinch out upon contact with masses
	No ice masses	No ice masses	Ice masses	Dense conc. of ice masses
	Relict ice	No relict ice	No relict ice	No relict ice

Table VII

Comparative features of four types of ground ice

	Relict ice	Ice wedge	Ice mass	Ice lens
Gross shape	Large continuous body, surface sculptured into circular or linear depressions	V-shaped bands, usually connected to form polygons. Wedges up to 1 meter wide	Amorphous. May be continuous or isolated. Size variable	Lenticular in horizontal plane
Bubble content	Variable, usually fairly high	High	None	None
Crystal size	0.5 to 6 cm^2	Young crystals 1 to 3 mm^2 Old crystals 0.5 to 3 cm^2	Up to 10 cm^2 in clean ice, less than 1 mm^2 around dirt particles	0,25 cm^2 close to dirt particles, up to 80 cm^2 in clean ice
Crystal shape	Irregular	Elongate	Irregular	Irregular
Inclusions	Dust; some silt and sand or pebbles at permafrost table	None except at sides of wedge	Silt, sand and pebbles in layers or randomly distributed	Some silt streamers and frost--shattered cobbles near base of lens, but generally very clean
Fabric *	*C*-axes approx. 45° to the vertical in a plane normal to the axial plane of the band as exposed at the permafrost table. One or two maxima with concentrations up to 25%	Young crystals in recent thermal contraction cracks are oriented horizontally and older crystals at each side are oriented near to the vertical, dipping steeply toward the axial plane of the wedge	Relatively weak concentrations of *c*-axes showing random orientation. Commonly a minimum in the horizontal plane	*C*-axes oriented at roughly 45° to the vertical with minima in the polar and equatorial planes. Concentrations may be numerous and scattered although one is usually stronger than the others and may be up to 18%

* General fabric pattern of the individual ice type is given. In contact with another type of ground ice the fabric may be affected greatly, as may also the crystal size and shape. Dirt inclusions may also affect crystal size, shape and orientation.

to develop sorting is possibly a result of the lack of great differences in density or thermal properties between the upper and lower portions of the active layer. As the boulder and large cobble fractions were absent from this area the large density or thermoł difference possible in Areas 3 and 4 could not develop and therefore could not cause extrusion of plugs of fines at the surface. Since only the material in the plugs was subject to mechanical analysis for pattern type 3, it is evident that the average percentage of fines for this type of active layer as a whole is considerably smaller than indicated by the grain size curves. Under these conditions it would seem advisable to raise the grain size limit defining fines from 0,02 to 0,074 mm and to maintain the percentage by weight limit at 2% to be relatively sure of obtaining a non-frost-susceptible soil material. It is also apparent that a large range in particle size, and particularly the presence of large quantities of cobbles and boulders is important either as a density or thermal unit in the formation of this pattern.

Comparative features of the four pattern types discussed above are given in table VI and those of the four types of ground ice in table VII. The descriptions given for each feature refer only to the archetype and do not represent the variations caused by the effect of one pattern or ice type upon another.

By plotting grain size curves from areas of pattern types 2, 3 and 4 (fig. 37), it is possible to define the limits of sorting and, roughly, of frost--susceptibility in terms of the percentage of fines. The sorted surface of the active layer is produced when the average percentage of fines in the plugs is between 3 and 8%. Although there may be a slight disturbance and vertical sorting of an active layer containing 2 to 3% fines, those containing less than 2% finer than 0,074 mm are generally not sorted or disturbed by frost action. Those containing more than 8% fines are highly susceptible to frost action although they may be unsorted at the surface. It is, however, a relatively simple matter to identify such an area from either a surface examination or from airphotos on the basis of its surface pattern.

ENGINEERING APPLICATIONS

In the outwash area near Thule, Greenland, a relationship exists between the surface morphology, the percentage of fines (200 ASA screen) in the active layer, and the type and distribution of ground ice in the permafrost. It is therefore possible to predict the amount of fines in the active layer (as a parameter for determining frost-susceptibility) and the ice distribution in the permafrost from a surface inspection or from airphotos.

The following predictions with regard to construction sites and sources for construction materials can be made on the basis of ground patterns.

Pattern type 1 (pl. 1), circular and linear depressions in unsorted outwash, is formed in materials (containing less than 2% fines) suitable for construction purposes if well drained, but such areas should be avoided as construction sites because they are underlain by a permafrost rich in ice. Care should be exercised when analyzing airphotos not to confuse this pattern with types 3 and 4, which contain more than 3% fines and are liable to frost action. Although each pattern is distinctive, under certain light conditions it might be possible to mistake one for another.

Pattern type 2, ice wedge polygons or polygonal troughs developed in unsorted outwash, is found in non-frost-susceptible outwash materials containing less than 2% fines. Ice wedges occur beneath the surface troughs, but within each polygon the permafrost is composed solely of frozen sands and gravels. Such an area would provide good construction sites and materials, although for a large installation steps would have to be taken to insulate or remove the ice wedges to prevent collapse as they melted. This pattern is easily identified from the air or ground (pl. 1) by the troughs and polygonal pattern formed by them, ranging from 50 to 100 feet in diameter of the individual polygon. The narrowing or disappearance of polygon troughs serves as a good indication of an increasing percentage of fines in the active layer and normally marks the boundary between this and pattern type 3 or 4.

Pattern type 3 (pl. 1), sorted circles or centers of fines in sorted frost--susceptible outwash, indicates an active layer and permafrost containing more than 2% fines and a permafrost rich in ice masses. Such an area should be avoided as a construction site or source for building materials [7]. In airphotos, pattern type 3 appears as a darker area, due either to lichen--covered boulder streams in which the centers occur or to the centers of fines themselves. Ice wedge troughs, if present, are reduced in size.

Pattern type 4 (pl. 1), irregular mounds and depressions of low relief and small size formed in unsorted outwash, indicates a high percentage of fines in the active layer and permafrost and a dense concentration of ice masses in the permafrost. The irregularity of the features of this pattern serves to differentiate it from pattern type 1 in airphotos. Because of the concentration of ice in the permafrost and the high percentage of fines (over 8% average) in the soil, areas exhibiting this pattern should be avoided as construction sites and borrow pits. Ice wedge troughs tend to disappear entirely within areas developing this pattern.

[7] However, recent work by Corte (1962) shows the formation of sorting, in the field and laboratory, in coarse material without fines.

On the basis of the work done to date on this subject, it is suggested that any outwash area in which ice wedge troughs tend to disappear or decrease sharply in size should be avoided as a construction site and analyzed for grain size before being selected as a source for building materials.

GLOSSARY

Active layer: that portion of the soil between the surface and the permafrost table which is subject to annual cycles of freeze and thaw.

Active layer, disturbed: a fine grained active layer averaging more than 4% fines and subject to frost heaving. Primary depositional features are contorted, broken, or entirely absent. Vertical sorting of fine material to the bottom and coarse to the top. Commonly referred to as „frost-susceptible".

Active layer, undisturbed: a dry coarse grained active layer averaging less than 1% fines and not susceptible to frost heaving. Contains primary depositional bedding and lacks vertical sorting commonly referred to as „non-frost-susceptible".

Cryoconite: originally a fine-grained dust found on the surface of glaciers which absorbed radiation to cause differential ablation and the formation of dust wells or cryoconite holes. Now expanded in definition to include any particle or particles which absorb sufficient radiation to produce cryoconite holes. Term was first used by Nordenskjöld, as *kryoconite*.

Evaporite: one of the sediments deposited from aqueous solution as a result of extensive or total evaporation of the solvent.

Fines: that fraction of the soil with a particle diameter less than 0,074 mm (200 ASA mesh); silt- and clay-sized fractions as a group.

Frost-susceptibility: the condition in which a soil is susceptible to frost-heaving when an adequate supply of moisture and the proper temperature gradient are available.

Ice lens: a lenticular body of clean transparent ice, as much as two feet thick in samples observed, sometimes containing suspended stones and sand grains thought to be cryoconites.

Ice mass: an amorphous body of transparent ice containing fine sediments in essentially parallel layers which may be horizontal, inclined or contorted. Layers may be continuous or broken. Apparently closely related to a frost-susceptible active layer averaging more than 4% fines.

Ice wedge: a linear body of bubbly ice, wedge-shaped in cross section, formed by the freezing of atmospheric moisture and/or melt-water in thermal contraction cracks. Normally interconnected to form a polygonal feature of large scale overlain by shallow trenches in the active layer.

Outwash: stratified drift deposited by meltwater streams beyond active glacier ice.

Permafrost (perennially frozen ground): a thickness of soil or other surficial deposit, or even of bedrock, at a variable depth beneath the surface of the earth, and in which a temperature below freezing has existed for a long time (from two to tens of thousands of years). (Although not as accurate a term as *perennially frozen ground* or *pergelisol*, the term *permafrost* is used in this report because it is simple, euphonious and commonly understood).

Permafrost table: a more or less irregular surface which represents the upper limit of permafrost.

Plug of fines: a feature of a disturbed active layer formed by the extrusion of a mass or neck of fine grained material, containing at least 4% of fines, from the general accumulation of fine material at the bottom of a vertically sorted active layer. It may reach the surface to form a „center of fines" or „sorted circle".

Relict ice: a large body of glacial ice whose surface has been sculptured by thermal or aqueous erosion to produce a kettled topography which has been later buried by conformal outwash deposits.

Sorted circle (center of fines): the surface expression of a „plug of fines" extruded from the active layer. Normally found as a center of finer material ranging from silt and clay sized particles to large pebbles and surrounded by washed cobbles and boulders.

Thermokarst: karst-like topographic features produced by the melting of ground ice and the subsequent settling or caving-in of ground.

Vertical sorting: sorting of coarser particle sizes to the top of the active layer and finer ones to the bottom to produce fully separated grain-size curves.

References

Beskow, G. 1934 — Tjälbildningen i vägarna och atgärder mot dess skadegörelse (Frost action on roads and countermeasures). *Svenska Väginstitutet, Tekniskekonomiska utredningar rörande vägvesendet,* Medd. 44; p. 292—345.

Black, R. F. 1951 — Structures in ice wedges of northern Alaska. *Bull. Geol. Soc. Amer.,* vol. 62; p. 1423—1424.

Black, R. F. 1952 — Growth of ice-wedge polygons in permafrost near Barrow, Alaska. *Bull. Geol. Soc. Amer.,* vol. 63; p. 1235—1236.

Black, R. F. 1954 — Ice wedges and permafrost of the arctic coastal plain of Alaska. Unpublished ms., 2 vol., 354 fig., 788 p. (Results of work under auspices of USGS).

Cailleux, A. & G. Taylor 1954 — Cryopédologie. Etude des sols gelés. 218 p., Paris.
Canada, National Research Council. Division of Building Research 1957 — Frost action in soils. *Canadian Builder,* vol. 7, no. 9; p. 49.

Casagrande, A. 1934 — Bodenuntersuchungen im Dienste des neuzeitlichen Strassenbaues. *Strassenbau,* Bd. 25; p. 25—28.

Colton, R. B. & C. B. Holmes 1954 — Geomorphology of the Nunatarssuak area. In: Operation Ice Cap 1953. Final report [on] the scientific program (program B), Stanford Res. Inst.; p. 27—52.

Commission de Morphologie Périglaciaire 1952 — Rapport préliminaires pour la 8e assemblée générale et le 17 congrès international. Union Géogr. Internationale, Washington, D. C.

Corte, A. E. 1959 — Experimental formation of sorted patterns in gravel overlying a melting ice surface. U. S. Army Snow, Ice and Permafrost Research Establishment, *Research Report* 55; 15 p.

Corte, A. E. 1961 — 1962 — Laboratory and field data for a new concept on the frost behavior of soils, Part I: Vertical sorting (1961). Part II Horizontal Sorting (1962). U. S. Army Snow, Ice and Permafrost Research Establishment, Corps of Engineers, *Research Report* 85.

Department of the Air Force 1954 — Airfield pavement design, Chapt. 4: Frost conditions. AFM 88—6; 21 p.

Dostovalov, B. N. 1958 — Tetragonalnye sistemy ledianykh jil (The tetragonal system of ice veins). Union géodésique et géophys. intern., Assoc. Hydr. Sci. C.-R. Assembl. gén. Toronto 1957, vol. 4; p. 149—157.

Dücker, A. 1956 — Gibt es eine Grenze zwischen frostsicheren und frostempfindlichen Lockergestein? *Strasse u. Autobahn,* Bd. 6; p. 78—82.

Espach, R. H., Jr. 1956 — Draft report on 1956 field work in patterned ground studies, Thule, Greenland. Unpublished ms, USA SIPRE Proj. 22. 3—5, CE Proj. 18.

Grim, R. E. 1952 — Relation of frost action to the clay-mineral composition of soil materials. In: Frost action in soils, A symposium. *Highway Research Board, Spec. Rept.* No 2; p. 167—172.

Jahn, A. 1946 — Badania nad strukturą i temperaturą gleb w zachodniej Grenlandii (summary: Research on the structure and temperature of the soils in western Greenland). *Bull. Acad. Polonaise Sci. et Lettr.,* Cl. Math., natur., Serie A; p. 50—59.

Krumbein, W. C. 1940 — Theory of pebble rounding. *Bull. Geol. Soc. Amer.,* vol. 51; p. 670.

Krumbein, W. C. & F. J. Pettijohn 1938 — Manual of sedimentary petrography. New York; 549 p.

Lambe, T. W. 1953 — Cold room studies. Third interim report of investigations (F. Y. 1952—1953), vol. 2, Appendix C: Mineral and chemical studies. Arctic Construction and Frost Effects Laboratory, *Technical Report* 43; 25 p. (Superseded by revised edition 1958).

Langway, C. C., Jr. 1958 — Ice fabrics and the universal stage. U. S. Army Snow, Ice and Permafrost Research Establishment, Corps of Engineers, *Technical Report* 62; 16 p.

Leffingwell, E. De K. 1919 — The Canning River region, northern Alaska. *U. S. Geol. Survey, Professional Paper* 109; p. 179—243.

Linell, K. A. & C. W. Kaplar 1959 — The factor of soil and material type in frost action. *Highway Research Board Bull.,* vol. 225; p. 81—128.

MacKay, J. R. 1953 — Fissures and mud circles on Cornwallis Island, N. W. T. *Canadian Geographer,* vol. 3; p. 31—37.

Marr, J. W. 1959 — Ecosystems of the South River boulder plain, Thule, Greenland. Unpublished ms., USA CRREL files.

Nakaya, U. 1956 — Properties of single crystals of ice revealed by internal melting. U. S. Army Snow, Ice and Permafrost Research Establishment, Corps of Engineers, *Research Paper* 13; 80 p.

Nakaya, U. & C. Magono 1944 — Tōjō no jikken-teki kenkyū (Experimental studies on frost heaving). *Teion-kagaku,* vol. 1; p. 37—51.

Nicolaou, A. D. 1958 — A preliminary application of geophysical methods in patterned ground studies in NW Greenland. Unpublished ms., USA CRREL files.

Osnovy geokriologii, merzlotovedeniia (Principles of geocryology). Part I; Obshchaya geokriologia (General geocryology). Inst. Merzlotovedeniia im. V. A. Obrucheva, Akad. Nauk SSSR; Moscow 1959, 459 p.

Osterberg, J. O. & W. N. Fead 1955 — Literature survey of moisture migration in soils due to thermal gradients. U. S. Army Snow, Ice and Permafrost Research Establishment, Corps of Engineers, *Special Report* 32; 13 p.

Popov, A. I. 1955 — Proiskhojdenie i razvitie moshchnogo iskopaemogo lda (Origin and evolution of fossil ice). *Materialy k osnovam ucheniya o merzlykh zonakh zemnoy kory,* vyp. 2; p. 5—24.

Powers, M. C. 1953 — New roundness scale for sedimentary particles. *Jour. Sedimentary Petrology,* vol. 23; p. 117—119.

Rigsby, G. P. 1951 — Crystal fabric studies on Emmons Glacier, Mount Rainier, Washington. *Jour. Geol.,* vol. 59; p. 590—598.

Rigsby, G. P. 1958 — Fabrics of glacier and laboratory deformed ice. In: Symposium of Chamonix, 16—24 Sept. 1958; Physics of the movement of ice. International Union of Geodesy and Geophysics, Association of Scientific Hydrology, Publication 47; p. 351—358.

Senstius, M. W. 1958 — Climax forms of rock-weathering. *American Scientist,* vol. 46; p. 355—367.

Shumski, P. A. 1955 — Osnovy strukturnogo ledovedeniya (Principles of the study of ice structure). Moscow, 492 p. (French transl.: Principes de glaciologie structurale; Annales du Centre d'études et de Documentation Paléontologiques, no 22, Oct. 1957; 262 p.).

Shvecov, P. F. 1956 — Proiskhojdenie i zakonomernosti rasprostraneniya podzemnykh ldov (The origin and regularity of fossil-ice distribution). *Vestnik Akad. Nauk SSSR,* 26; p. 66—69.

Taber, S. 1930 — Freezing and thawing of soils as factors in the destruction of road pevements. *Public Roads,* vol. 11; p. 113—132.

Taber, S. 1943 — Perennially frozen ground in Alaska: its origin and history. *Bull. Geol. Soc. Amer.,* vol. 54; p. 1433—1548.

Taylor, R. S. 1956 — Studies on patterned ground. U. S. Army Snow, Ice and Permafrost Research Establishment, Report 32 (unpublished).

Troll, C. 1944 — Strukturboden, Solifluktion und Frostklimate der Erde. *Geol. Rundschau,* Bd. 34; p. 545—694.

U. S. Army Engineer Waterways Experiment Station 1957 — The unified soil classification system, Appendix B: Characteristics of soil groups pertaining to roads and airfields. *Technical memorandum* No. 3—357, (revised June 1957).

Vilborg, L. 1955 — The uplift of stones by frost. *Geogr. Annaler,* vol. 37; p. 164—169.

Wadell, H. 1932 — Volume, shape and roundness of rock particles. *Jour. Geol.,* vol. 40; p. 443—451.

Washburn, A. L. 1956 — Classification of patterned ground and review of suggested origins. *Bull. Geol. Soc. Amer.* vol. 67; p. 823—865.

Watkins, W. I., A. Casagrande & S. Taber 1931 — Discussion on frost heaving. *Highway Research Board, Proc.,* vol. 11; p. 165—177.

Appendix A: Associated studies

ECOLOGY

by Dr. John W. Marr

Ecological studies of areas 3, 4 and 4a were carried out by the above author using the stand ecosystem method, a research approach based upon the principle that the landscape is mosaic of relatively discrete units called stand ecosystems. Since a stand is the result of the interaction of all the environmantal factors, such as available plant forms, climate, soil, water supply, and both macro- and micro-topographical features, its study involves investigation of many external and internal processes.

Two maps were prepared covering the stand distribution for areas 3, 4 and 4a. Some of these stand features are reported in the main body of this report. In spite of the fact that not all the environmental factors were investigated and that this is the first study of this kind in the Thule area, it is possible to present the following conclusion by combining the results of the ecological studies with those of the geological studies. Three stand types are related to three of the patterns described in this report. These are:

(1) Pattern type 2, well-developed ice wedge polygons formed in a coarse, dry, undisturbed active layer without fines, supports stable stands of sparse rock lichens and lush lichens (areas 3, 4). Lower areas with less wind and slightly more soil moisture support stable stands of *Carex nardina* (area 3). The stability is an indication of both the dryness and the lack of fines;

(2) Pattern type 3, sorted circles or centers of fines formed in a disturbed active layer with more than 3% fines, generally occurs in lower areas than type 2, and is characterized by more complex ecological stands — *Salix* and *Cassiope* in area 3 and *Dryas*, *Salix* and *Carex rupestris* in the same pattern in area 4 (*Carex rupestris* indicates a relatively high soil moisture in this area). The stands are stable in area 3, except for wind exposed parts, and show all degrees of stability and instability in area 4;

(3) Pattern type 4, mounds and depressions of low relief in unsorted outwash (area 4 a), is developed in a disturbed active layer which averages more than 8% fines. The pattern is stable one except for one center of fines, and supports a stable stand of rock lichens, *Carex nardina*, and *Dryas*. Plugs are formed in the active layer but fail to reach the surface. The stability of the ground surface and the plant stands is considered the result of the relatively stable active layer which lacks the very coarse material necessary to force centers of fine material to the surface and thereby create unstable conditions.

In addition to these primary stands related to ground patterns there are 22 other stands which are related to micro-ground patterns formed as the product of the interaction of various factors, such as temperature, moisture balance, wind, soil structure, grain size, mineral composition of soil, and micro- and macro-topographical features, most of which are continually changing. As the composition of such stands is a valuable indicator of the mineral composition, grain size, structure and moisture content of the soil (as well as climatic and other conditions), it is recommended that further studies be conducted in areas with fewer variables and that the roles of the variable be studied in greater detail.

GEOPHYSICAL

by Anthony D. Nicolaou

Seismic refraction and electric direct current resistivity surveys were conducted in the research areas to determine their potential as methods for locating and defining ice bodies in the permafrost. The seismic velocities obtained, however, were not in agreement with those of larger scale seismic surveys made in the area, and the resistivity survey led to contradictory results in some cases. Further investigations would appear to be necessary before any conclusions can be reached on the applicability of these methods for the location of ice bodies in the permafrost.

Appendix B

RECOMMENDATIONS FOR FURTHER FIELD AND LABORATORY WORK

(1) The geographical distribution of pattern type 1 should be determined, as this, to the author's knowledge, is the first time it has been reported in the literature.

(2) Studies similar to those reported herein should be made in active layers developed in residual soils from different parent materials, cutting trenches to determine whether or not surface sorting is related to the presence of ice masses and plugs of fines.

(3) More studies of unsorted areas with frost-susceptible active layers (e. g. area 4a) should be made in order to develop more limiting grain size curves to define the part played by both the coarse and fine fractions of the soil in the process of forting.

(4) Low, cobbles areas in former stream and river channels in the Thule outwash plain (pl. 1) show faint polygonal troughs which are either incompletely developed or are no longer actively developing. This type of area should be trenched and examined to determine the reason for this faint pattern and its relationship to the fully developed polygonal pattern and to areas where no pattern develops at all.

(5) The process whereby glacial or other land ice is buried by outwash material should be studied and evaluated in terms of the pattern developed in areas 1 and 5. Several excellent locations for such a study exist currently along the edge of the ice cap near Camp Tuto, as mentioned in the text.

(6) Fabric analyses should be made on different types of ground ice from samples cut deeper beneath the permafrost table to determine more

about the pattern of stresses which affect growth and development of the ice.

(7) Laboratory experiments should be conducted in freezing cabinets to determine the effect of freeze—thaw cycles on a layer of fines covered by an uneven layer of coarse gravel. This will clarify the role of densities in the formation of centers of fines.

(8) Samples of ice with known and preferred *c*-axis orientation should be subjected to stresses under different temperatures to determine the effect on *c*-axis orientation.

Appendix C

RECOMMENDATIONS FOR FIELD AND LABORATORY TECHNIQUES

When mounting samples of dirty ground ice for fabric analysis it is not practicable to use the melting method: placing the thin section on a warmed glass slide and allowing it to freeze on. Dirt in the sample does not permit a good tight bond. It is therefore recommended that a few drops of water slightly above the freezing point be placed on a cold glass slide. If the thin section is placed on the slide quickly before these drops have a chance to freeze they will spread beneath the sample and freeze to form a good bond without any noticeable melting of the sample. By this method a good transparent thin section can be obtained without any of the „feathery" crystals or air bubbles often formed when the warmed slide method is used.

The best temperature for cutting and mounting thin sections was found to be between -5 and $-10\,^{\circ}$C. At temperatures below this the ice becomes brittle and chips easily.

Ground ice samples were cut on a bandsaw using standard steel blades. In this way a slice about 3 mm thick may be cut. One face is smoothed and polished on carborundum screen laid over a piece of plate glass so the section can be mounted. Once mounted on a glass slide (4" × 4" × 1/16"), the section may be thinned to 1 or 1,5 mm on the carborundum screen.

When trenching the active layer to obtain ice samples from the underlying permafrost it is bothersome but important to protect the ice from radiation by providing some means for covering the excavation. Tyndall figures develop rapidly when the ice is exposed to radiation, thereby destroying the original Tyndall figure pattern which may indicate something of the past history of the ice such as earlier exposure to radiation and subsequent burial by outwash sediments.

Obtaining an undisturbed ground ice sample is difficult if an ice chisel is used and impossible if explosives are employed because both cracking in the ice. A chain saw was found to be a most efficient and convenient means for cutting samples and is highly recommended.

For a complete study of the active layer and distribution of ground ice in the permafrost, a bulldozer is a prime requisite for cutting of trenches. It was found in the studies reported here that structure of the active layer and distribution of ground ice in the permafrost may change radically within short distances, and particularly so where two ground patterns converge. A trench through the entire active layer is therefore the only practical method of exposing a cross-section, obtaining selective soil samples, and observing variations in structure and composition. A D-8 bulldozer, if available, is advisable for cutting the trench because of the very coarse nature of much of the soil material, but a small D-2 would be extremely valuable for removing the last thin layer above the permafrost table to expose the ground ice. The larger machine tends to chew up the ice surface and its large blade will not completely bare the ice in many cases because of the irregularity of the surface. The smaller blade of the D-2 would do a much better job, without disturbing the ice surface. At best, a tremendous amount of shovel work is required to expose the top of the permafrost table for full length of a trench, but a small-bladed machine can save hours, and even days, of shovelling.

Pl. 1. Airphoto of study area, showing ground pattern types and outlines of excavations made

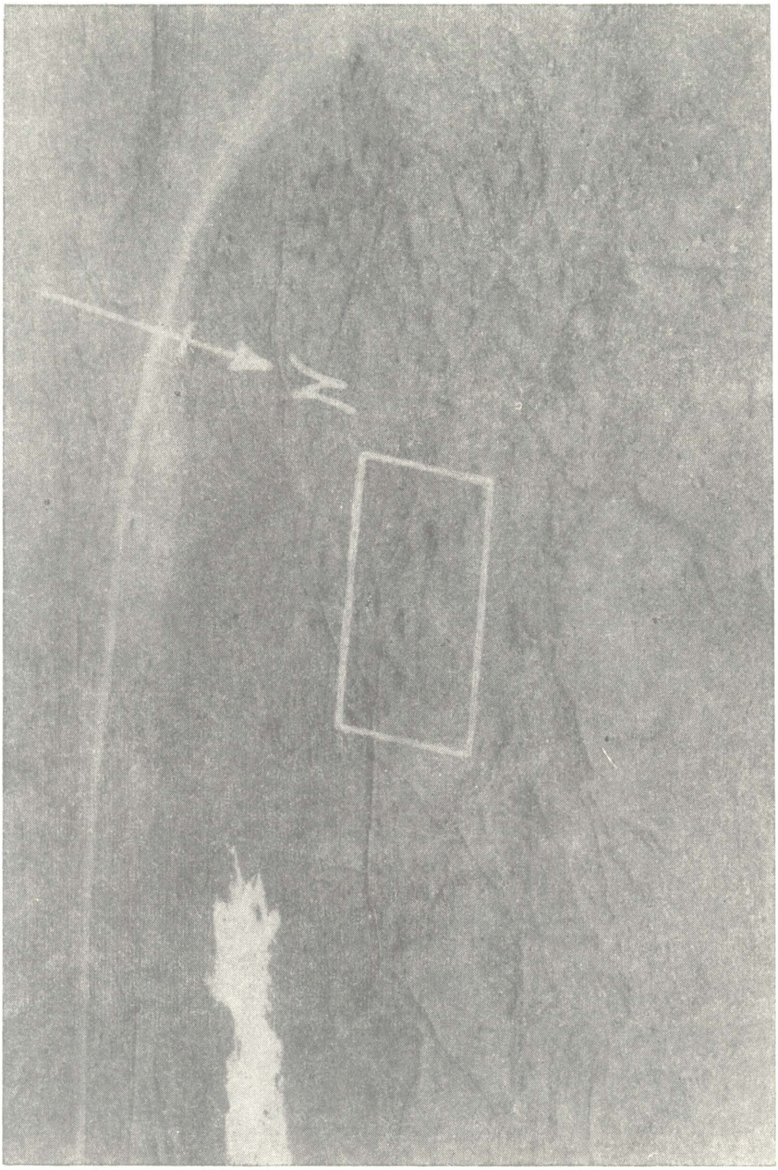

Pl. 2. Area 1. Box represents outline of surface map, fig. 2

Pl. 3. Pattern type 1, showing unsorted surface and size range of material

Pl. 4. Ice-wedge trough, Area 1

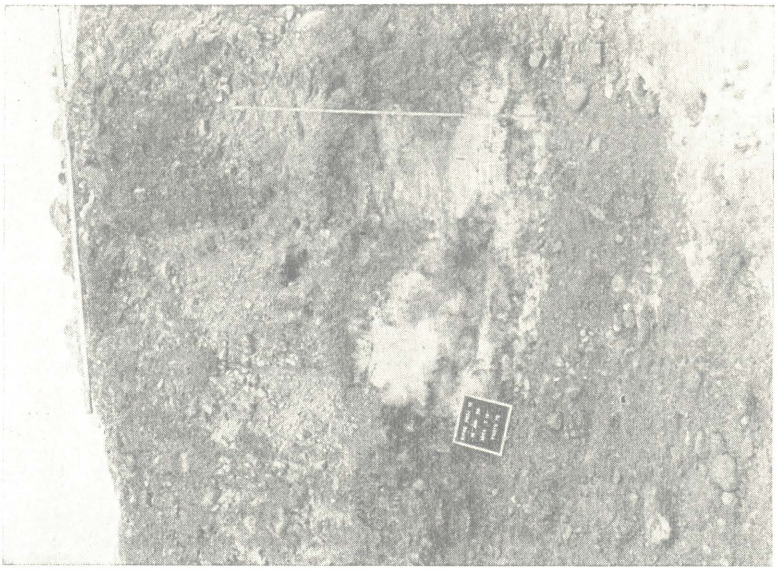

b)

a)

Pl. 5. Ground ice beneath pattern type 1

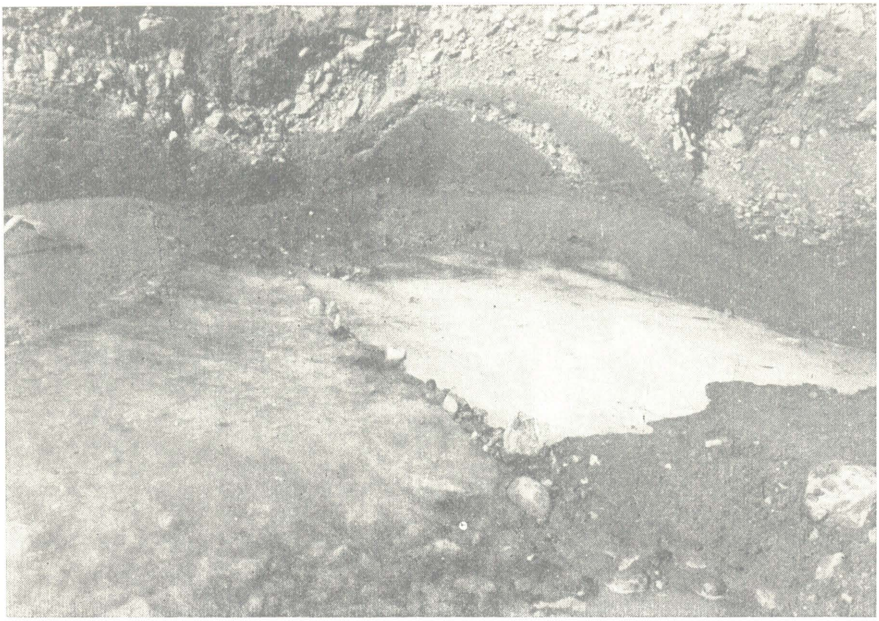

Pl. 6. Ice lens (at left) separated from relict ice (at right) by wall of vertically oriented cobbles

Pl. 7. Vertical view of edge of ice lens, Area 1, showing washed bed (beneath knife) contrasted with sandy permafrost at lower left. Dashed line indicated edge of the lens. Note also wavy bands or streamers of silt

Pl. 8. Photographic view of section shown in fig. 7

Pl. 9. Outwash material covering the edge of the ice cap near Camp Tuto

Pl. 10. Glacial ice exposed beneath outwash deposits at the edge of the ice cap near Camp Tuto

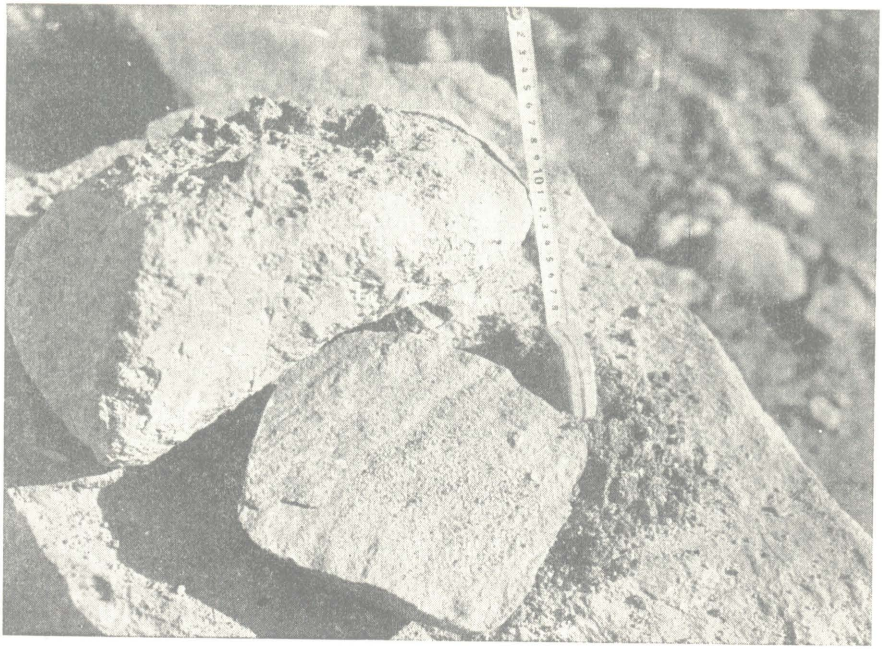

Pl. 11. Accumulated deposit of fines on top of a boulder

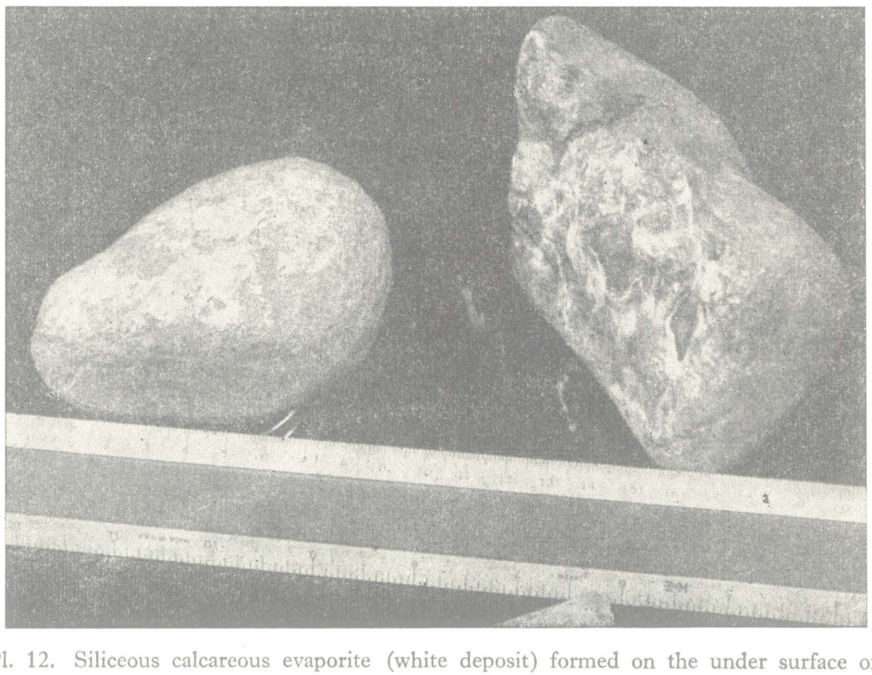

Pl. 12. Siliceous calcareous evaporite (white deposit) formed on the under surface of cobbles

Pl. 13. Aerial view of Area 5 showing trench. Area 1 excavation is seen in the background

Pl. 14. Northwest wall of Area 5 trench, showing relict ice sample location and orientation of stones in the active layer

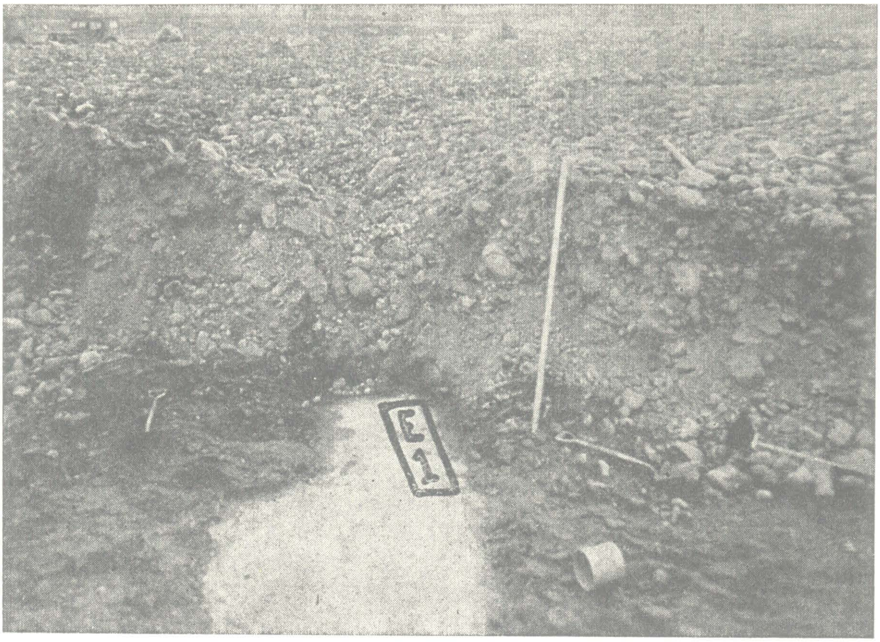

Pl. 15. Ice wedge and relict ice beneath surface trough, Area 5
View looking west (mag.)

Pl. 16. Typical ice-wedge trough

Pl. 17. Large center of fines or sorted circle

Pl. 18. Small sorted circle with raised center

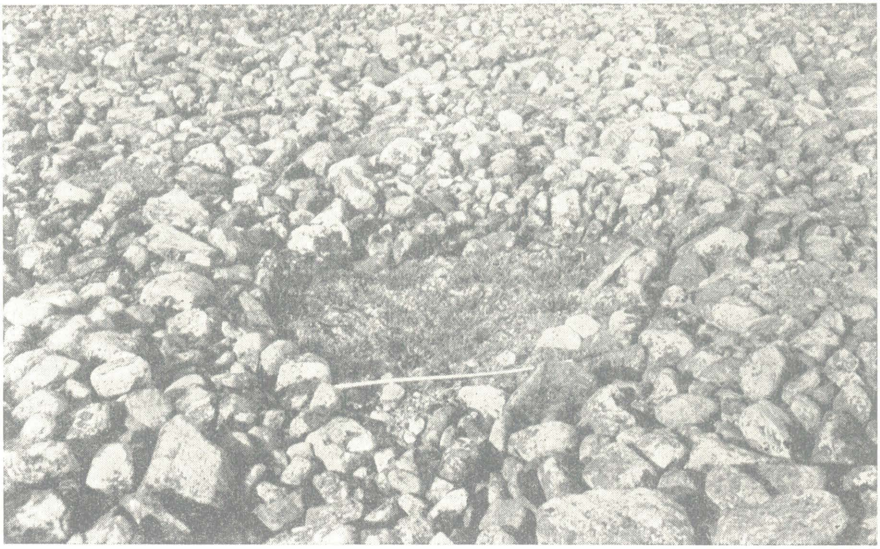

Pl. 19. Depressed center of fines or sorted circle

Pl. 20. Closely spaced centers of fines

Pl. 21. Center of fines or sorted circle composed of pebbles and small cobbles

Pl. 22. Contact between pattern types 2 and 3 showing decrease in size or complete disappearance of ice wedge troughs upon contact with centers of fines (foreground and just above left center)

Pl. 23. Ice wedge in the permafrost beneath its surface trough, Area 3

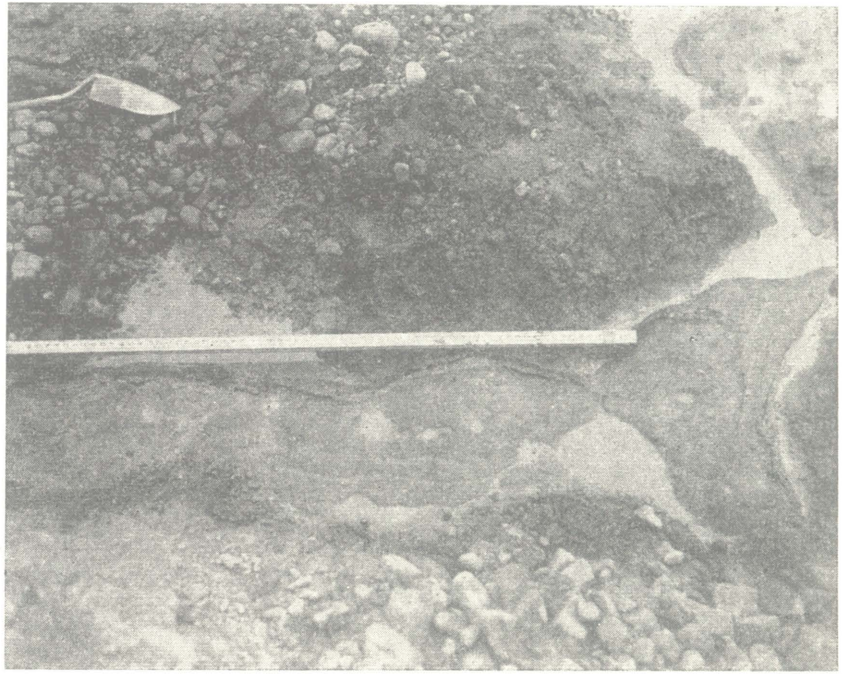

Pl. 24. Ice mass showing „contour lines" of infolded layers of sediments (see fig. 32)

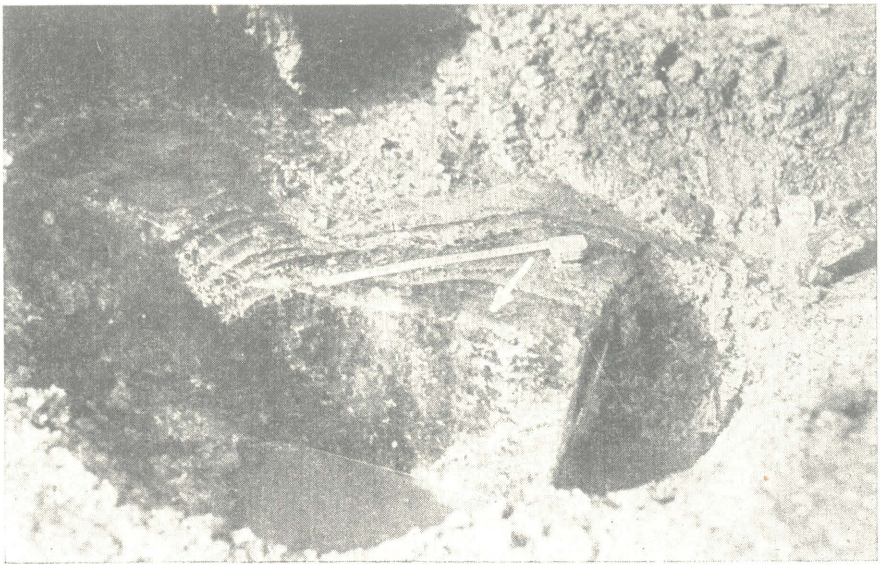

Pl. 25. Ice mass excavated to show randomly scattered silt inclusions (in front face) and folded layers beneath and behind

Arrow indicates orientation of sample C-3

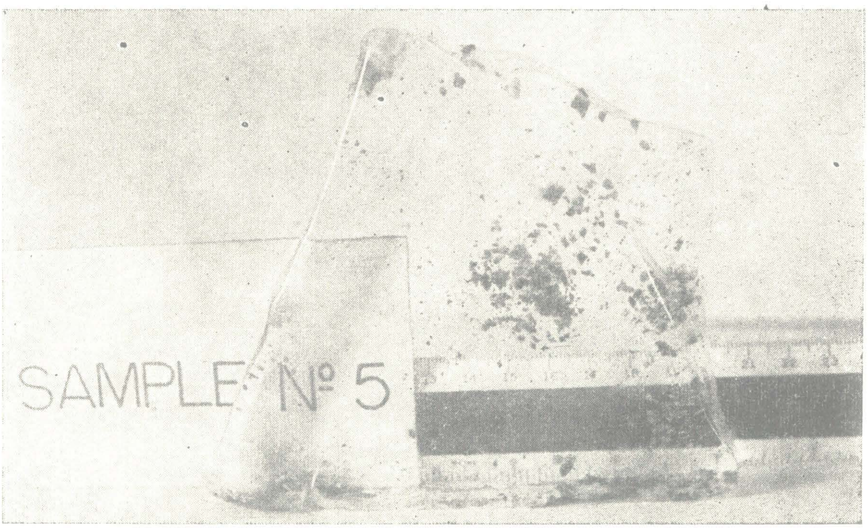

Pl. 26. Thin section of mass ice showing scattered inclusions of sediments

Pl. 27. Dense pattern of centers of fines in Area 4, with ice wedge polygons in the background

Pl. 28. Pattern type 4, Area 4 a

Compare surface texture with that of pattern type 1, pl. 3

Pl. 29. Aerial view of Area 4a showing its relationship to Areas 3 and 4

Note widespread occurrence of pattern type 4 in the surrounding area. Numbers 1 through 6 indicate ice wedge troughs which fade out upon contact with pattern type 4

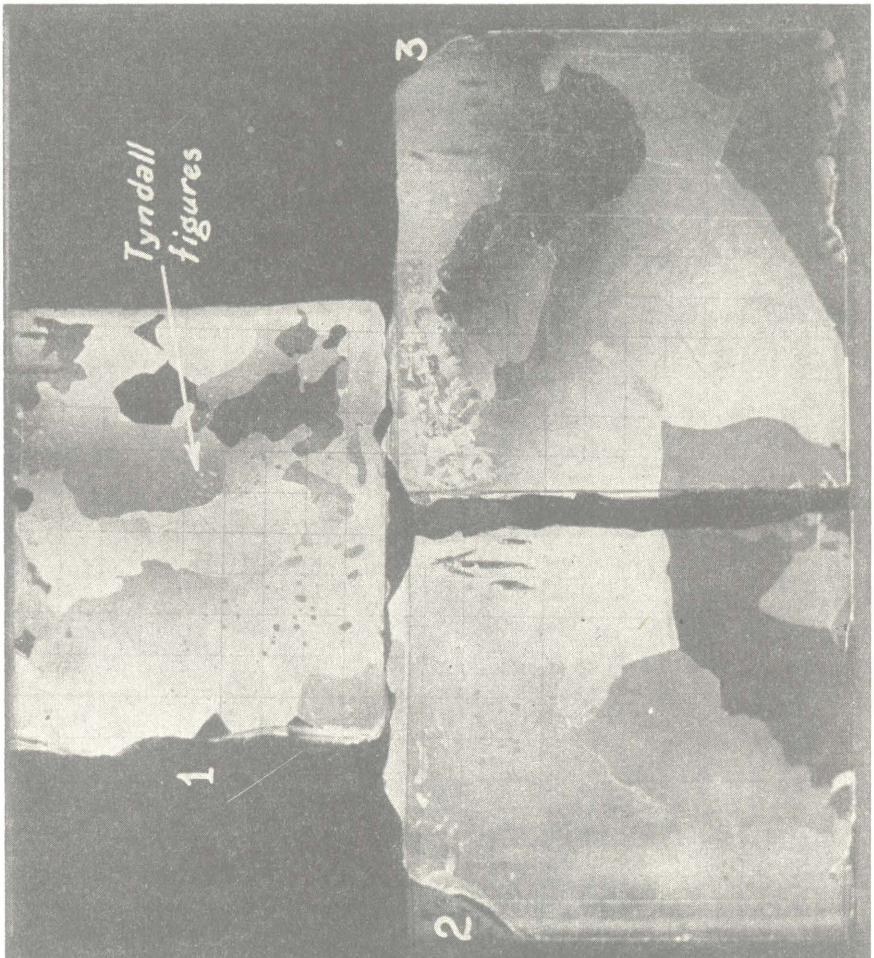

Pl. 30. Vertical thin sections, lens-ice sample A-9

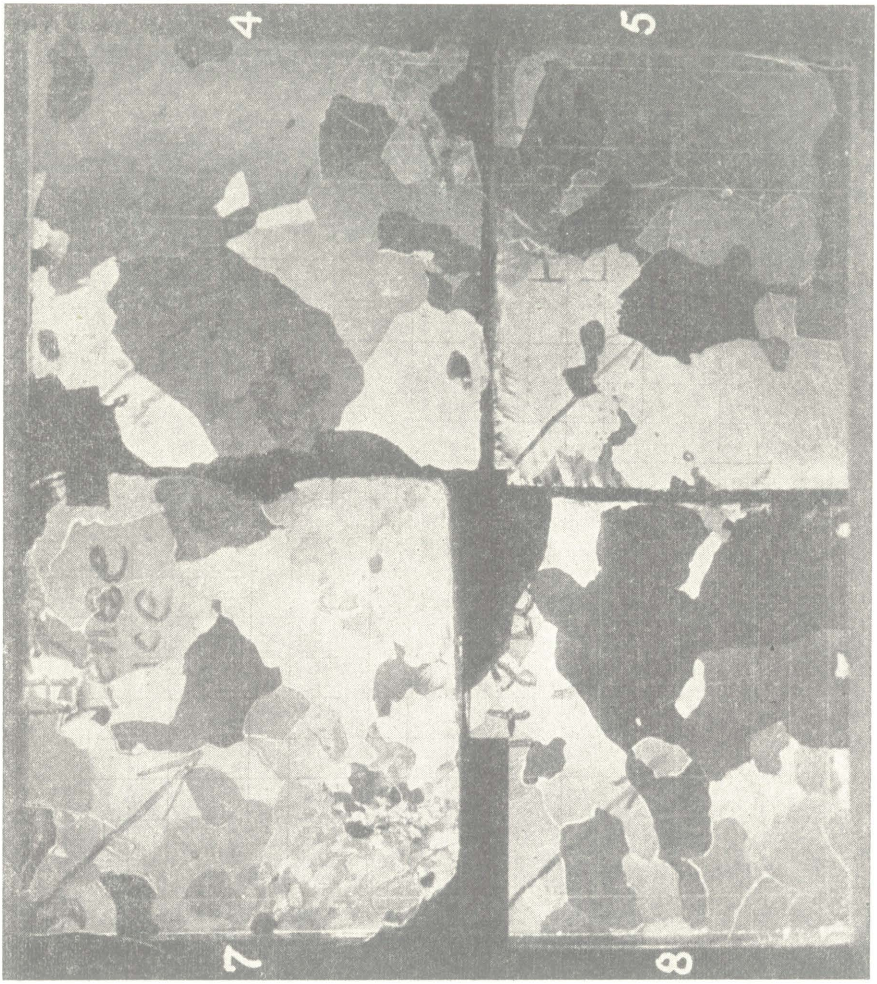

Pl. 31. Horizontal thin sections, lens-ice sample A-9

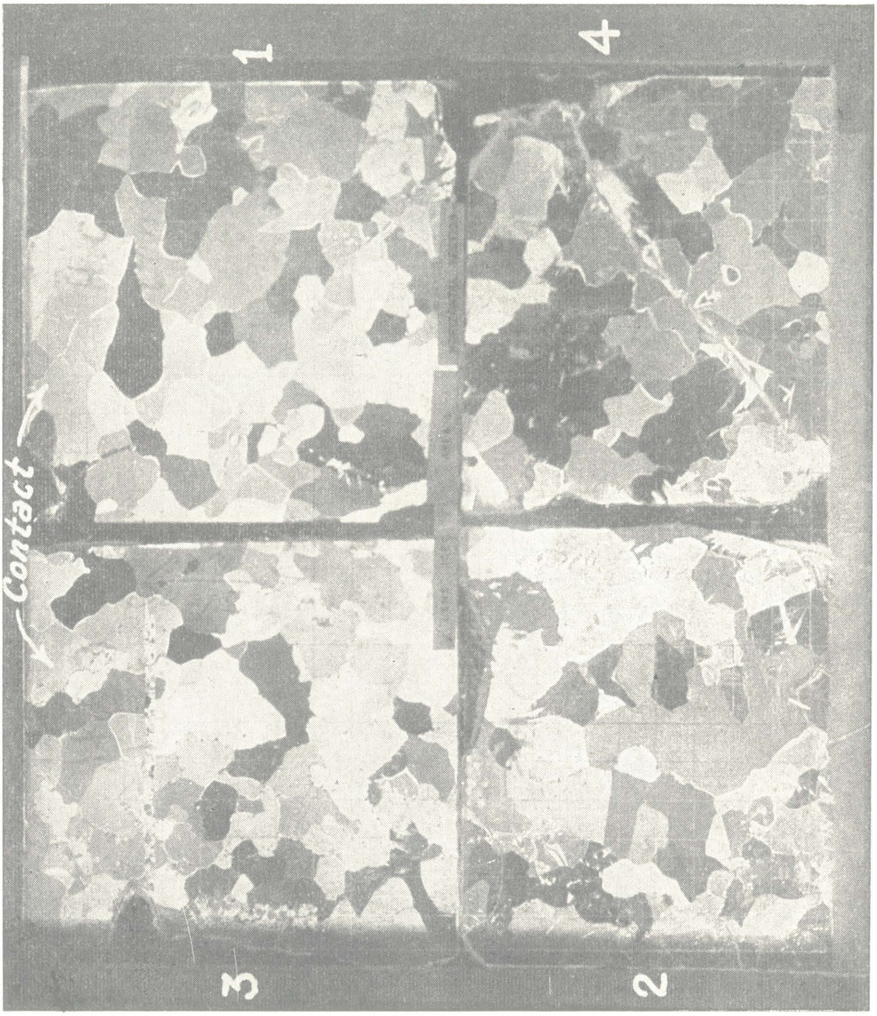

Pl. 32. Horizontal thin sections, lens-ice sample A-11

Pl. 33. Vertical thin sections, lens-ice sample A-11

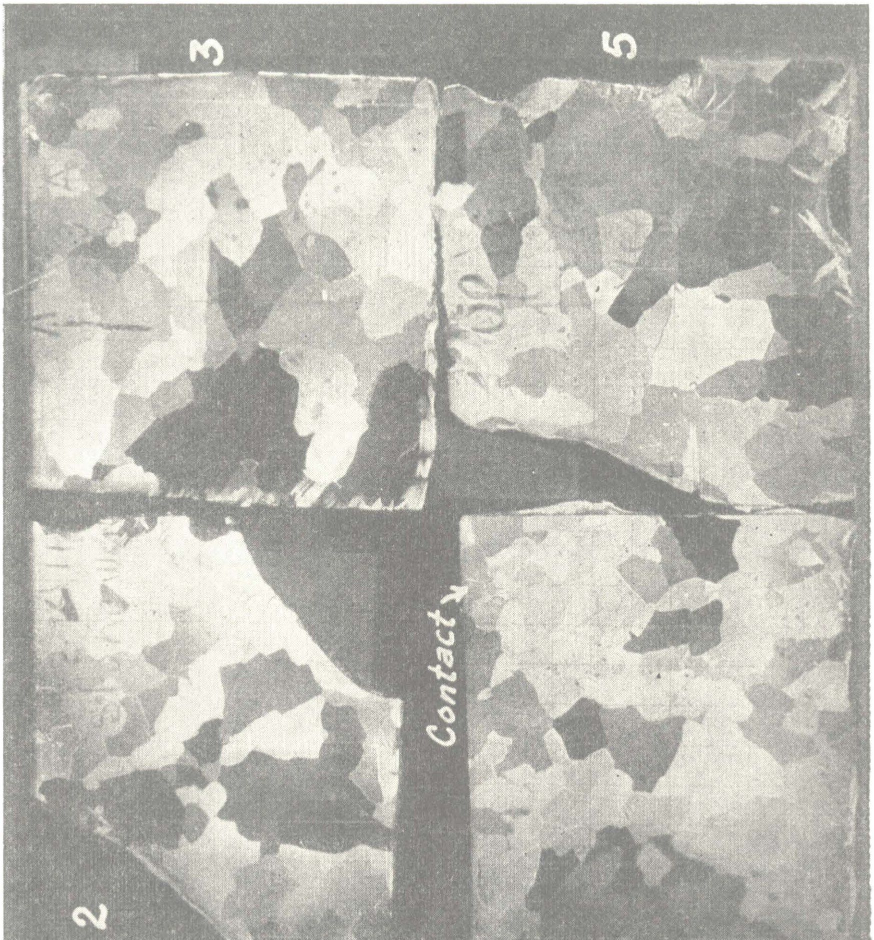

Pl. 34. Vertical thin sections, right face (close to stone wall) of sample A-11

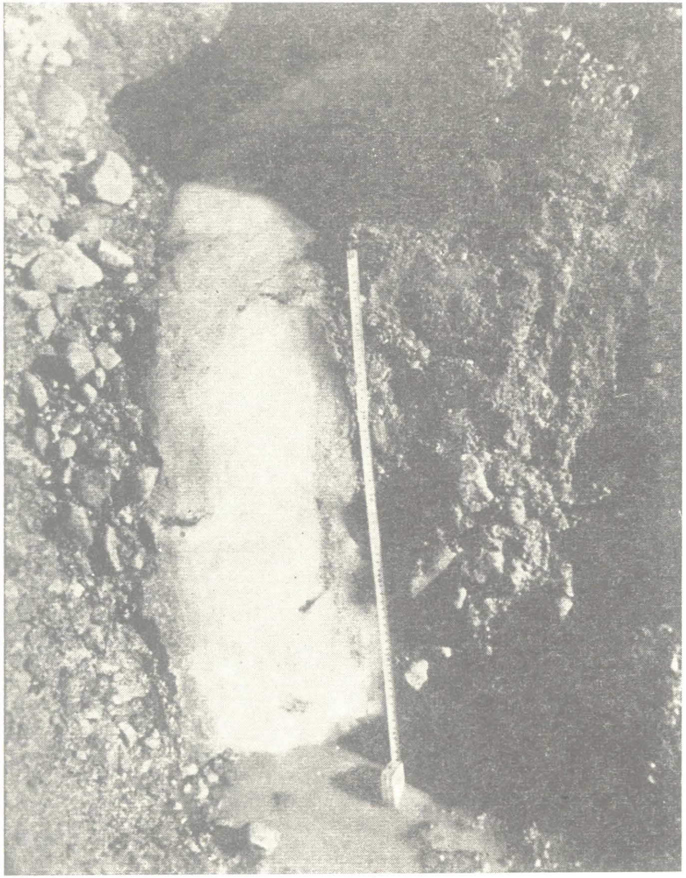

Pl. 35. Cross section of small ice wedge, Area 1

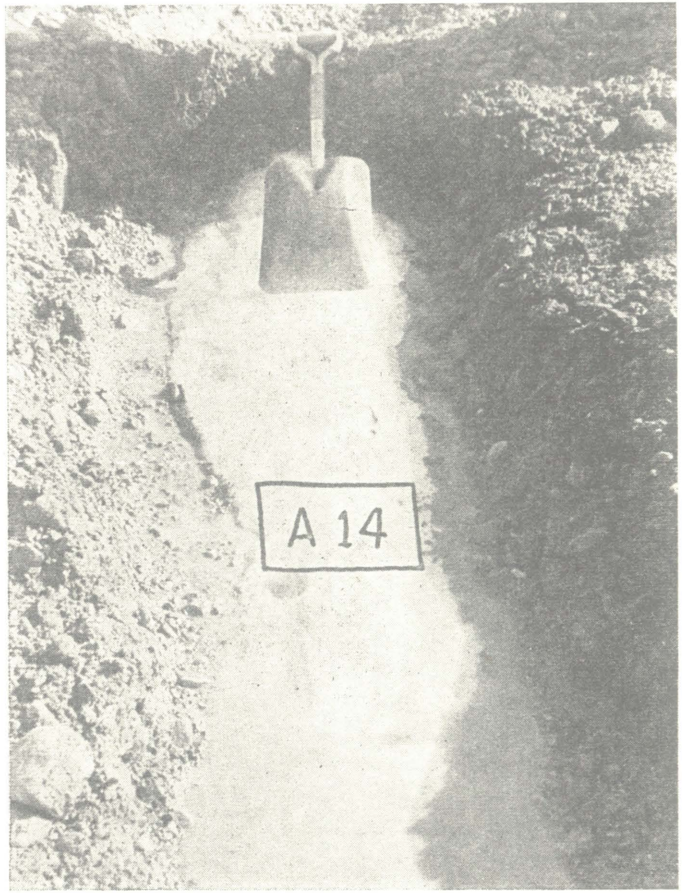

Pl. 36. Ice wedge, Area 1, showing A-14 sample location

Pl. 37. Thin section of wedge ice under crossed polaroids showing fine thermal contraction crack. Thickness of section is 2 to 4 mm. Section too thick to show crystal size and shape adequately

Pl. 38. Section in pl. 37 thinned to 1 mm to show variations in crystal size and shape

Pl. 39. Sections of relict ice bands shortly after being uncovered

Exposure to sun's rays later thawed frozen gravel between the three sections so it could be removed to expose one continuous band

Pl. 40. Section of relict ice exposed at the permafrost table. Note convex form, with surface dipping beneath frozen gravel at the edges

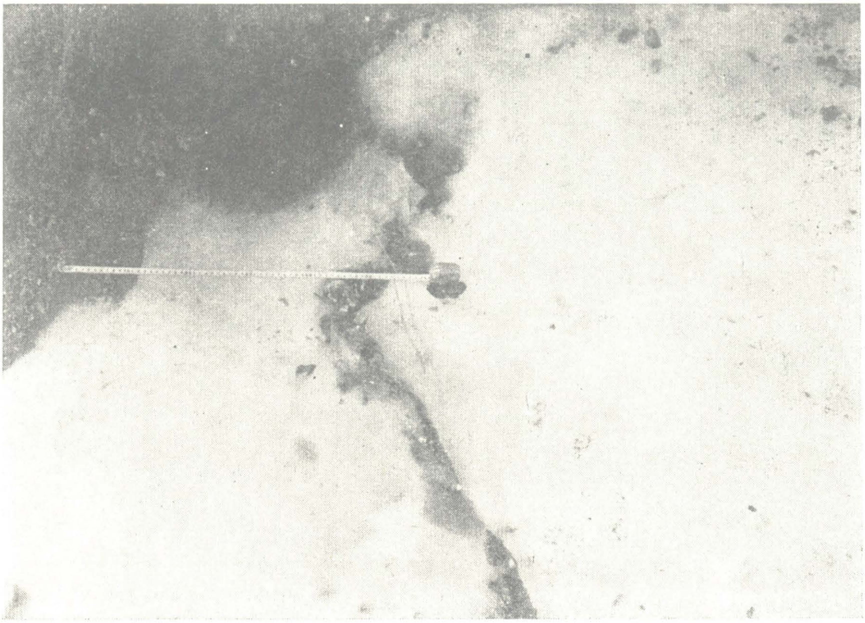

Pl. 41. Line of small stones frozen into relict ice and leading to small patch of clear ice containing some streamers of fine material

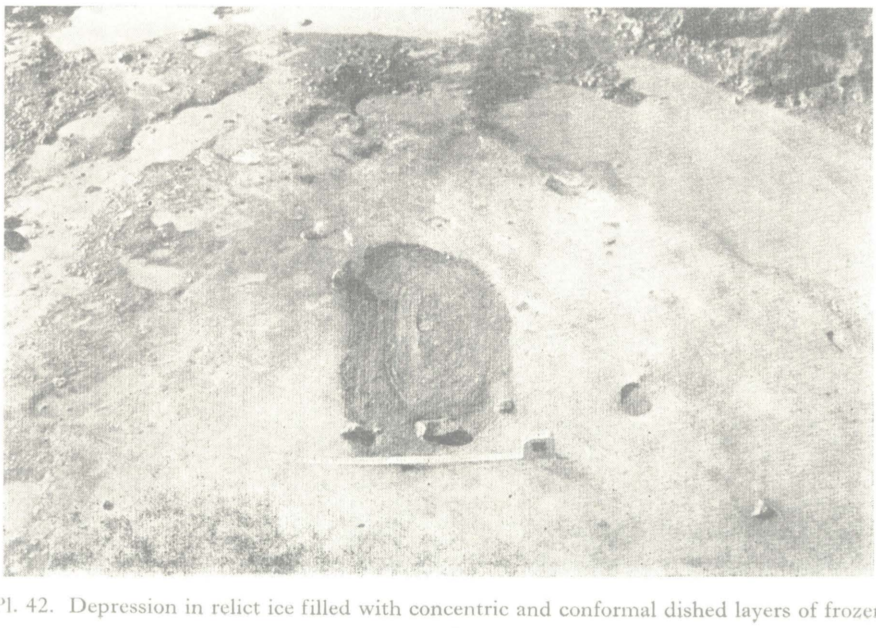

Pl. 42. Depression in relict ice filled with concentric and conformal dished layers of frozen sand

Pl. 43. Milky appearance of relict ice, showing vertical bands of Tyndall figures

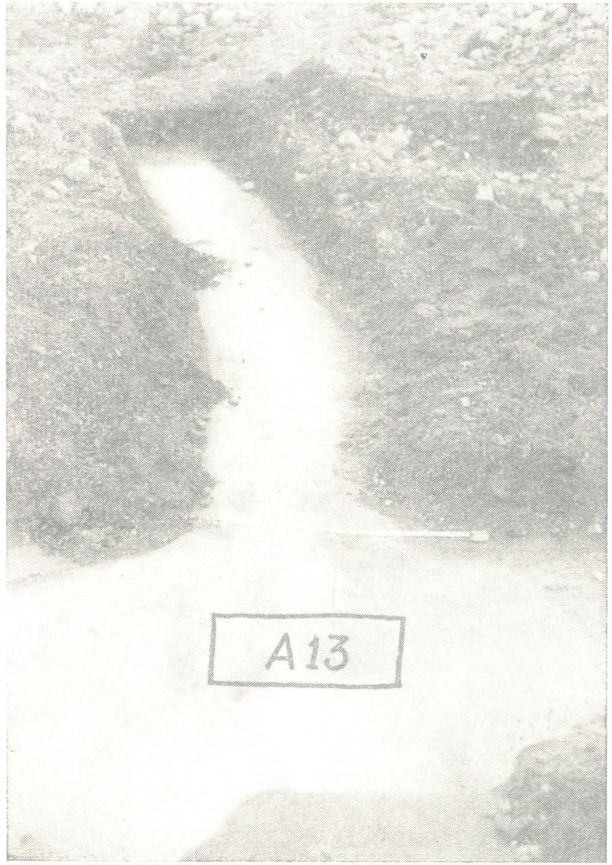

Pl. 44. Variations in Tyndall figure content in relict ice cause variations in transparency as affected by insolation. Relict band in foreground with ice wedge intruding from behind

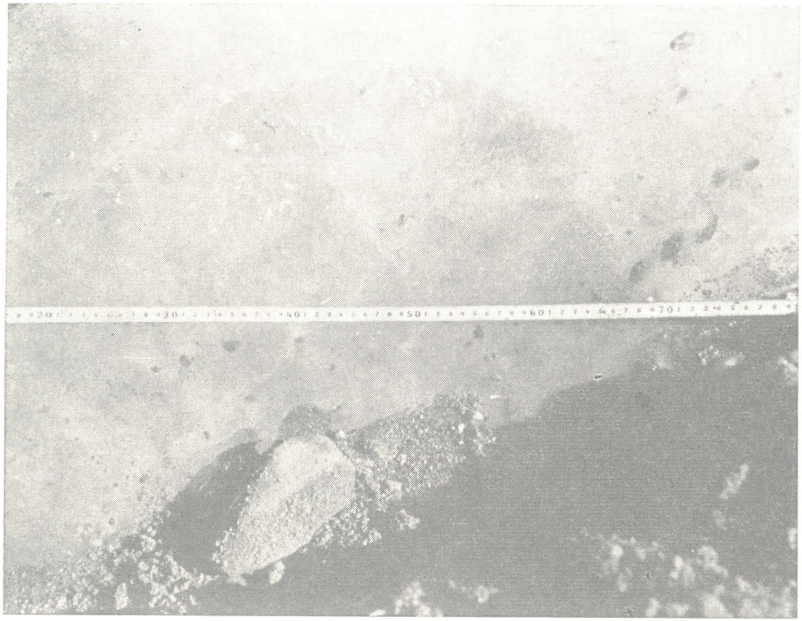

Pl. 45. Small section of more transparent relict ice

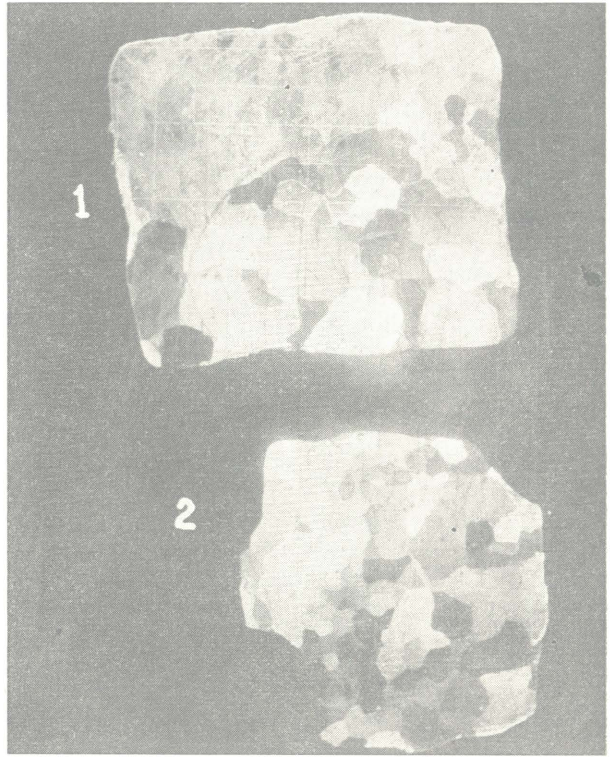

Pl. 46. Vertical (upper) and horizontal (lower) sections of relict ice, sample A-15

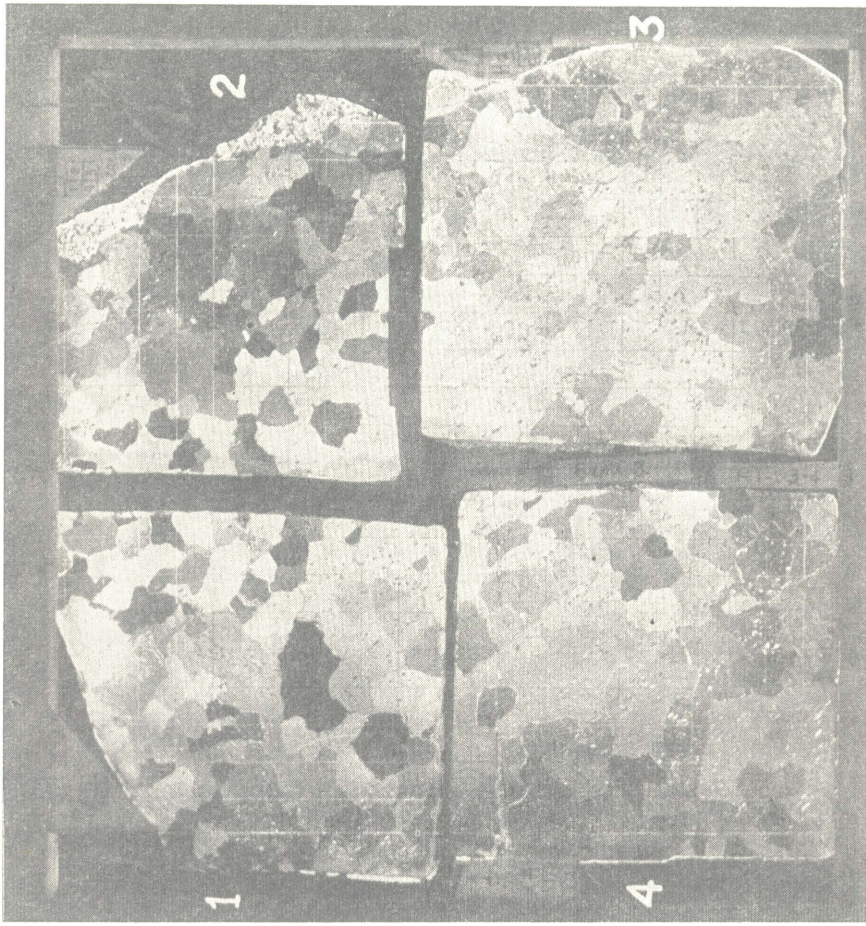

Pl. 47. Horizontal thin sections, relict ice, sample A-18

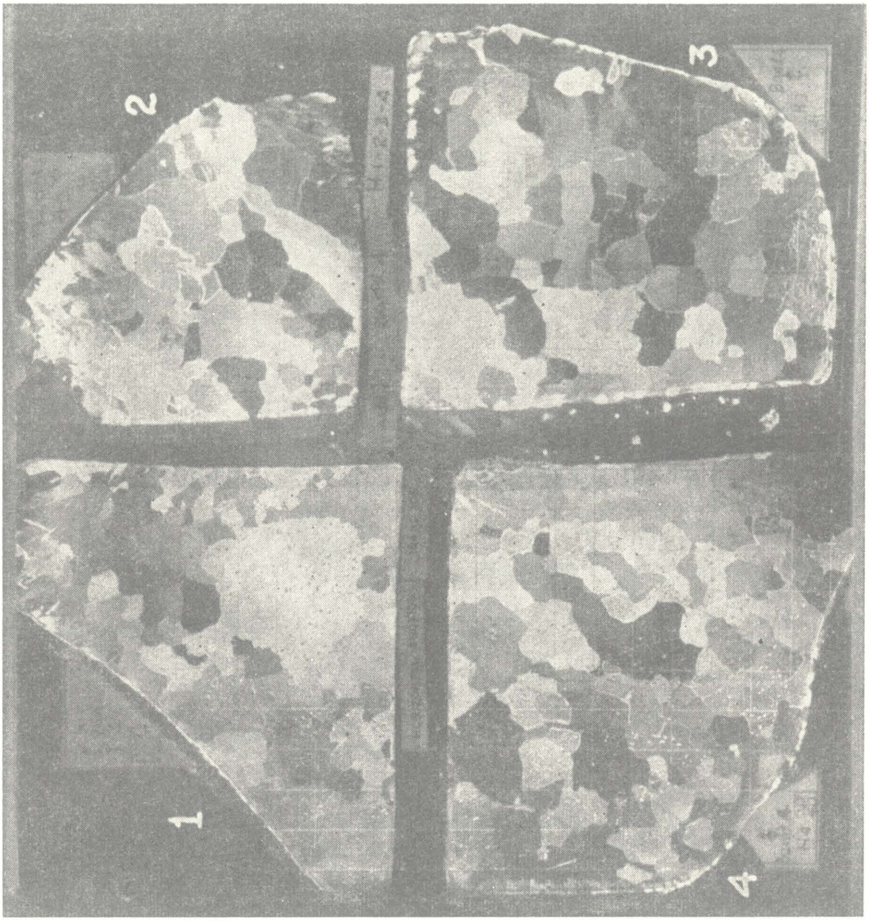

Pl. 48. Horizontal thin sections, relict ice, sample A-19

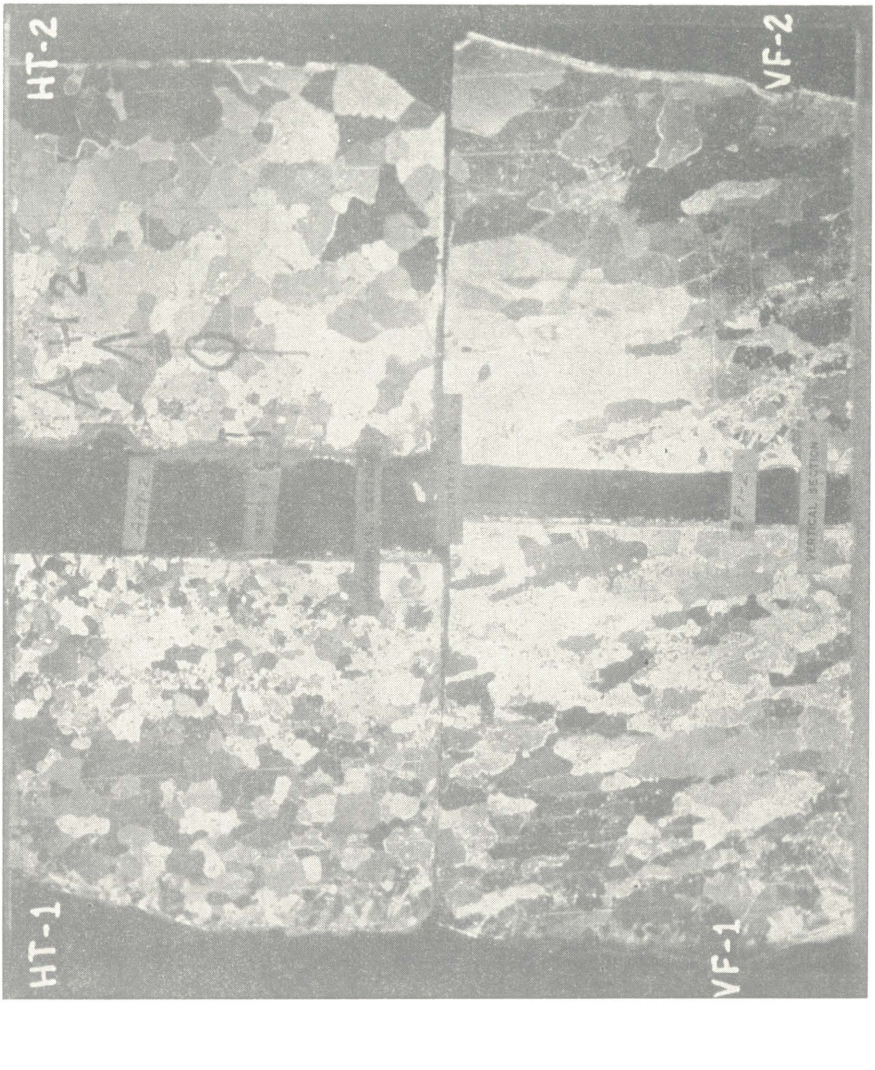

a)

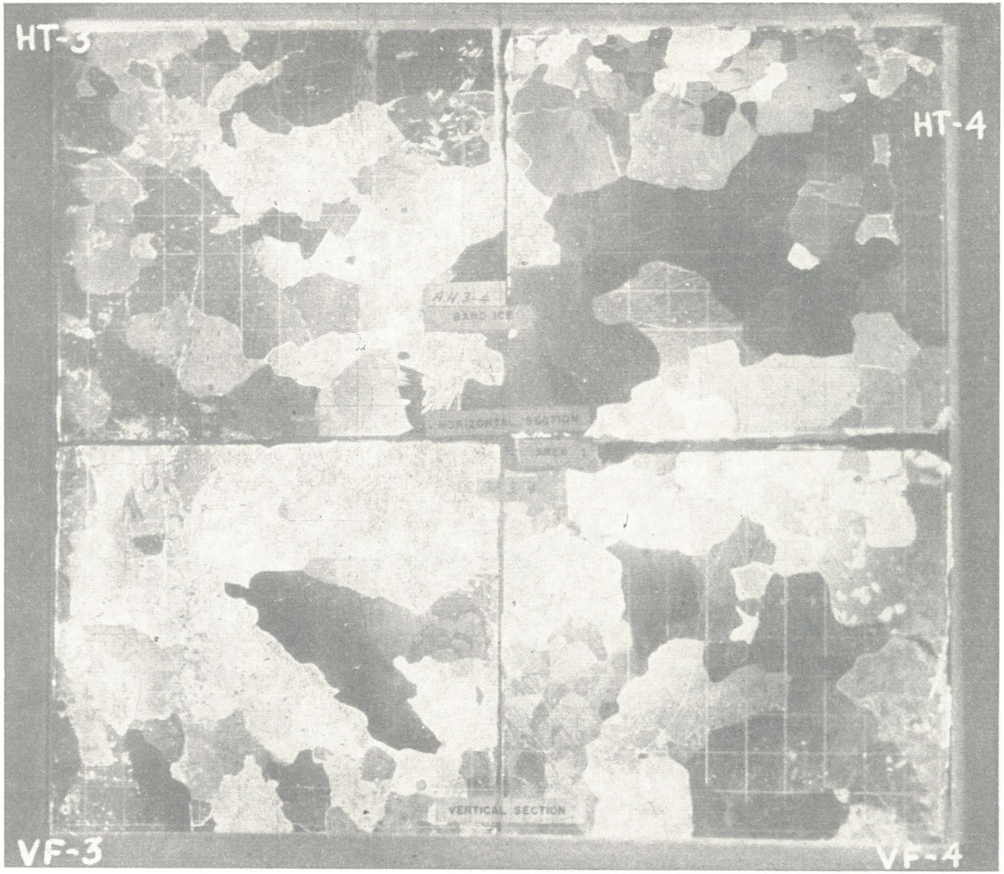

b)

Pl. 49. Top horizontal and corresponding vertical front thin sections from sample A-13 to show variation in crystal size and form across a contact of wedge ice (HT-1, VF-1) with relict ice (HT-4, VF-)

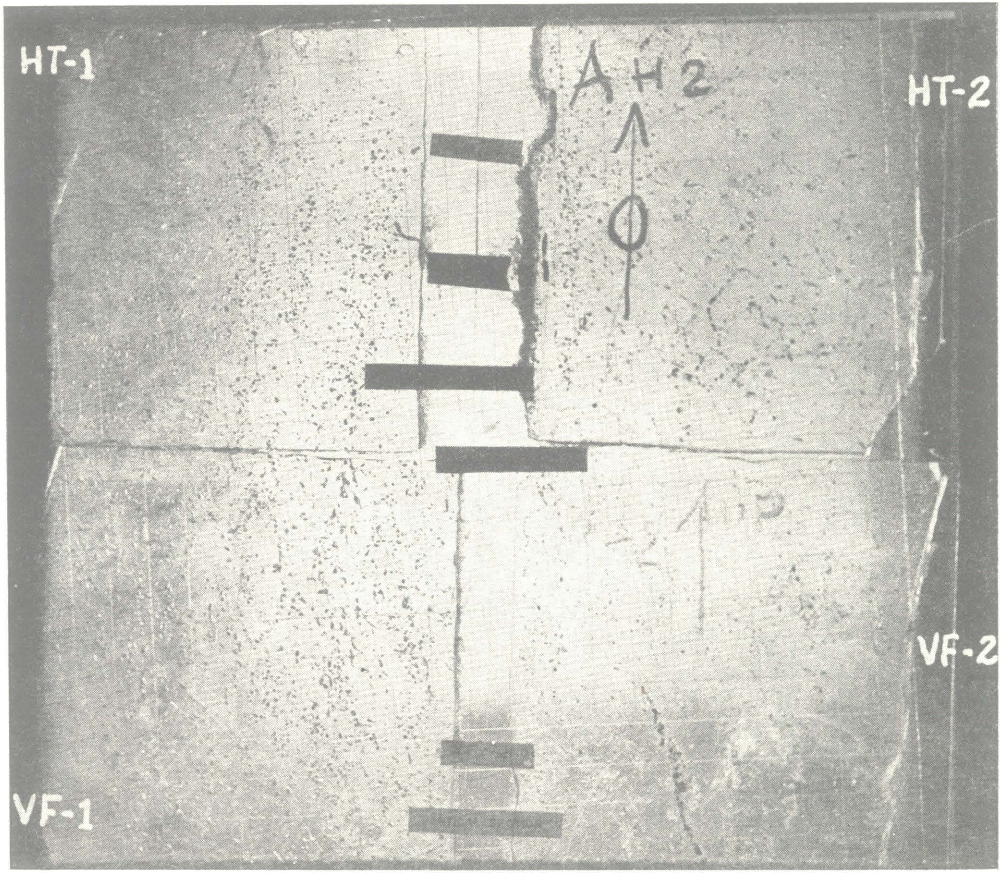

Pl. 50. Horizontal and vertical thin sections from sample A-13 through single polaroid to show bubble structure at contact (HT-2, VF-2) between wedge (HT-1, VF-1) and relict ice

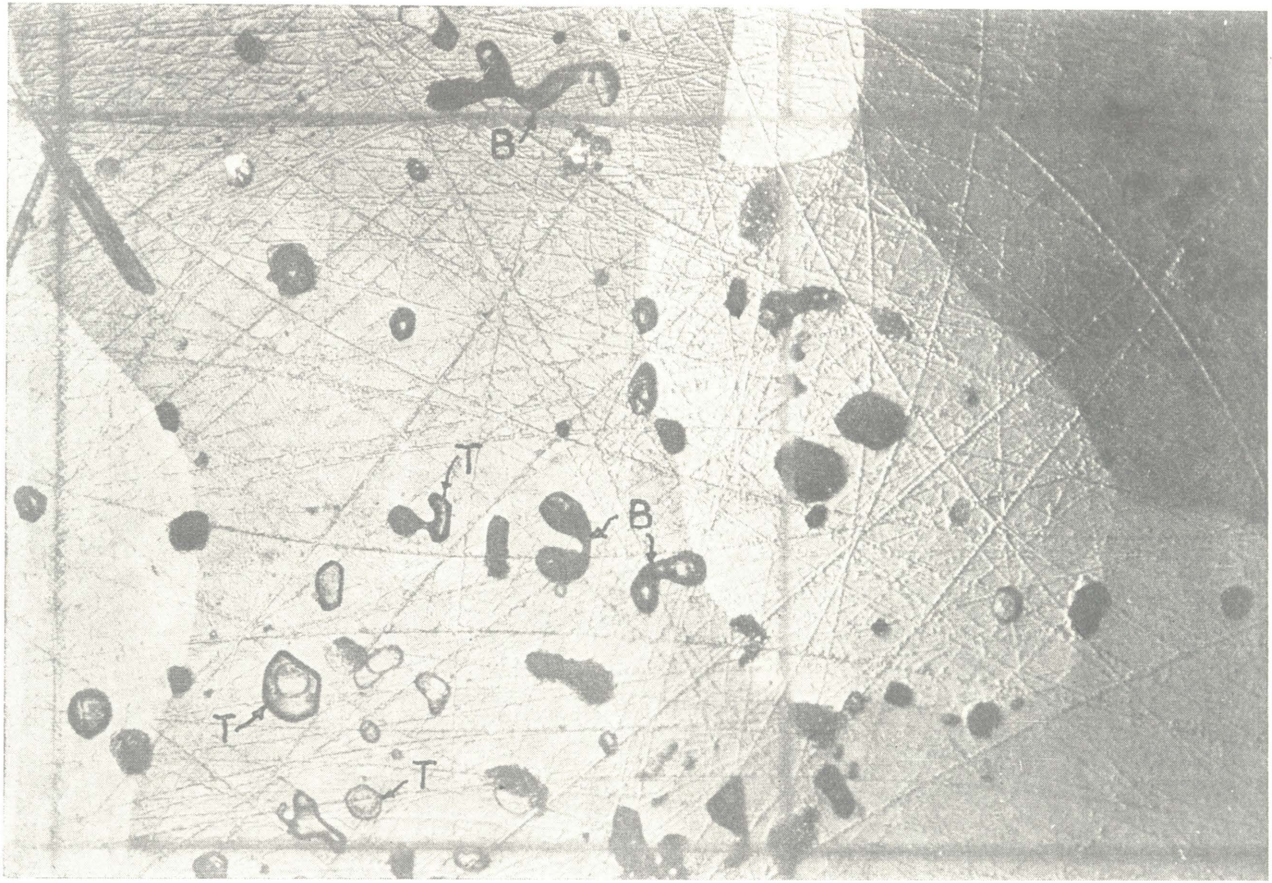

Pl. 51. Section of wedge ice under 10 × magnification, crossed polaroids. Dirt particles are opaque bodies located primarily at crystal interfaces. Air bubbles are the rounded worm-like structures and Tyndall figures are the geometric, primarily hexagonal, plates. Section cut normal to crystal *c*-axis

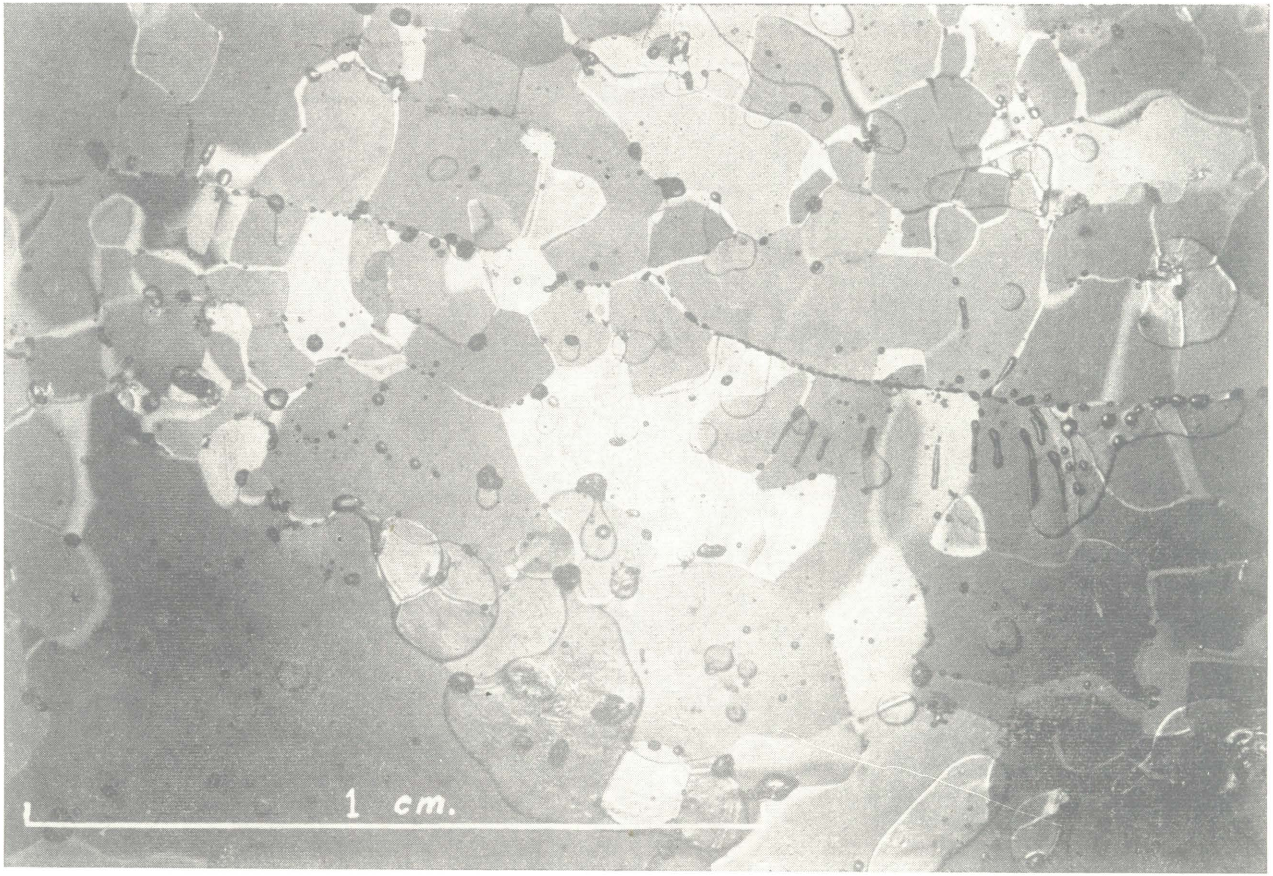

Pl. 52. Thin section of small new ice wedge crystals under 10 × magnification. Air bubbles are worm-like structures along crystal interfaces. Dirt particles appear concentrated along interfaces as well, often inclosed in air bubbles, and particularly along the crack running across the section

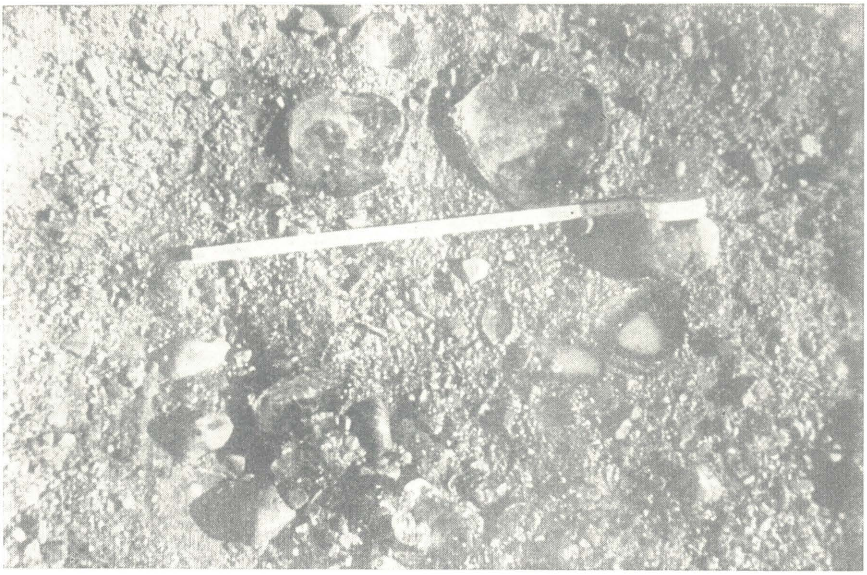

Pl. 53. Ice sockets, Area 1

Pl. 54. Ice wedge containing dirt bands along border, Area 5

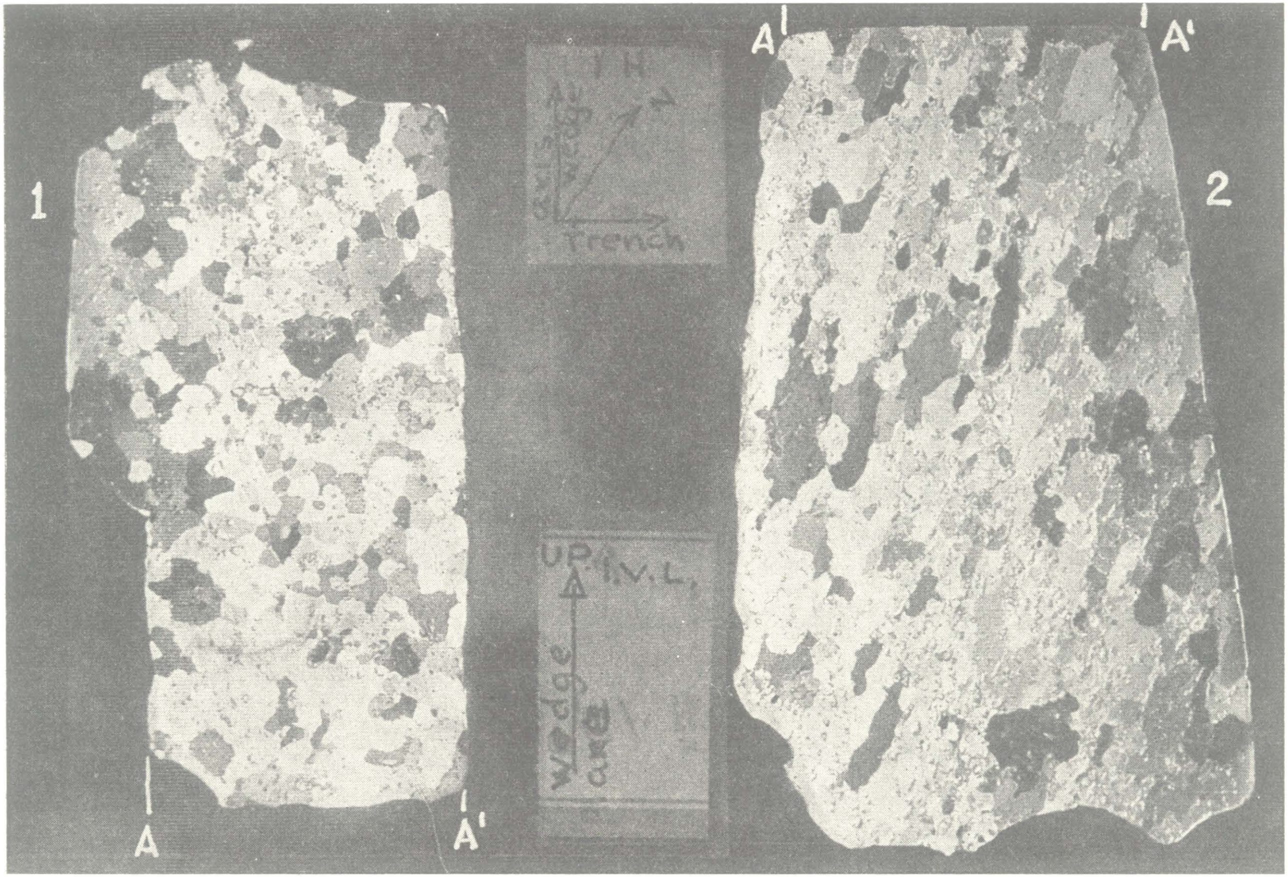

XXXVIII

Pl. 55. Horizontal (sect. 1) and vertical (sect. 2) thin sections of ice wedge, sample E-1

Note vertical line of new wedge crystals, particularly in section 2

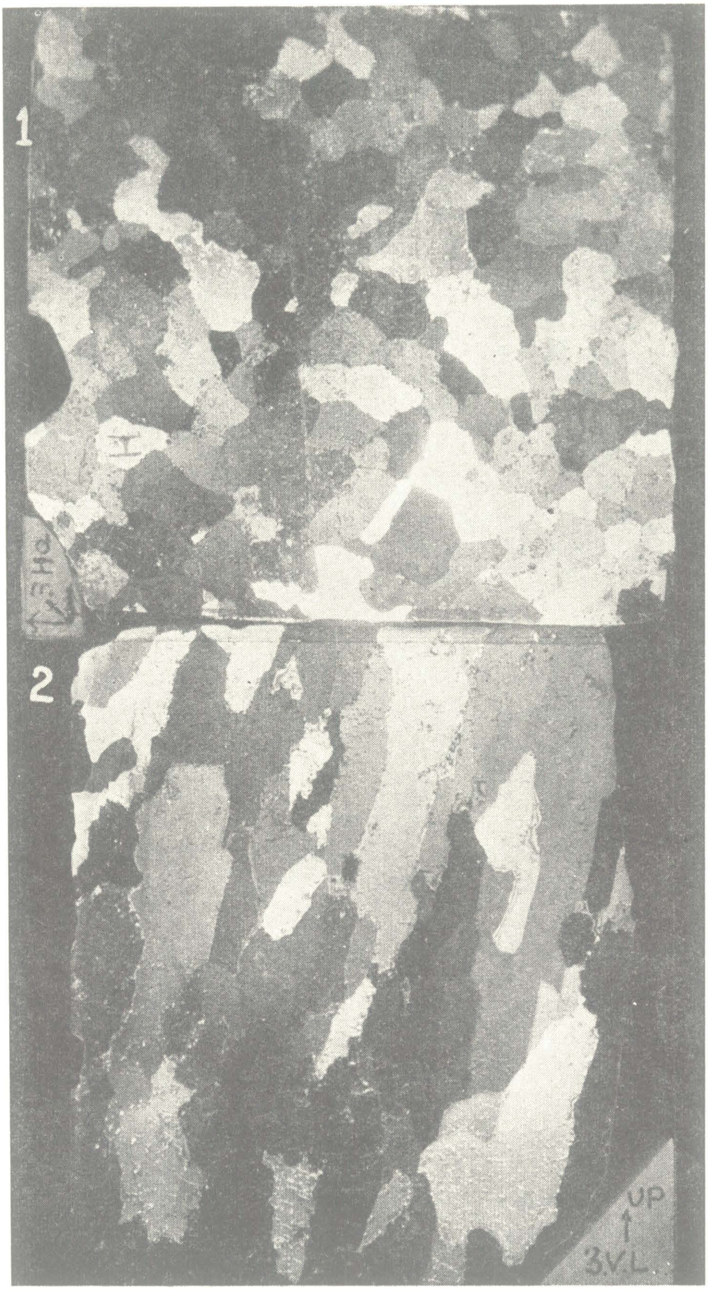

Pl. 56. Horizontal (sect. 1) and vertical (sect. 2) thin sections from older wedge crystals, sample E-1

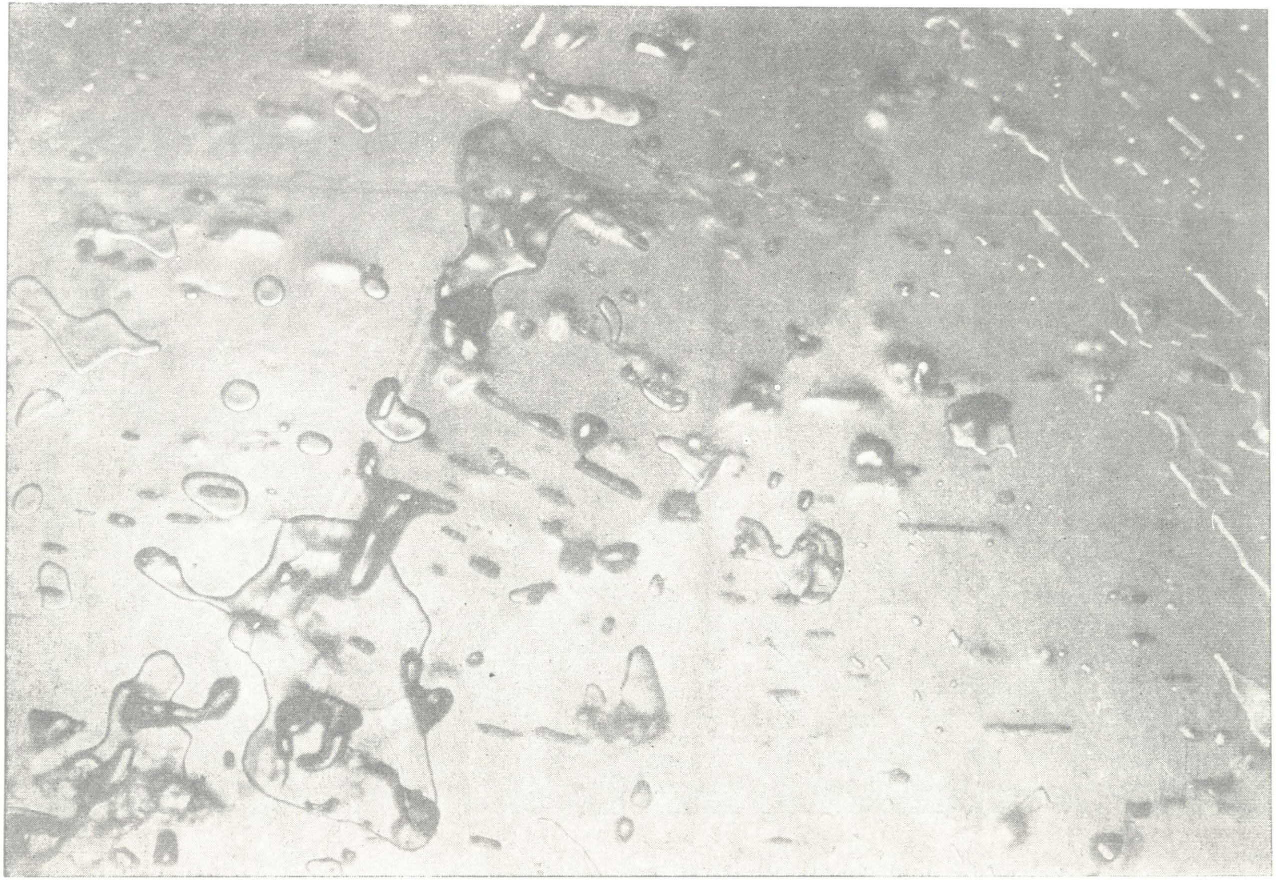

Pl. 57. Vertical thin section of wedge ice (E-1-VL-3) under approx. 8,5 × magnification. Tyndall figures are rod-shaped structures normal to plane of crystal elongation

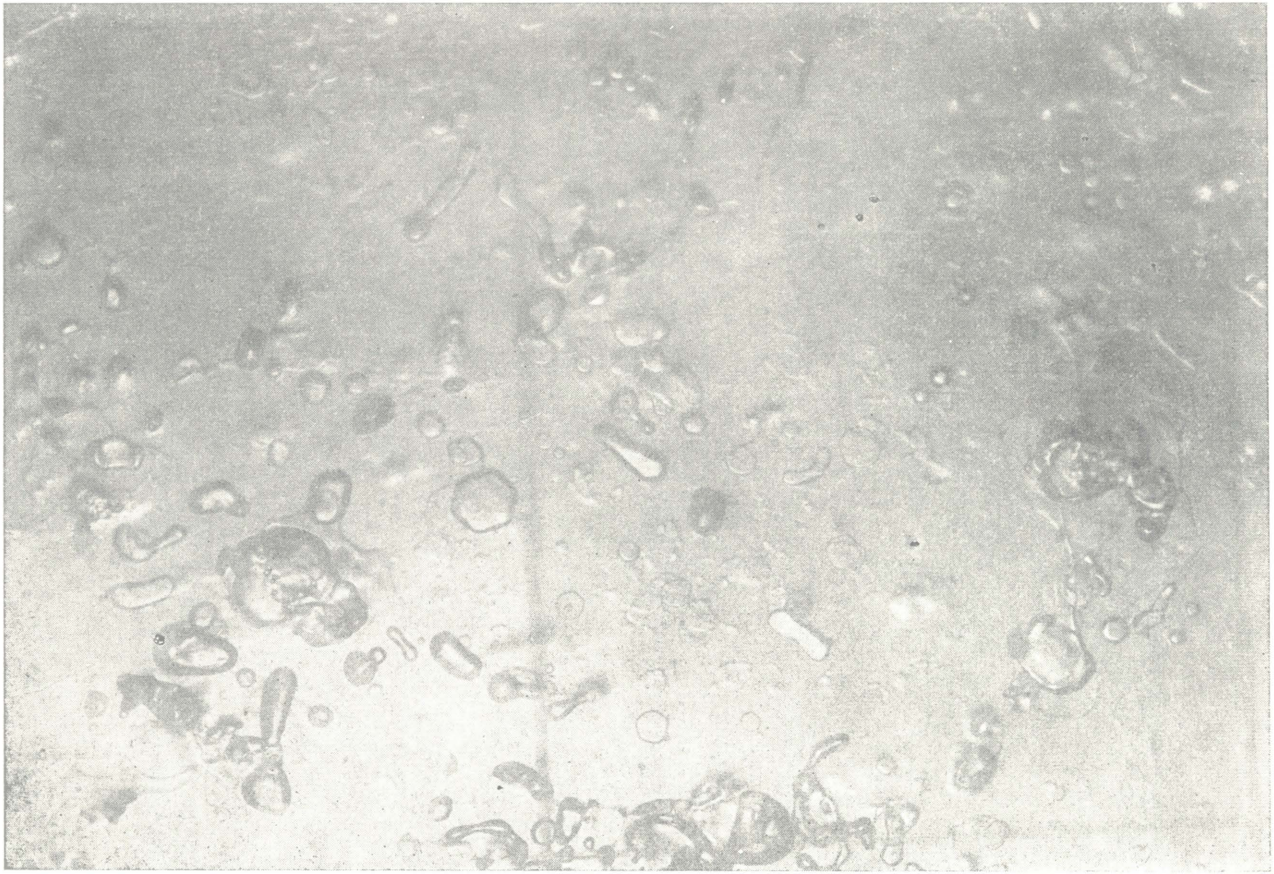

Pl. 58. Horizontal thin section of wedge ice (E-1-HT) under approx. 8,5 × magnification. Tyndall figures appear as polyhedral (primarily hexagonal) plates about 1 mm in diameter (grid in photo is in cm^2)

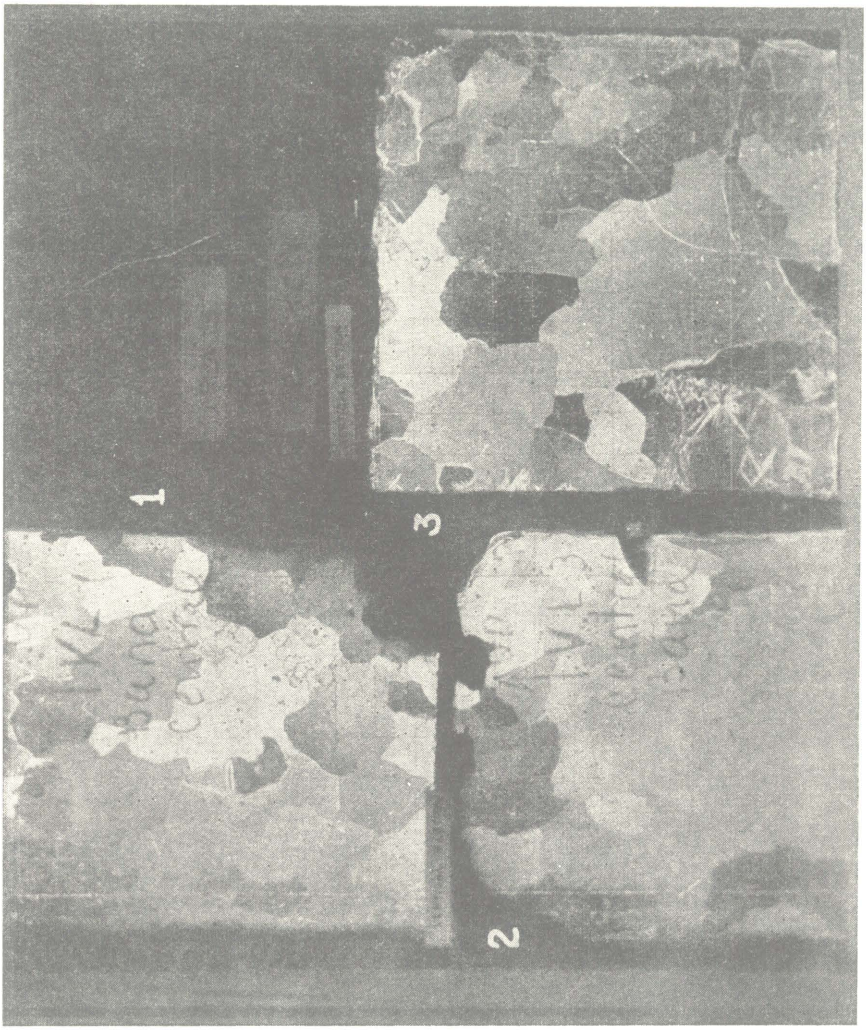

Pl. 59. Vertical thin sections of relict ice, sample E-2

Pl. 60. Alternating bands of sand and clear ice at the edge of a band of relict ice. Location of sample E-3

Pl. 61. Top view of ice mass (sample C-3) showing apparently scattered dirt inclusions (compare with pl. 62)

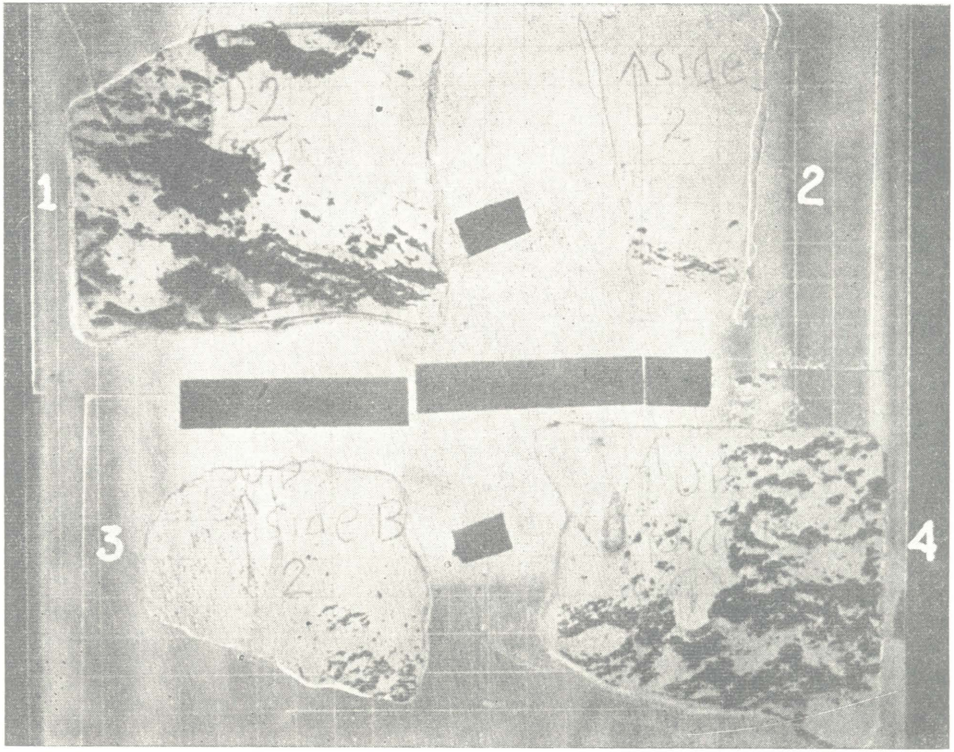

Pl. 62. Vertical sections from ice mass (sample C-3) showing discontinuous layered structure of inclusions (compare with pl. 61)

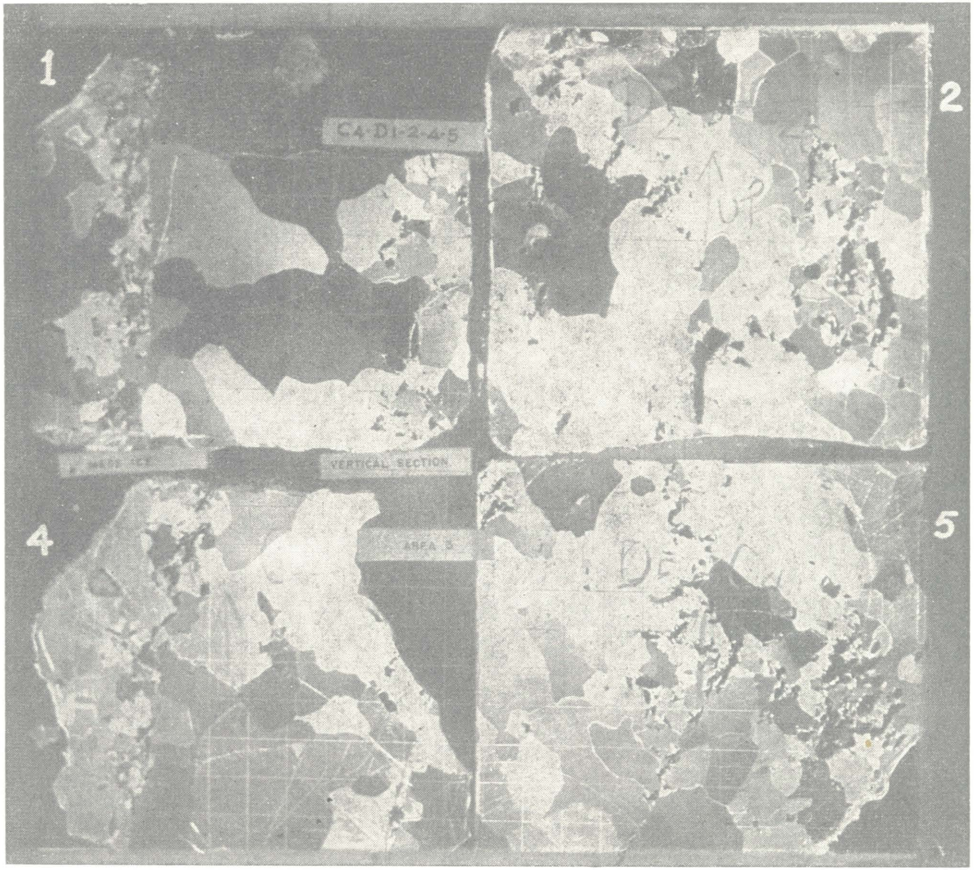

Pl. 63. Vertical thin sections of ice mass C-4 containing vertical to 45° oriented layers of soil particles

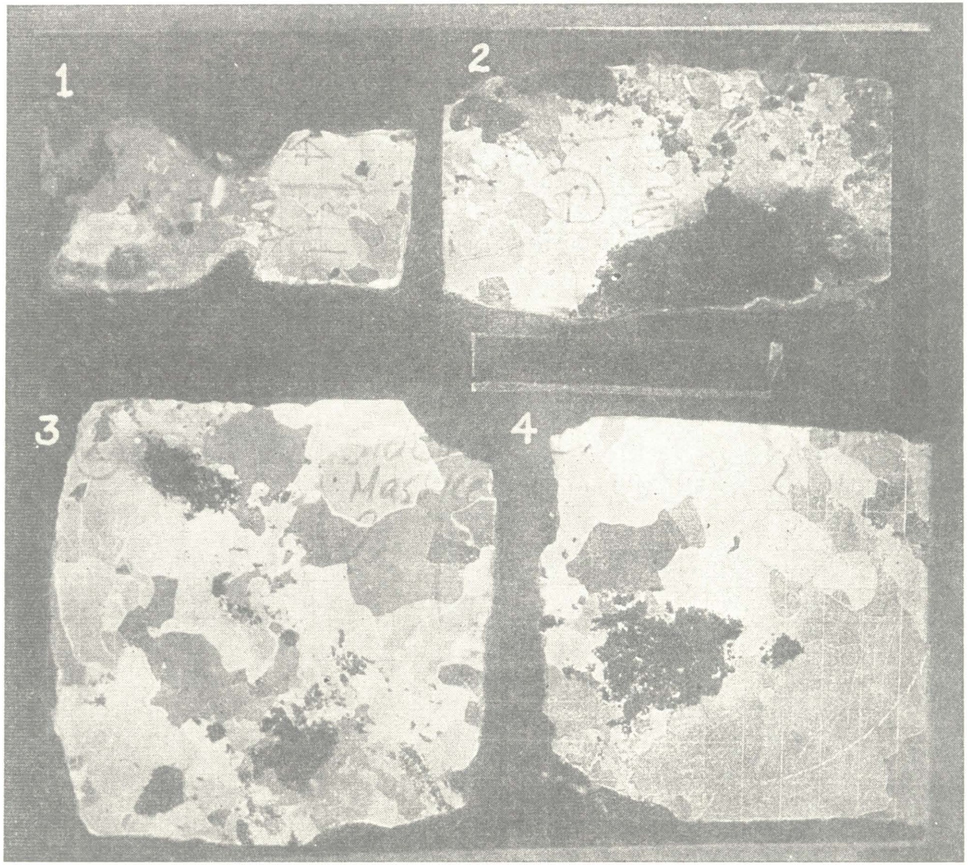

Pl. 64. Horizontal thin sections of ice mass C-3 containing discontinuous layered inclusions of soil particles oriented 0° to 20° to the horizontal

Pl. 65. Three-pronged junction of ice wedges, Area 3. Block excavated is sample C-1

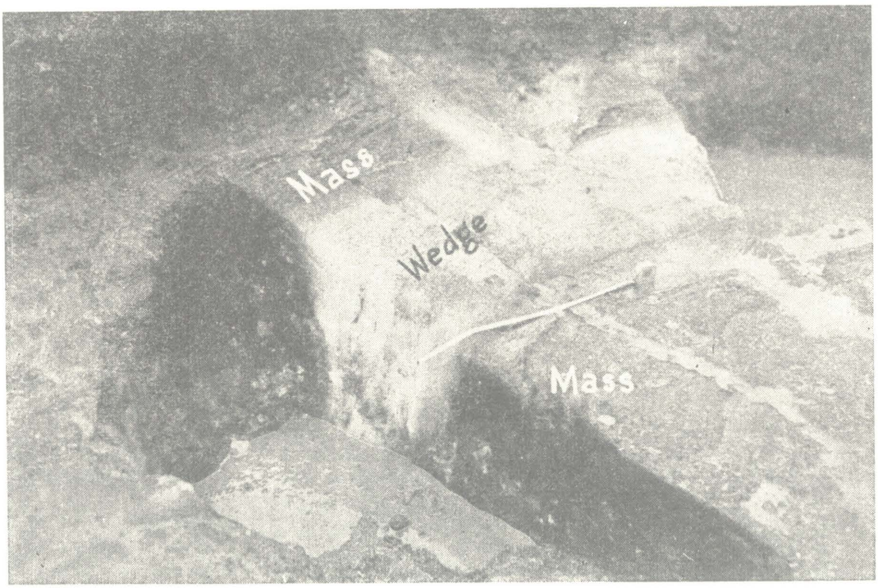

Pl. 66. Ice wedge inclosed by ice masses, Area 3

Note orientation of dirt layers parallel to contact and marked difference between dark mass ice and milky wedge ice

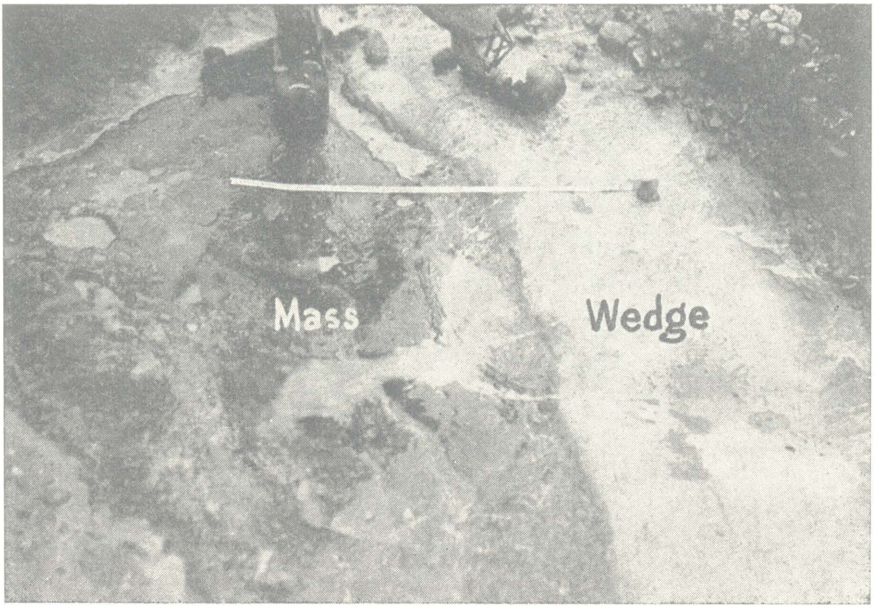

Pl. 67. Ice wedge in contact with ice mass, Area 3

In this sample, no clear layering of soil particle inclusions is apparent in the mass

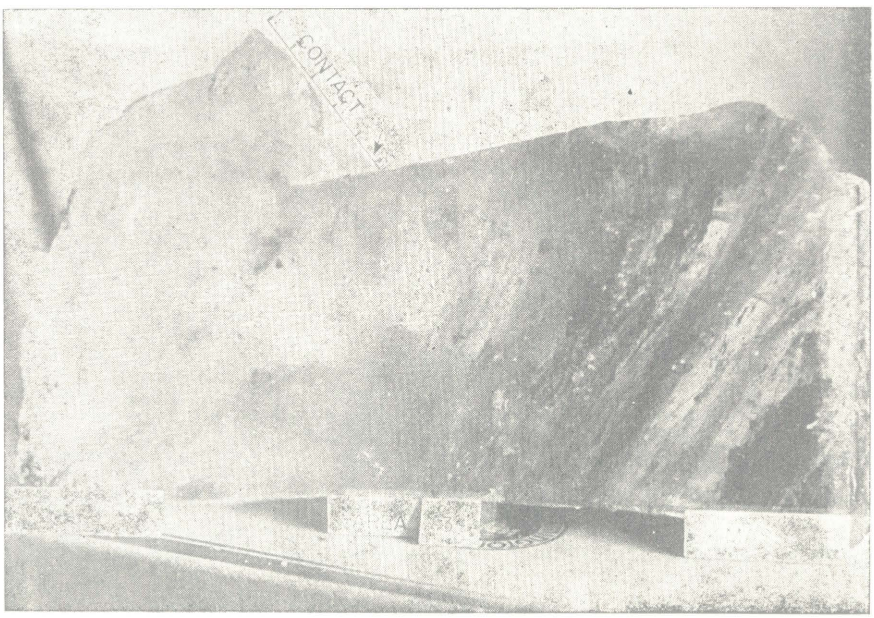

Pl. 68. Cross section („back") of sample C-5 showing contact between wedge and mass ice